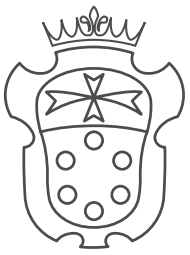

SCUOLA
NORMALE
SUPERIORE

Classe di Scienze

Corso di perfezionamento in
Matematica

XXXV ciclo

Bestvina–Brady Morse theory on hyperbolic manifolds

Settore Scientifico Disciplinare **MAT/03**

Candidato
dr. Matteo Migliorini

Relatore
Prof. Bruno Martelli

Supervisione interno
Prof. Andrea Malchiodi

Anno accademico 2022–2023

Acknowledgements

I would like to express my deepest appreciation to my advisor, Bruno Martelli, for guiding me along this journey. I am very grateful to him, in particular for suggesting this beautiful project which was very much enjoyable and fulfilling.

I would also like to extend my sincere thanks to Federica for all the emotional and mathematical support she has given me in these years. She always kept my motivation high, and was always there to encourage me when I was feeling disheartened.

Special thanks should also to my family, on which I know that I can always rely on, and to my friends, who accompanied me through this experience and made it a lot more enjoyable.

Introduction

Among all fiber bundles, the simplest to study are certainly the ones with the circle as base space. Indeed, whenever a manifold fibers over S^1, it can be easily described as a product $F \times [0,1]$ where we identify the two boundary components with a certain diffeomorphism $\varphi\colon F \to F$, called *monodromy*. Although this construction is very simple, a wide range of manifolds arises in this way.

For example, although the hyperbolic geometry is the richest among the eight geometries that classify the 3-manifolds (as per Thurston's Geometrization Theorem), Agol and Wise proved [AGM13, Wis21] that every hyperbolic 3-manifold admits a finite cover that fibers over the circle. This result is, from a certain perspective, quite surprising, since fibrations do not behave very well with hyperbolicity.

The first sign of this misbehaviour comes from an Euler characteristic argument. In fact, the Euler characteristic of a fibering manifold is always zero, but a generalization of Gauss-Bonnet Theorem implies that in even dimension the Euler characteristic of a hyperbolic manifold M is proportional to the volume, and therefore never vanishes.

So a fibration of a hyperbolic manifold can only happen when the dimension is odd. In the even-dimensional case, one can be interested in having a smooth map to S^1 with the least amount of critical points allowed by the Euler characteristic. Such a function is called *perfect circle-valued Morse function*.

Moreover, one should not think that the fibers are embedded in M in a geometric way. Since every fibering hyperbolic 3-manifold has a hyperbolic surface F as a fiber, it would be tempting to assume that F is totally geodesic inside M.

Actually, this could not be farther from the truth. If one considers the liftings of F and M to their respective universal covers

$$\begin{array}{ccc} \mathbb{H}^2 & \xrightarrow{\tilde{\iota}} & \mathbb{H}^3 \\ \downarrow & & \downarrow \\ F & \xrightarrow{\iota} & M \end{array}$$

then $\tilde{\iota}(\mathbb{H}^2)$ is not a hyperplane inside $\mathbb{H}^3$ (as it should be if the fiber were totally geodesic), instead it is a topological disk whose boundary is a Peano curve on the sphere.

The situation gets even more paradoxical if we move to a higher dimension. The fiber F is homotopically equivalent to $F \times \mathbb{R}$, which carries a natural hyperbolic metric (being the cyclic cover of M), so this implies that F is aspherical. Despite this, it cannot be hyperbolic as a consequence of Mostow Rigidity (which does not apply in dimension 2, and that is why we can have hyperbolic surfaces as a fiber). The fiber must therefore be an intrinsically complicated object, which explains the difficulty in finding even a single example in dimension higher than 3.

A possible approach for constructing fibering hyperbolic manifolds comes from Bestvina-Brady Morse theory. Introduced in [BB97], it is the piecewise-linear analogue of the more classical smooth version. By constructing hyperbolic manifolds as combinatorial objects, one can try to define a piecewise-linear linear function to S^1, and hope that there are no critical points (or, at least, they are controlled in some sense).

The way to proceed was described in [JNW19]. The rough idea is to take some right-angled hyperbolic polytope, glue some copies of it to obtain a manifold, and then consider the dual tessellation, which is a cube complex C. By choosing an orientation of the edges of C that is *coherent*, meaning that parallel edges in a square should have the same orientation, one can define a canonical *diagonal map* from every cube to S^1, which glues together to a global map $f : C \to S^1$. After that, one can use Bestvina-Brady theory to check for critical points, which appear only in the vertices of the cube complex.

In this thesis, we generalize this approach by not enforcing coherency in the orientation of the cube complex. Then, we consider the barycentric subdivision of the cube complex, and we provide a canonical way to define some piecewise-linear map on this subdivision.

The downside of this is that, in general, the critical points can now also appear on all the barycentres of the cubes. Therefore, we need some tools that allow us to be sure that most of them are not actually critical; for example, we will see that if a cube is coherently oriented, then its barycentre is not critical, so we are not losing anything to the original algorithm.

Actually, the barycentre is regular even if we only ask that the cube is coherently oriented in some direction (that is, all the edges which are parallel to some coordinate axis are oriented in the same way). This allows us to leave only a small amount of cubes to check.

We will then employ this algorithm with a family of hyperbolic polytopes, obtaining different results in different dimensions. In particular, we will be able

to prove the following.

Theorem 1. *There exists a cusped finite-volume hyperbolic* 5*-manifold which fibers over the circle.*

Theorem 2. *There exists a cusped finite-volume hyperbolic* 6*-manifold admitting a perfect circle-valued Morse function.*

In dimension 7 and 8 we will not obtain a fibration (or perfect circle-valued Morse function), but we will still get an interesting result.

Theorem 3. *For* $n = 7, 8$ *there exists a finite volume hyperbolic* n*-manifold* M^n *along with a map* $f\colon M^n \to S^1$ *such that the induced map in homotopy* $f_*\colon \pi_1(M^n) \to \mathbb{Z}$ *has finitely presented kernel.*

The cover $\widetilde{M^n}$ *associated with this kernel has finitely presented fundamental group, and infinitely many cusps of maximal rank. In particular, it has infinite Betti number* b_{n-1}*.*

Theorems 1 and 3 are obtained in a joint work with Italiano and Martelli [IMM22, IMM20], while Theorem 2 is currently in preparation with Italiano.

Structure of the paper

This thesis is structured as follows:

- In Chapter 1 we will compare different versions of Morse theory, mainly the smooth one and the piecewise-linear one (introduced by Bestvina and Brady). We will then see that, up to dimension 7, a Bestvina-Brady Morse function with non-degenerate singularities can be smoothened to a Morse function with critical points of the same indices.
- In Chapter 2 we will see how to extend a cellular 1-cocycle on a cell complex to a piecewise-linear map on its barycentric subdivision, and prove some useful properties of this map.
- In Chapter 3 we will describe Jankiewicz, Norin, and Wise's algorithm, adapted to this fairly more general setting.
- In Chapter 4 we will apply the algorithm to a family of hyperbolic polytopes, proving the main theorems stated above.

- In Chapter 5 we will investigate a bit more the 5-dimensional fibering manifold by finding a small quotient that still fibers over the circle. We will also see some geometric intuition behind this algorithm, as well as some consequence this fibration has from the geometric group theory point of view.

Contents

1

Circle-valued Morse theory

Morse theory is a tool that can be adapted to different settings: smooth, piecewise-linear, or combinatorial. In this chapter, we will see two different implementations of this theory and the relationships between them. In particular, we are interested in the circle-valued version of Morse theory.

The general setting is the following. Let M be a compact n-manifold, and let $f\colon M \to S^1$ be a map. It is intended that if M has any additional structure (smooth, PL), then we require that f preserves that structure.

We consider the following pullback:

$$\begin{array}{ccc} \widetilde{M} & \xrightarrow{\widetilde{f}} & \mathbb{R} \\ \downarrow{\scriptstyle \pi} & & \downarrow \\ M & \xrightarrow{f} & S^1 = \mathbb{R}/\mathbb{Z} \end{array}$$

where, by definition, $\widetilde{M} = \{(x,t) \in M \times \mathbb{R} : f(x) - t \in \mathbb{Z}\}$. This pullback is called the *cyclic cover* of M with respect to f.

We denote by $[f]$ the pull back of the fundamental coclass of S^1 through f, which is an element of $H^1(M)$.

Remark 1.1. The case $[f] = 0$ is of little interest to us, as f is homotopic to a constant and everything becomes fairly trivial: in this case, f lifts to a map $g\colon M \to \mathbb{R}$, and $\widetilde{M}$ is homeomorphic to $M \times \mathbb{Z}$, with $\widetilde{f}(x,n) = g(x) + n$.

1.1 Morse theory

Let us delve into the different categories in which we can define a Morse function, starting from the smooth one.

1.1.1 Smooth Morse theory

In this section we will follow the definitions given in [MSW69], and we refer to it for the proofs.

Let M be a smooth compact n-manifold (with or without boundary).

Definition 1.2. A circle-valued smooth Morse function is a smooth function $f\colon M \to S^1$ such that its critical points, i.e. the points $x \in M$ with $df_x = 0$, are non-degenrate, meaning that the Hessian Hf_x is non-degenerate.

If ∂M is non-empty, we also require that the restriction $f|_{\partial M}$ is a circle-valued Morse function without critical points.

If x is a critical point, then the *index of* x is the index of negativity of Hf_x. We denote by c_i the number of critical points of index i. Moreover, we say that an element $y \in S^1$ is a *regular* (resp. *critical*) *value* if $f^{-1}(y)$ does not (resp. does) contain critical points.

Proposition 1.3. *Non-degenerate critical points are isolated.*

If $f\colon M \to S^1$ is a circle-valued Morse function, then its lift $\widetilde{f}\colon \widetilde{M} \to \mathbb{R}$ is a (real-valued) Morse function. This is useful in order to speak about sublevels, which are needed for the deformation lemma.

Theorem 1.4. *Suppose f is a smooth circle-valued Morse function on M. Let $a < b \in \mathbb{R}$ be such that $\widetilde{f}$ has no critical values between a and b. Then the sublevel $\widetilde{M}_{\leq b} := \widetilde{f}^{-1}((-\infty, b])$ deformation retracts on $\widetilde{M}_{\leq a}$ (and in particular they are diffeomorphic).*

Note that the boundary of a sublevel $\partial\widetilde{M}_{\leq a}$ can be naturally split into the union of $\partial\widetilde{M} \cap \widetilde{M}_{\leq a}$ and $\widetilde{f}^{-1}(a)$.

It is useful to know what happens to sublevels when we cross a critical point. We recall that attaching an i-handle means gluing to the boundary of a manifold a copy of $D^i \times D^{n-i}$ along $S^{i-1} \times D^{n-i} \subset \partial(D^i \times D^{n-i})$.

Theorem 1.5. *Suppose f is a smooth Morse function, and suppose $a < b \in \mathbb{R}$ are regular values such that $\widetilde{f}^{-1}([a, b])$ contains a single critical point of index i. Then $\widetilde{M}_{\leq b}$ can be obtained from $\widetilde{M}_{\leq a}$ by attaching an i-handle to $f^{-1}(a)$.*

The critical indices c_i are in relation with the Euler characteristic of M.

Theorem 1.6 (Euler characteristic)**.** *We have $\chi(M) = \sum_{i=0}^{d}(-1)^i c_i$.*

We will be interested in circle-valued Morse function with few critical points.

Definition 1.7. A circle-valued Morse function $f\colon M \to S^1$ is said to be *perfect* if it has $|\chi(M)|$ critical points.

When $\chi(M) = 0$, a perfect Morse function has no critical points and is therefore a fibration over the circle.

1.1.2 Polytopes

Before switching to the piecewise-linear category, we recall some definitions and properties of affine polytopes, as they are a recurring object throughout this document.

Definition 1.8. An *affine polytope* is the convex hull of a finite number of points in $\mathbb{R}^d$.

Remark 1.9. The definition above is actually for *convex* affine polytopes. While there exists a notion of non-convex polytope, the polytopes considered here will all be convex, so we can safely drop the adjective.

Affine polytopes can also be defined in terms of half-spaces.

Theorem 1.10 ([Min89, Wey34])**.** *A subset $P \subseteq \mathbb{R}^d$ is an affine polytope if and only if it is a bounded intersection of finitely many half-spaces.*

An in-depth explanation of the relationships between these two definitions, including the proof of the above theorem, can be found for example in [BS18, Chapter 3].

Definition 1.11. Let P be an affine polytope of dimension n. A *supporting hyperplane* is the boundary of a half-space containing P. A *face* of P is the intersection of P with a (possibly empty) family of supporting hyperplanes. We include the empty set and the whole P in this definition; faces which are distinct from $\varnothing$ and P are called *proper*.

Moreover, we refer to 1-codimensional faces as *facets*, 2-codimensional faces as *ridges*, 1-dimensional faces as *edges* and 0-dimensional faces as *vertices*. Dually, if F is a face of P, we say that P is a *coface* of F, and if F is a facet we say P is a *cofacet* of F.

We are interested in studying affine polytopes from a combinatorial point of view. An affine polytope is, in particular, a cell complex, so it carries the natural structure of a partially ordered set.

Definition 1.12. Let P be an affine polytope. The *face lattice* of P, denoted by $\Phi(P)$, is the set of faces of P partially ordered by inclusion. We conventionally include P and $\varnothing$ inside $\Phi(P)$.

Definition 1.13. Two affine polytopes P and Q are *combinatorially isomorphic* if their face lattices are isomorphic posets.

If P and Q are combinatorially isomorphic then they are isomorphic as cell complexes, but they may not be isometric.

Definition 1.14. An affine polytope P is *simple* if the intersection of any k distinct facets is either empty or a k-codimensional face.

Definition 1.15. Two facets are *adjacent* if they intersect in a ridge. The *adjacency graph of* P is the graph whose vertices correspond to facets of P; its edges join adjacent facets, and so they correspond to ridges of P.

Remark 1.16. Two facets may not be adjacent but still intersect in a face of codimension at least 3: for example, in the octahedron, two facets may intersect in a single vertex, and are therefore not adjacent. This pathology is ruled out if the polytope is simple.

The adjacency graph can be seen concretely using duality.

Definition 1.17. Let P, Q be polytopes of the same dimension. We say that Q is *dual* to P if $\Phi(P)$ is isomorphic to the opposite poset of $\Phi(Q)$, or equivalently, if we have a bijection between k-faces of P and $(n-k-1)$-faces of Q for every k which reverses inclusion.

A dual of a convex polytope always exists and can be constructed using polar reciprocation [Bar02, Chapter IV]. We will denote a dual of an affine polytope P by P^*; this is well-defined up to combinatorial isomorphism.

Using the dual, we can note the following.

Proposition 1.18. *If P and Q are dual, the adjacency graph of P is isomorphic to the 1-skeleton of Q.*

1.1.3 Affine cell complexes

Let us study to the piecewise-linear (PL for short) category. We give some definitions, following [RS82].

Definition 1.19. A *polyhedron* is a subset $X \subseteq \mathbb{R}^d$ such that every point x has a neighbourhood N which is a cone with vertex x and base some compact $L \subset X$; we denote this cone by xL.

The set L is called a *link* of x, and N is called a *star* of x.

Remark 1.20. Be careful that the word *polyhedron* has been used with different meanings in literature; here we attain to the notation used in [RS82].

The choice of the link $L \subseteq X$ is not unique; however, we may restrict to links that are polyhedra, and two such links are PL homeomorphic. The link of x is therefore well-defined up to PL homeomorphism, and is denoted by $\mathrm{Lk}(x)$.

Definition 1.21. We say that a topological space X has a *PL structure* if X is equipped with an atlas, where charts map neighbourhoods of X to polyhedra, and transition maps are PL.

A PL structure on X gives rise to a *PL n-manifold* if we require that charts map to the standard n-simplex.

The simplex carries a natural structure of a PL manifold with boundary; we refer to this manifold as *PL ball*, and to its boundary as *PL sphere*.

Every PL manifold can be triangulated, i.e. it is PL homeomorphic to a simplicial complex. Vice versa, every simplicial complex has a natural PL structure, but is not necessarily a PL manifold: to ensure this, we need to require links to be PL spheres.

To study Morse theory in the PL category, we need a notion of a cell structure which is compatible with the piecewise-linear one. The following definition is taken from [BB97].

Definition 1.22. An *affine cell complex* X is a cell complex where every cell is identified with some affine polytope inside $\mathbb{R}^n$. Moreover, the inclusion map between any two cells $\sigma \subset \tau$ must translate to an affine map between the corresponding polytopes.

A simplicial complex is in particular an affine cell complex.

Remark 1.23. An affine cell complex whose cells are simplices may not be a simplicial complex, as cells might intersect in the union of more than one face.

Since cells of an affine cell complex are affine polytopes, we employ the same terminology used for them.

Definition 1.24. Let X be an affine cell complex, and σ, τ be two cells. We say that τ is a *face* of σ, or equivalently that σ is a *coface* of τ, if τ is contained in σ. In this case, we also write $\tau < \sigma$, as cells of an affine cell complex form a partially ordered set under inclusion.

Analogously, we say that τ is a *facet* of σ, or that σ is a *cofacet* of τ, if τ is a face of codimension 1 inside σ.

An affine cell complex X has a natural PL structure, which allows us to define links and stars. Links and stars have a natural cell structure, induced by the cell structure of X; more precisely, if we define $\mathrm{Lk}(v, \sigma)$ to be the link of v inside a cell σ which has v as a vertex, then $\cup_\sigma \mathrm{Lk}(v, \sigma)$ gives the desired cell decomposition.

In this piecewise-linear setting, we also need an analogue of the concept of smooth deformation retract. There are two different natural definitions, depending on whether we are working with manifolds or affine complexes.

Definition 1.25. Let X be an affine cell complex. Suppose that X has a maximal cell with a *free facet*, which is a facet not contained in any other cell.

An *elementary collapse* is the removal of that maximal cell, along with one free facet. We say that X *collapses* on $Y \subseteq X$ if Y can be obtained from X by a sequence of elementary collapses; if X collapses to a point, we say that X is *collapsible*.

Remark 1.26. Note that collapsibility is stronger than contractibility. We refer to [RS82] for the example of the *house with two rooms*.

Definition 1.27. Let M be a PL n-manifold with boundary, and let $B \subseteq M$ be a PL n-ball such that $B \cap \partial M$ is a PL $(n-1)$-ball. An *elementary shelling* is the removal of $\mathrm{Int}\, B \cup \mathrm{Int}(B \cap \partial M)$.

The manifold M is said to *shell to* $N \subset M$ if N is obtained by a sequence of elementary shellings.

Note that collapsing does not preserve the homeomorphism class; indeed, one may start from a manifold and obtain a complex which is not pure-dimensional. Shelling, however, preserves the PL homeomorphism class.

One can promote a collapse to a shelling by taking regular neighbourhoods.

Definition 1.28. Let $C \subseteq X$ be a subcomplex of an affine cell complex. Denote by $\mathrm{sd}^r X$ the r-th iterated barycentric subdivision of X.

The *r-th derived neighbourhood* $\mathcal{N}^r C$ is the subcomplex of $\mathrm{sd}^r X$ spanned by the simplices which intersect $\mathrm{sd}^r C$.

Taking the first derived neighbourhood might cause some pathologies: for example, the first derived neighbourhood of the boundary of the simplex is the barycentric subdivision of the whole simplex, which is not homotopy equivalent to its boundary. To fix this, it suffices to consider the second derived neighbourhood, as we shall soon see.

Definition 1.29. A subcomplex $Y \subseteq X$ of an affine cell complex is *full* if for every cell $e \in X$ such that $\partial e \subseteq Y$, then $e \in Y$.

A full subcomplex is determined by its vertices, and it is the largest subcomplex with those vertices.

Lemma 1.30. *[RS82, Corollary 3.30] If X is a simplicial complex, and $Y \subseteq X$ is a full subcomplex, then $\mathcal{N}^1 Y$ collapses to Y.*

Sketch of proof. Every full subcomplex of the boundary of a simplex which is proper (i.e. not empty and not the whole complex) is also collapsible, since it is necessarily a simplex. This allows to collapse all the barycentres of the simplices in $\mathcal{N}^1 Y$ which are not in Y. □

When Y is a subcomplex of X, then $\mathrm{sd}\, Y$ is full in $\mathrm{sd}\, X$: by applying the above lemma one obtains the following.

Proposition 1.31. *Let X be an affine cell complex. The second derived neighbourhood $\mathcal{N}^2 Y$ of a subcomplex $Y \subseteq X$ collapses on Y.*

Moreover, if X is a PL manifold, then $\mathcal{N}^2 Y$ is a PL-submanifold (possibly with boundary).

If Y is an affine cell complex embedded in a PL manifold M, one can define a class of well-behaved neighbourhoods called *regular neighbourhoods* (see Chapter 3 of [RS82]). If additionally M is an affine cell complex such that Y is a subcomplex of M, then $\mathcal{N}^2 Y$ is a regular neighbourhood of Y.

Theorem 1.32. *Let $Y \subseteq X \subseteq M$ be subcomplexes in an affine cell complex M which is also a PL manifold. Suppose that X collapses to Y. Then a regular neighbourhood of X in M shells to a regular neighbourhood of Y in M.*

All the proofs can be found in [RS82].

1.1.4 PL Morse theory

Morse functions for affine cell complexes were introduced by Bestvina and Brady in [BB97].

Definition 1.33. Let Σ be an affine polytope of dimension n. We say that a map $f\colon \Sigma \to S^1$ is *affine* if its lift $\widetilde{f}\colon \Sigma \to \mathbb{R}$ is.

Definition 1.34. Let X be an affine cell complex. A map $f\colon X \to S^1$ (or $X \to \mathbb{R}$) is *Bestvina-Brady Morse*, or simply *Morse*, if it is affine and non-constant on every positive-dimensional cell.

When the codomain of a Morse function f is the circle, we call it *circle-valued*; if its codomain is $\mathbb{R}$ we call it instead *real-valued*.

Let us see how the sublevels of a Bestvina-Brady Morse function change when crossing a vertex. The key object is the following.

Definition 1.35. Let $f\colon X \to S^1$ be a Morse function on an affine cell complex X, and let $v \in X$ be a vertex. The *descending link* of f at v is defined as

$$\mathrm{Lk}_{\downarrow}(v; f) := \bigcup \{\mathrm{Lk}(v, \sigma) : \sigma \text{ is a cell of } X, v \in \sigma,\ \widetilde{f} \text{ attains maximum at } v\},$$

where $\widetilde{f}\colon \sigma \to \mathbb{R}$ is the lift of $f|_\sigma$.

Similarly, the *ascending link* is defined as

$$\mathrm{Lk}_{\uparrow}(v; f) := \bigcup \{\mathrm{Lk}(v, \sigma) : \sigma \text{ is a cell of } X, v \in \sigma,\ \widetilde{f} \text{ attains minimum at } v\}.$$

In the notation, we will omit the function f when it is clear from the context, and simply write $\mathrm{Lk}_{\uparrow/\downarrow}(v)$.

Using descending links we can obtain a deformation lemma. Suppose that $f\colon X \to \mathbb{R}$ is a real-valued Morse function on an affine cell complex X, and let $a < b \in \mathbb{R}$. Denote with X' the affine cell complex obtained from X by subdividing affine cells along $f^{-1}(a)$ and $f^{-1}(b)$; the sublevels $X_{\leq a} \subseteq X_{\leq b}$ are naturally subcomplexes of X'.

Proposition 1.36 ([BB97])**.** *Suppose that $f\colon X \to \mathbb{R}$ is a real-valued Morse function on an affine cell complex X, and let $a < b \in \mathbb{R}$.*

If there are no vertices of X with value in $(a, b]$, then $X_{\leq b}$ collapses to $X_{\leq a}$. If there is a single vertex v with value in $(a, b]$, then $X_{\leq b}$ collapses to $X_{\leq a}$ with a cone attached over $\mathrm{Lk}_{\downarrow}(v)$, where $\mathrm{Lk}_{\downarrow}(v)$ embeds naturally inside $f^{-1}(a)$.

Theorem 1.37 ([BB97])**.** *Let X be an aspherical affine cell complex, and let $f\colon X \to S^1$ be a circle-valued Morse function.*

- *If all the descending links are connected, then the induced map $f_* : \pi_1(X) \to \mathbb{Z}$ has finitely generated kernel.*
- *If all the descending links are simply connected, the kernel is also finitely presented.*

1.2 Smoothing PL Morse functions

In this thesis, our main objective is to build smooth perfect Morse functions on some hyperbolic manifolds. The way we do that is by equipping the manifolds with a PL structure, constructing a Bestvina-Brady Morse function on them, and using it to define the smooth Morse function. The goal of this chapter is to produce a tool that transforms circle-valued Bestvina-Brady Morse functions into smooth Morse functions.

Note that there might not even be a compatible smooth structure on a PL manifold: however in dimension $n \leq 7$ the compatible smooth structure exists, and moreover it is unique if $n \leq 6$.

In particular, we have the following theorem.

Theorem 1.38 ([Mun60], [HM74])**.** *Suppose that M is a PL manifold of dimension $n \leq 7$, with a PL handle decomposition with c_i handles of index i. Then M admits a smooth structure and a smooth handle decomposition with c_i smooth handles of index i.*

There is a substantial difference between Bestvina-Brady and smooth Morse functions: sublevels of a smooth Morse function always change by attaching a handle, since critical points are non-degenerate; for a Bestvina-Brady Morse function, however, the descending links may be very complicated, so the topology of the sublevel manifold may change a lot when crossing a vertex. We need to translate the notion of non-degenerate critical vertex to the PL setting.

Definition 1.39. Let X be an affine cell complex, and $f\colon X \to S^1$ be a Bestvina-Brady Morse function. We say that a vertex is *regular* if its descending link is collapsible.

Moreover, we say that a vertex is *non-degenerate critical of index i* if the descending link collapses to a PL $(i-1)$-sphere.

To smoothen a Bestvina-Brady Morse function, we need vertices to be regular or non-degenrate critical. It turns out that this requirement suffices; the rest of this chapter will be devoted to prove the following.

Theorem 1.40. *Let M be an affine cell complex which is a compact PL manifold of dimension $n \leq 7$, with possibly non-empty boundary, and $f\colon M \to S^1$ be a Bestvina-Brady Morse function.*

Suppose f has only regular and non-degenerate critical vertices. Suppose the latter are all contained in the interior of M, and that the restriction $f|_{\partial M}$ is Morse with only regular vertices.

Then there exists a compatible smooth structure on M and a smooth Morse function $g\colon M \to S^1$ with the same amount of critical points for every index as f.

The smoothing process will be divided into three steps:

- we produce a PL handle decomposition from the given Bestvina-Brady Morse function;
- we smoothen this PL handle decomposition and turn it into a smooth handle decomposition;
- we construct the smooth Morse function from the smooth handle decomposition.

We need some care as handle decompositions are usually used in combination with real-valued Morse functions, while here we are dealing with circle-valued functions.

The handle decomposition may be produced from the Bestvina-Brady Morse function by using discrete Morse theory, as it can be seen from [Ben16] (the paper also contains a survey on the differences between smooth and PL category). We will take however a more topological approach, by proving the following local lemma.

Lemma 1.41. *Let M be a PL n-manifold with boundary, and let B be a PL n-ball. Let $C \subseteq \partial B$, $C' \subseteq \partial M$ be PL $(n-1)$-submanifolds with (possibly empty) boundary, with a PL homeomorphism $C \cong C'$; let M' be obtained by attaching B on M along $C \cong C'$, as in Figure 1.1.*

The following hold.

- *If C is collapsible, then M' shells to M.*

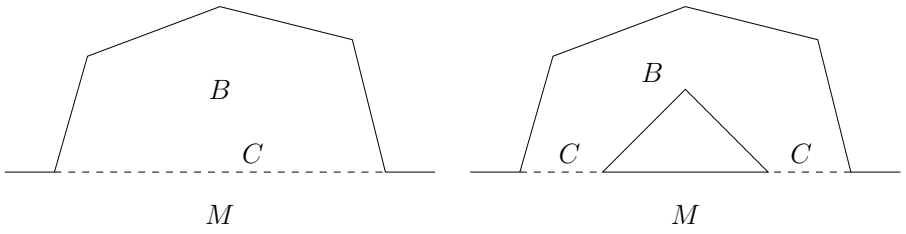

Figure 1.1: Attaching a ball B to a manifold. If the attaching locus C is collapsible, this is a shelling (left); if C instead collapses to an $(i-1)$-sphere, we are attaching an i-handle (right, with $i = 1$).

- *If C collapses to a PL $(i-1)$-sphere, then there exist PL manifolds $M \subseteq X \subset Y \subseteq M'$ such that X shells to M, M' shells to Y and Y is obtained by attaching an i-handle to X.*

Corollary 1.42. *In the second case of the lemma above, M' is PL homeomorphic to M with an i-handle attached.*

Proof. Since shelling is a PL homeomorphism invariant, we have $M \cong X$, $M' \cong Y$, so we conclude. □

Proof of Lemma 1.41. We translate the proof of [Ben16, Theorem 2.2] to the *PL* setting.

If C is collapsible, then the pair (B, C) is PL homeomorphic to the pair of standard simplices (Δ^n, Δ^{n-1}), so M' shells to M.

Suppose now that C collapses to a PL sphere S. Pick a PL triangulation of ∂B, such that C and S are subcomplexes, and cone it to a point v to obtain a triangulation of B. The cone $B' = vS$ is a *PL* i-ball, so up to performing some barycentric subdivisions on B' we can choose an i-simplex σ of B' such that $Z := B' \setminus \operatorname{Int}\sigma$ collapses on S [Ben16, Lemma 2.22 and Definition 2.17]. Since $M \cup Z$ collapses on M then we can find regular neighbourhoods $X := \mathcal{N}(M \cup Z)$ and $\mathcal{N}M$ such that the first shells to the second. Moreover, if Y denotes an appropriate neighbourhood of $M \cup B'$, by Lemma 2.10 in the same paper, Y is obtained from X by attaching an i-handle.

It remains to show that M' shells to Y, but this is true because M' collapses on $M \cup vC$ (we can collapse every simplex not in vC from its free face on $\partial M'$) which in turns collapses to $M \cup vS$, so again by taking regular neighbourhoods we obtain the shelling. □

Note that the sphere S could be knotted inside ∂B, so B itself may not be a handle. This explains why we do not get that M' is obtained by attaching a handle directly to M, but we need to add these intermediate shellings.

Consider the following example.

Example 1.43. Let D, D' be two 4-dimensional disks, and let K be a knot in $S^3 = \partial D = \partial D'$. Let M' be $D \cup_{\mathcal{N}(K)} D'$, i.e. we are attaching two identical disks along a neighbourhood of K via the identity map. The previous proposition implies that M' is obtained by attaching a 2-handle to a ball.

While D' is clearly not a 2-handle, we can note that M' is homeomorphic to $D \cup (\mathcal{N}(K) \times I) \cup D'$, where D and D' are glued on the opposite ends of $\mathcal{N}(K) \times I$.

If A and B are closed 3-balls such that $A \cup B = \mathcal{N}(K)$, then $X = D \cup (A \times I) \cup D'$ is homeomorphic to a 4-ball, and $B \times I$ is a 2-handle. So indeed M' is obtained by attaching a 2-handle $B \times I$ to a ball X that shells to D. In fact B can be taken as a regular neighbourhood of an arc α contained in K, and so $B = \alpha \times D^2$; $B \times I$ is then attached along $D^2 \times \partial(\alpha \times I)$. In this case the handle is attached to a connected sum of K with itself.

By putting everything together, we obtain the following.

Proof of Theorem 1.40. Pass to the cyclic cover $\widetilde{M}$, and consider $N = \widetilde{f}^{-1}([0,1])$. We assume that 0 is not the image of any vertex, and that vertices have distinct images under $\tilde{f}$ (both can be achieved with a small perturbation). We want to study N by using the sublevels of $\widetilde{f}$.

Let $0 < a_1 < \cdots < a_k < 1$ be real numbers such that $\widetilde{f}^{-1}((a_i, a_{i+1}])$ contains exactly a vertex.

By Proposition 1.36, the sublevel $M_{\leq a_{i+1}}$ collapses to $M_{\leq a_i}$ with the descending link of the vertex coned off; by passing to a regular neighbourhood, we obtain that $M_{\leq a_{i+1}}$ is PL homeomorphic to $M_{\leq a_i}$ with a PL ball B attached along some submanifold C of $f^{-1}(a_i)$ which is a neighbourhood of the descending link. So we obtain that:

- either v is regular, and so C is collapsible;
- or v is non-degenerate critical of index i, so C collapses to an $(i-1)$-sphere.

By Lemma 1.41, the map $\widetilde{f}$ produces a relative PL handle decomposition, that is, we are describing N as $\widetilde{f}^{-1}([0, \varepsilon])$ with some handles attached. Indeed, when we cross the sublevel of a critical vertex, we are attaching a PL handle.

Note that these handles are always contained in the interior of N, as there are no critical points on the boundary. By Theorem 1.38, this handle decomposition can be made smooth, and can be turned into a Morse function $\widetilde{g} : N \to [0, 1]$. By gluing back the boundaries $\widetilde{f}^{-1}(0)$ and $\widetilde{f}^{-1}(1)$ we obtain our desired smooth circle-valued map. □

2

From cellular cocycles to Morse functions

The aim of this chapter is to describe a simple procedure to construct, given a cellular cocycle on some affine cell complex, a circle-valued Morse function of which we can compute the descending links.

For the whole chapter, we let X denote an affine cell complex, which is always tacitly assumed to be connected.

We fix an arbitrary orientation on each cell of X. Associated to X we have the cellular cochain complex $C^\bullet(X, R)$ with coefficients in the ring $R = \mathbb{R}, \mathbb{Z}$, and we denote by $Z^\bullet(X, R)$ and $B^\bullet(X, R)$ the cocycles and coboundaries respectively. Finally, we denote by $H^\bullet(X, R) = Z^\bullet(X, R)/B^\bullet(X, R)$ the cellular cohomology of X. If no ring of coefficients is specified, real coefficients are assumed.

Our focus is primarily on 1-cocycles. We have the inclusions $Z^1(X, \mathbb{Z}) \subset Z^1(X, \mathbb{R})$ and $H^1(X, \mathbb{Z}) \subset H^1(X, \mathbb{R})$; the elements in $Z^1(X, \mathbb{Z})$ and $H^1(X, \mathbb{Z})$ are called *integral cellular* 1*-cocycles* and *integral classes*.

Recall, by using the universal coefficients theorem, that

$$H^1(X, \mathbb{Z}) = \mathrm{Hom}(H_1(X, \mathbb{Z}), \mathbb{Z}) = \mathrm{Hom}(\pi_1(X), \mathbb{Z}),$$

which in turn is equal to the set of continuous functions from X to S^1 up to homotopy. Therefore, any continuous map $f : X \to S^1$ represents an integral class $[f] \in H^1(X, \mathbb{Z})$.

2.1 Low barycentric affine extension

Let X be an affine cell complex, and let α be an integral cellular 1-cocycle. We want to define a PL function $f\colon X \to S^1$ such that $[f] = [\alpha]$.

Actually, we require a bit more. Let e be an edge of X, with an arbitrary orientation; denote by e_- and e_+ its endpoints, where the signs are chosen in such a way that $\partial e = e_+ - e_-$. Restrict f to e, and lift it to a map $\widetilde{f} : e \to \mathbb{R}$. The difference $\widetilde{f}(e_+) - \widetilde{f}(e_-)$ does not depend on the chosen lift; we denote it with $df(e)$. This defines a cellular 1-cocycle df; we require that f satisfies $df = \alpha$.

If we replace X with an affine cell complex Y whose cells are simplices, such a function can be constructed directly.

Lemma 2.1. *Let σ be an affine n-simplex with vertices $v_0, \dots, v_n$, and let $a_0, \dots, a_n$ be real numbers. There is a unique affine map $f\colon \sigma \to \mathbb{R}$ such that $f(v_i) = a_i$ for $i = 0, \dots, n$.*

Proof. Since every affine simplex is affinely equivalent to the standard simplex $\Delta^n \subset \mathbb{R}^{n+1}$, we can assume $\sigma = \Delta^n$. Since f is affine, it must satisfy

$$f(x_0, \dots, x_n) = a_0 x_0 + \dots + a_n x_n,$$

which in turn defines the required map. □

Lemma 2.2. *Let Y be a connected affine cell complex whose cells are simplices, and let α be a cellular 1-cocycle on Y representing an integral class in cohomology. There is a function $f\colon Y \to S^1$ which is affine on every simplex and satisfies $df = \alpha$.*

Such a function is unique up to post-composing by a rotation of S^1.

Proof. Pass to the universal cover $\widetilde{Y}$, where we pull back the cocycle α to a cocycle $\widetilde{\alpha}$.

We start by defining a real valued map $\widetilde{f}$ on the vertices of $\widetilde{Y}$. Fix a base vertex v_0, and pick any vertex v. Consider any path joining v_0 with v, which is a collection of oriented edges $\ell_1, \dots, \ell_k$. We define

$$\widetilde{f}(v) = \sum_i \widetilde{\alpha}(\ell_i),$$

which is the "integral" of $\widetilde{\alpha}$ over the path joining the two vertices. This does not depend on the chosen path, since $\widetilde{\alpha}$ is a cocycle and $\widetilde{Y}$ is simply connected.

We can extend $\widetilde{f}$ to the whole $\widetilde{Y}$, by using Lemma 2.1 on every simplex. Since α represents an integral class in cohomology, for every points $x, y \in Y$ with the same projection on Y, the difference $\widetilde{f}(x) - \widetilde{f}(y)$ is an integer. In particular $\widetilde{f}$ passes to the quotient, and yields a map $f\colon Y \to S^1$ which satisfies $df = \alpha$. □

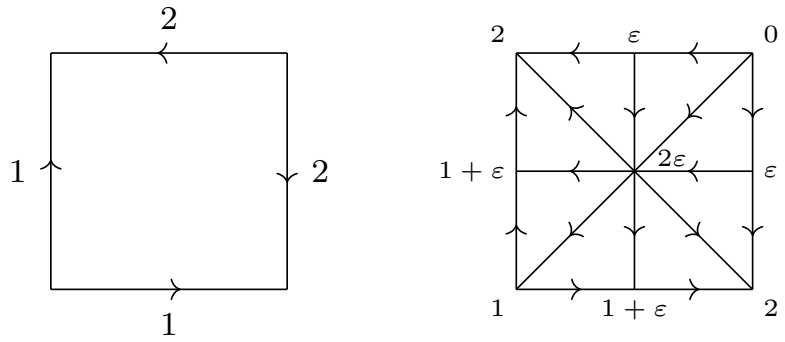

Figure 2.1: On the left, an integral 1-cocycle α on the square. On the right, a description of the low-barycentric affine extension f_α; the numbers near vertices denote the values of the lift of f_α.

Let us turn back to the general case of an affine cell complex X, equipped with an integral cellular cocycle α. To define a function $f : X \to S^1$ satisfying $df = \alpha$ we proceed as follows.

Notation. If X is an affine cell complex, we denote by $X^{(n)}$ the n-skeleton of X. In particular, $X^{(0)}$ denotes the set of vertices.

Fix a small $\varepsilon > 0$, and let σ be a cell of X. Let $g\colon \sigma^{(0)} \to \mathbb{R}$ be a 0-cocycle with $dg = \alpha$; such a g is unique up to a constant.

We now consider the barycentric subdivision $\operatorname{sd}\sigma$; for every non-empty face τ of σ we have the corresponding barycentre $\hat{\tau}$, which is a vertex of $\operatorname{sd}\sigma$. We want to extend g to a map $\hat{g}$ defined on all the vertices of $\operatorname{sd}\sigma$.

If τ is a k-dimensional cell contained in σ, we set

$$\hat{g}(\hat{\tau}) = \min\{g(v) : v \in \tau^{(0)}\} + k\varepsilon. \tag{1}$$

The map $\hat{g}$ induces a cellular 1-cocycle $d\hat{g}$ on $\operatorname{sd}\sigma$, which we denote by β_σ; for an example, see Figure 2.1.

Lemma 2.3. *Let $\tau < \sigma$ be two cells of X. Then β_τ is the restriction of β_σ to τ.*

Proof. Follows directly from the definition of $\hat{g}$. □

This implies that all the cellular 1-cocycles β_σ glue together nicely, giving rise to a cellular 1-cocycle β on $\operatorname{sd} X$. Note that by construction $[\beta] = [\alpha]$, so in particular β represents an integral class.

Definition 2.4. Let X be an affine cell complex, and let α be an integral cellular cocycle. We perform a barycentric subdivision $\operatorname{sd} X$ on X, on which we define an integral cellular 1-cocycle β as above.

We denote by f_α the circle-valued function on $\operatorname{sd} X$ obtained by applying Lemma 2.2 on the integral cellular 1-cocycle β; we call it the *low-barycentric affine extension* of α.

Remark 2.5. The reason behind this name is that the value of $\hat{g}$ on the barycentre of a cell σ is close to the minimum of g on the vertices of σ. One could similarly define a high-barycentric extension by putting the barycentre near the maximum, or a median version where one puts the barycentre at the average height of the vertices. While the latter seems more natural, the low-barycentric affine extension allows us to control well the descending and ascending links.

Lemma 2.6. *The low-barycentric affine extension of any integral cellular* 1*-cocycle* α *is Morse on* $\operatorname{sd} X$*.*

Proof. By construction, f_α is affine on every simplex of $\operatorname{sd} X$. Moreover, thanks to the small perturbation by ε, it is also non-constant on every edge and, therefore, on every cell. □

2.1.1 Ascending and descending links

As we have just seen, we can build a circle-valued Morse function f_α from an integral cellular 1-cocycle α on an affine cell complex X. In this section, we study the ascending and descending links of this function.

We must be careful that f_α is Morse on $\operatorname{sd} X$, and not on the original complex X. In particular, when v is a vertex of X, we need to distinguish between $\operatorname{Lk}(v, X)$ and $\operatorname{Lk}(v, \operatorname{sd} X)$, as they come with two different cell structures (the latter is the barycentric subdivision of the former).

Let us start by studying the structure of the link at a barycentre of a cell. To this purpose, the following regularity condition is helpful.

Definition 2.7. An affine cell complex X is *regular* if every cell is embedded in X.

If X is a regular affine cell complex, then $\operatorname{sd} X$ is a simplicial complex. This is not true without assuming regularity, as one can see by taking the 2-torus T with the cellularization with one vertex, two edges and one square: in this case, cells are not embedded in T, as all their vertices are mapped to the same point of T, and $\operatorname{sd} T$ is not simplicial.

Remark 2.8. Regularity is not a critical assumption, in the sense that all the following works without assuming regularity of affine cell complexes. However, regularity allows us to make some definitions clearer, and on the other hand we are not losing anything, as the affine cell complexes we are interested in are regular.

Let Y be a simplicial complex which, as we already observed, is naturally an affine cell complex; let $v \in Y$ be a vertex. For simplicial complexes, there is a notion of *simplicial star* and *simplicial link* of v: the former is the smallest subcomplex containing all simplices that contain v, while the latter is the subcomplex of the simplicial star made of simplices that do not contain v. The simplicial star and simplicial link satisfy the definition of star and link given in the PL setting.

For the following, we let X be a regular affine cell complex, and we consider its barycentric subdivision $\operatorname{sd} X$. Since $\operatorname{sd} X$ is a simplicial complex, the links and stars of its vertices are naturally embedded in $\operatorname{sd} X$ as simplicial stars and simplicial links respectively.

Definition 2.9. Let σ be a cell of a regular affine cell complex X. The *face link* of σ, denoted by $\mathrm{fLk}(\sigma)$, is the full subcomplex of $\mathrm{Lk}(\hat{\sigma}, \operatorname{sd} X)$ spanned by barycentres of faces of σ. Similarly, the *coface link* of σ is the full subcomplex of $\mathrm{Lk}(\hat{\sigma}, \operatorname{sd} X)$ spanned by barycentres of cofaces of σ, and is denoted by $\mathrm{cofLk}(\sigma)$.

The face link of σ is in particular the barycentric subdivision of $\partial\sigma$.

Lemma 2.10. *Let $\hat{\sigma}$ be the barycentre of a cell σ. Then $\mathrm{Lk}(\hat{\sigma}, \operatorname{sd} X)$ is the join of $\mathrm{fLk}(\sigma)$ and $\mathrm{cofLk}(\sigma)$.*

Proof. By definition of barycentric subdivision, the barycentres of a collection S of cells of X span a simplex in $\mathrm{Lk}(\hat{\sigma}, \operatorname{sd} X)$ if and only if $\sigma \notin S$ and $S \cup \{\sigma\}$ is totally ordered with respect to inclusion. We can therefore split $S = S^+ \cup S^-$, where $S^+ = \{\tau \in S : \tau > \sigma\}$ and $S^- = \{\tau \in S : \tau < \sigma\}$. Barycentres of cells in S^+ and S^- span simplices in $\mathrm{cofLk}(e)$ and $\mathrm{fLk}(e)$ respectively, which give the desired equality. □

We can therefore analyse the descending and ascending links by splitting them into two parts, as follows.

Definition 2.11. Let f be some real- or circle-valued Morse function on the barycentric subdivision $\operatorname{sd} X$ of a regular affine cell complex X, and let σ be a cell of X; its barycentre $\hat{\sigma}$ is a vertex of $\operatorname{sd} X$.

The *ascending/descending face link* of f at σ, denoted by $\mathrm{fLk}_{\uparrow/\downarrow}(\sigma; f)$, is the intersection $\mathrm{Lk}_{\uparrow/\downarrow}(\hat{\sigma}; f) \cap \mathrm{fLk}(\sigma)$. We define similarly the *ascending/descending coface link* as $\mathrm{cofLk}_{\uparrow/\downarrow}(\sigma; f) := \mathrm{Lk}_{\uparrow/\downarrow}(\hat{\sigma}; f) \cap \mathrm{cofLk}(\sigma)$.

Lemma 2.12. *The descending link* $\mathrm{Lk}_{\downarrow}(\hat{\sigma}; f)$ *at any barycentre* $\hat{\sigma}$ *is the join* $\mathrm{fLk}_{\downarrow}(\sigma; f) * \mathrm{cofLk}_{\downarrow}(\sigma; f)$. *Similarly,* $\mathrm{Lk}_{\uparrow}(\hat{\sigma}; f) = \mathrm{fLk}_{\uparrow}(\sigma; f) * \mathrm{cofLk}_{\uparrow}(\sigma; f)$.

Proof. Analogous to the proof of Lemma 2.10. □

From now on we consider only the low-barycentric affine extension f_α, obtained from an integral cellular cocycle α on a regular affine cell complex X; we will therefore omit specifying the function when referring to a link.

Definition 2.13. Let σ be a cell in a regular affine cell complex X, equipped with an integral cellular 1-cocycle α. Let $g\colon \sigma^{(0)} \to \mathbb{R}$ be such that $g(e_+) - g(e_-) = \alpha(e)$ for every oriented edge e of σ. We say that a vertex v of σ is:

- a *local minimum of* σ if $g(v) \leq g(w)$ for any vertex w of σ connected to v by an edge;
- a *global minimum* (or simply a *minimum*) *of* σ if $g(v) \leq g(w)$ for any vertex w of σ.

These two definitions do not depend on the choice of g, as it is unique up to a constant. Note that the map g is the same map that aided us in Definition 2.4.

Remark 2.14. Checking whether a vertex v is a local minimum of σ can be done directly by evaluating α on the edges of σ incident in v.

Lemma 2.15. *Let* $\tau < \sigma$ *be two cells of* X*, with their barycentre denoted by* $\hat{\sigma}$ *and* $\hat{\tau}$*. The following are equivalent:*

(1) $\hat{\sigma} \in \mathrm{cofLk}_{\uparrow}(\tau)$*;*

(2) $\hat{\tau} \in \mathrm{fLk}_{\downarrow}(\sigma)$*;*

(3) any minimum of τ *is also a minimum of* σ*.*

Proof. The equivalence between (1) and (2) follows from the definition.

By the definition of low-barycentric affine extension, since $\tau < \sigma$ and ε is small, the only way that $f_\alpha(\hat{\sigma}) > f_\alpha(\hat{\tau})$ is when the two minima coincide; this proves (1) $\Rightarrow$ (3). On the other hand, since $\dim \sigma > \dim \tau$, when the minima coincide we obtain by applying the definition that $f_\alpha(\hat{\sigma}) > f_\alpha(\hat{\tau})$ as desired. This concludes the equivalence with (3). □

This tells us that the descending face link of a cell σ is spanned by the barycentres of faces that contain a minimum of σ.

Ascending and descending face links are easy to compute in the cases which interest us. Whenever they are collapsible, we do not need to compute coface links, as we already know that the whole ascending and descending links are collapsible by Lemma 2.12. When this is not the case, however, we will need some tools to help us to compute ascending and descending coface links.

Computing the coface link of vertices is particularly important: in this case, the face link is empty, and the coface link is the whole link.

Let v be a vertex of a cell $\sigma \in X$. Suppose that $\hat{e} \in \mathrm{Lk}_\uparrow(v) = \mathrm{cofLk}_\uparrow(v)$ for every edge e in σ with endpoint v; it would be tempting to guess that $\hat{\sigma} \in \mathrm{Lk}_\uparrow v$, but this is in general not true, as it can be seen in Figure 2.1 (bottom left vertex).

The problem is that v is a local minimum, but not a global minimum. When the two notions coincide, the following holds.

Lemma 2.16. *Let X be a regular affine cell complex, equipped with the low-barycentric affine extension f_α. Let v be a vertex of a cell σ, and suppose that local minima of σ are global minima of σ. Then $\hat{\sigma} \in \mathrm{Lk}_\uparrow(v)$ if and only if v is a local minimum in σ.*

Proof. By applying Lemma 2.15 with $\tau = v$, we obtain that $\hat{\sigma} \in \mathrm{Lk}_\uparrow(v)$ if and only if v is a global minimum in σ, which is equivalent to v being a local minimum. □

This lemma can be generalized to barycentres of cells of any dimension.

Proposition 2.17. *Let X be a regular affine cell complex, equipped with the low-barycentric affine extension f_α. Suppose that every cell of X is a simple affine polytope, and suppose that in every cell of X local minima are global minima.*

Let $\tau < \sigma$ be two cells. Then $\widehat{\sigma} \in \mathrm{cofLk}_\uparrow(\tau)$ if and only if for every cofacet τ' of τ contained in σ, we have $\widehat{\tau'} \in \mathrm{cofLk}_\uparrow(\tau)$. Conversely, the barycentre $\widehat{\sigma} \in \mathrm{cofLk}_\downarrow(\tau)$ if and only if there is some cofacet of τ contained in σ whose barycentre is in $\mathrm{cofLk}_\downarrow(\tau)$.

This proposition tells us that we can calculate the ascending and descending coface link of a cell by only looking at cofacets.

Remark 2.18. The coface link of a cell σ is the barycentric subdivision of a cell complex Y, whose vertices correspond to cofacets of τ, and cells correspond to cofaces. Since cells are simple polytopes by assumption Y is a simplicial complex;

denote with $Y_\uparrow$ and $Y_\downarrow$ the full subcomplexes spanned by cofacets which have barycentre in $\mathrm{cofLk}_\uparrow(\sigma)$ and $\mathrm{cofLk}_\downarrow(\sigma)$ respectively.

In the setting above, by Proposition 2.17, the coface link $\mathrm{cofLk}_\uparrow(\sigma)$ coincides with the barycentric subdivision $\mathrm{sd}\, Y_\uparrow$, while $\mathrm{cofLk}_\downarrow(\sigma)$ is the first derived neighbourhood of $Y_\downarrow$; in particular, $\mathrm{cofLk}_\downarrow(\sigma)$ collapses on $\mathrm{sd}\, Y_\downarrow$.

These two simplicial complexes $Y_\uparrow$ and $Y_\downarrow$ are particularly easy to compute when $\sigma = v$ is a vertex. Choose the orientation of edges incident in v that points away from v. Then $Y_\uparrow$ is spanned by midpoints of edges e with $\alpha(e) \geq 0$, and $Y_\downarrow$ is spanned by midpoints of edges e with $\alpha(e) < 0$.

We conclude the section by proving Proposition 2.17.

Proof of Proposition 2.17. If $\hat{\sigma} \in \mathrm{cofLk}_\uparrow(\tau)$, then by Lemma 2.15 we have that minima of τ are also minima of σ, and therefore they are minima of all cofacets of τ contained in σ; this proves that all the barycentres of cofacets are in $\mathrm{cofLk}_\uparrow(\tau)$.

Vice versa, suppose that for every cofacet τ', contained in σ, we have that $\widehat{\tau'} \in \mathrm{cofLk}_\uparrow(\tau)$. Let v denote a minimum in τ.

We claim that v is a local minimum in σ. Indeed, let e be an edge in σ which has v as endpoint, with the orientation pointing away from v; if e is in τ, then $\alpha(e) \geq 0$ since v is a minimum in τ. Otherwise, since σ is simple, there is exactly one cofacet τ' of τ such that $e < \tau' < \sigma$; this is because $\mathrm{Lk}(v, \sigma)$ is a simplex, and τ' is the only face of σ satisfying $\mathrm{Lk}(v, \tau') = \mathrm{Lk}(v, e) * \mathrm{Lk}(v, \tau)$. Since v is a minimum in τ, by hypothesis and Lemma 2.15 it is also a minimum in τ', and therefore is a minimum in $e < \tau'$, i.e. we have that $\alpha(e) \geq 0$, as desired.

So v is a local minimum in σ, and therefore a global minimum. This implies, by Lemma 2.15, that $\hat{\sigma} \in \mathrm{cofLk}_\uparrow(\tau)$. □

2.1.2 Direct products and duality

We conclude the chapter by studying the behaviour of the low-barycentric extension on the products of affine cell complexes.

Suppose to have two affine cell complexes X and Y, each equipped with a 1-cocycle representing an integral class denoted respectively with α and β. The product $X \times Y$ has a natural structure of affine cell complex; denote by $\pi_X \colon X \times Y \to X$ and $\pi_Y \colon X \times Y \to Y$ the projections.

We can pull back α and β to cocycles $\pi_X^*(\alpha)$ and $\pi_Y^*(\beta)$ of $X \times Y$; we denote with γ the sum of these two cocycles.

We are now interested in the low-barycentric affine extension of γ in $X \times Y$. We have the following.

Lemma 2.19. *The low-barycentric affine extension f_γ coincides with $f_\alpha \circ \pi_X + f_\beta \circ \pi_Y$, where π_X, π_Y are the two projections.*

Proof. This is true on the 0-skeleton, as the sum is precisely the function whose differential is γ. The equality holds on the barycentres as well, since for any pair of cells $\sigma \in X$, $\tau \in Y$ we have that

$$\begin{aligned}\min\{f_\gamma(v \times w) : v \in \sigma^{(0)}, w \in \tau^{(0)}\} = \quad & \min\{f_\alpha(v) : v \in \sigma^{(0)}\} \\ & + \min\{f_\beta(w) : w \in \tau^{(0)}\}\end{aligned}$$

and $\dim(\sigma \times \tau) = \dim \sigma + \dim \tau$. □

We would like to understand the relationship between the descending face link of a product cell $\sigma \times \tau$ and the descending face links of σ and τ. It turns out that it becomes clearer if one considers the dual.

Recall from Section 1.1.2 that given some affine polytope P of dimension n, one can construct its dual P^*.

The barycentric subdivision of the boundary, denoted with $\operatorname{sd} \partial P$, can be defined in terms of the face lattice $\Phi(P)$: vertices correspond to proper faces of P, and cells correspond to chains, i.e. totally ordered subsets of $\Phi(P)$. In particular, if P and Q are combinatorially isomorphic, then $\operatorname{sd} \partial P$ and $\operatorname{sd} \partial Q$ are isomorphic simplicial complexes.

This holds even if the isomorphism between the lattices reverses inclusions: in particular, we have that $\operatorname{sd} \partial P$ and $\operatorname{sd} \partial P^*$ are isomorphic.

Given two polytopes P and Q, there are two natural ways to construct a higher-dimensional polytope. The first one is just taking the product $P \times Q$, while the second is the join $P * Q$, intended as follows.

Let n and m denote the dimension of P and Q respectively, and embed $P \hookrightarrow \mathbb{R}^n$, $Q \hookrightarrow \mathbb{R}^m$ in such a way that the origins are in the interior of the polytopes. Then one can embed them both in $\mathbb{R}^{n+m}$ via the inclusions $\mathbb{R}^n \times \{0\} \hookrightarrow \mathbb{R}^{n+m}$ and $\{0\} \times \mathbb{R}^m \hookrightarrow \mathbb{R}^{n+m}$, and then take the convex hull. We denote the polytope obtained in this way by $P * Q$, with a slight abuse of notation: to be precise, we should say that its boundary is the join of ∂P and ∂Q.

One can study the face lattices of these two objects: let us start from the direct product. Its non-empty faces are of the form $F \times F'$, and so are in correspondence

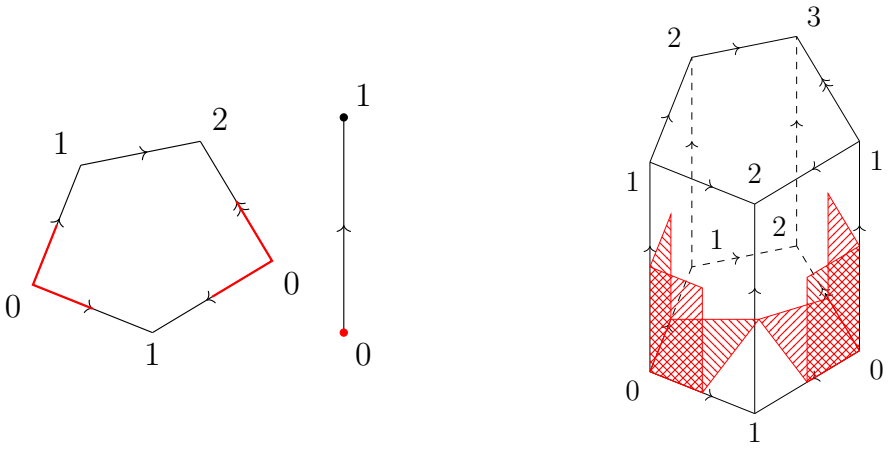

Figure 2.2: On the left, the descending link of a pentagon and of an interval, both in red: they are the full subcomplexes generated by barycentres of cells containing a minimum. On the right, the descending link of the product. It can be noted that the descending link on the right is isomorphic to a subdivision of the join of the ones on the left.

with the pairs (F, F') where F and F' are non-empty faces of P and Q respectively. Here *non-empty* is crucial: all the pairs $(F, \varnothing)$ and $(\varnothing, F')$ get mapped to the same, empty face of $P \times Q$, while the top face $P \times Q$ comes naturally from the pair (P, Q).

The situation is reversed when considering the join $P * Q$: its faces are naturally of the form $F * F'$, where F and F' may be empty (these correspond to the copies of P and Q inside $P * Q$). However, we do not have facets of the form $P * F'$ and $F * Q$.

In particular, we have the following:

Lemma 2.20. *If P and Q are two polytopes, then $(P \times Q)^*$ and $P^* * Q^*$ are combinatorially isomorphic polytopes. This produces an isomorphism between $\operatorname{sd} \partial(P \times Q)$ and $\operatorname{sd} \partial(P^* * Q^*)$.*

Proof. If F and F' are non-empty faces of P and Q, one can map $F \times F'$ to $F^* * F'^*$. This is a bijection which reverses inclusions, so it produces an isomorphism of posets between $(P \times Q)^*$ and $P^* * Q^*$. □

Now, suppose that σ and τ are cells of X and Y. The descending face link $\mathrm{fLk}_\downarrow(\sigma \times \tau)$ is a subcomplex of $\operatorname{sd} \partial(\sigma \times \tau)$, which by what we said above is isomorphic to $\operatorname{sd} \partial(\sigma \times \tau)^* \cong \operatorname{sd} \partial(\sigma^* * \tau^*)$.

We are now ready to state the following:

Proposition 2.21. *The descending face link* $\mathrm{fLk}_{\downarrow}(\sigma \times \tau)$ *is isomorphic to a subdivision of the join* $\mathrm{fLk}_{\downarrow}(\sigma) * \mathrm{fLk}_{\downarrow}(\tau)$.

In Figure 2.2 we can see an example, where σ is a pentagon and τ is a segment.

Proof. Descending face links of σ and τ are the barycentric subdivision of subcomplexes of $Z \subseteq \sigma^*$, $Z' \subseteq \tau^*$, since if the barycentre of a face $F < \sigma$ belongs to $\mathrm{fLk}_{\downarrow}(\sigma)$, then all barycentres of cofaces of F do (and the same holds for τ).

The barycentre of a face $F \times F'$ belongs to $\mathrm{fLk}_{\downarrow}(\sigma \times \tau)$ if and only if it contains a minimum $v \times w$ of $\sigma \times \tau$. This holds if and only if F contains a minimum v of σ and F' contains a minimum w of τ, which is in turn equivalent to both the barycentres of F and F' belonging to the descending link of σ and τ respectively.

So $\mathrm{fLk}_{\downarrow}(\sigma \times \tau)$ is the barycentric subdivision of $Z * Z'$, so it is a subdivision of $\mathrm{sd}\, Z * \mathrm{sd}\, Z' = \mathrm{fLk}_{\downarrow}(\sigma) * \mathrm{fLk}_{\downarrow}(\tau)$. □

3

Constructing manifolds from polytopes

In this chapter, we review the work of Jankiewicz, Norin and Wise [JNW19] in which they build a manifold equipped with a circle-valued Bestvina-Brady Morse function starting from some right-angled polytope.

We have already defined affine polytopes inside $\mathbb{R}^n$: we now see the analogous definition for the hyperbolic space.

Definition 3.1. A hyperbolic polytope is a finite-volume intersection of a finite collection of half-spaces inside $\mathbb{H}^n$.

Note that hyperbolic polytopes are not necessarily bounded; they are only finite-volume. It is still true that hyperbolic polytopes are the convex hull of a finite number of points, with the caveat that some of these points may be at infinity; these are called ideal vertices.

The faces of a hyperbolic polytope are defined as the intersection of P with its supporting hyperplanes, i.e. boundaries of half-spaces containing P. However, be careful that we defined a polytope as a subset of $\mathbb{H}^n$, and not of the closure $\overline{\mathbb{H}^n}$. In particular, *ideal vertices are not faces*.

For the same reason, by boundary of a hyperbolic polytope we intend its boundary inside $\mathbb{H}^n$, so the boundary is a sphere with (possibly none) punctures, with one puncture for each ideal vertex.

We employ the same terms used for affine polytopes to refer to faces of various dimensions: facets, ridges, and edges. We refer to 0-dimensional faces as *finite vertices*, to emphasize the fact that they are points in $\mathbb{H}^n$, and to distinguish them from ideal vertices. The definitions of face lattice, adjacent faces, and simple polytope carry out to hyperbolic polytopes without modifications.

Remark 3.2. In a 2-dimensional polygon, two edges that are incident in the same ideal vertex are not adjacent: we must only look at their intersection inside $\mathbb{H}^2$, which is empty.

Remark 3.3. An affine 3-dimensional octahedron is not simple, as four faces intersect in a vertex, which has codimension 3. However, an ideal hyperbolic octahedron, i.e. an octahedron where all vertices are ideal, is indeed simple; now four faces are incident in an ideal vertex, so their intersection in $\mathbb{H}^3$ is empty, which is allowed by the definition of simple.

We would like to have some notion of duality for hyperbolic polytopes. Let P be a hyperbolic polytope; one can always give P a Euclidean structure, by looking at P with the Klein coordinates of the hyperbolic space. This model identifies the hyperbolic space with the open unit ball B^n, sending hyperbolic hyperplanes to affine hyperplanes intersected with B^n. This allows us to interpret P as an affine polytope, that we denote by $\overline{P}$ since it is obtained from P by adding its ideal vertices. From $\overline{P}$ one can construct a dual affine polytope Q.

Dual to an ideal vertex v of P there is a facet of Q. However, v is not a face of the hyperbolic polytope P: this information should be preserved when passing to the dual. This motivates the following definition.

Definition 3.4. Let P be a hyperbolic polytope. Let Q be an affine polytope, with possibly some facets marked as *ideal*. We say that P is *dual* to Q if $\overline{P}$ and Q are dual as affine polytopes, and the duality maps ideal vertices of P to ideal facets of Q.

Moreover, if Q is an affine polytope with ideal facets, we define its *boundary* as the subcomplex of all proper faces of Q, excluding ideal facets.

We denote with P^* a dual of a hyperbolic polytope P. Similarly to affine polytopes, this is only well-defined up to combinatorial isomorphism, but this is not a problem since we are only interested in its cell structure.

When P is simple, its dual has a nice description as simplicial complex.

Proposition 3.5. *Let P be a simple hyperbolic polytope. The boundary of its dual P^* is a simplicial complex, whose vertices correspond to facets of P, and whose k-simplices correspond to $k+1$ pairwise intersecting facets.*

Example 3.6. Let P be a hyperbolic octahedron with ideal vertices. In this case the dual P^* is a cube, with all its facets marked as ideal. Therefore, the boundary ∂P^* is the 1-skeleton of the cube (and is in particular a simplicial complex).

3.1 The algorithm

Given some hyperbolic polytope, we plan to give it some additional combinatorial structure in order to build a manifold equipped a Morse function.

3.1.1 Colourings

Let P be a polytope.

Definition 3.7. Let $\mathcal{F}$ denote the set of facets of P, and let $\mathcal{C}$ be a finite set of cardinality k, which we call *palette of colours* and whose elements we call *colours*. A *k-colouring* for P is a surjective map $c\colon \mathcal{F} \to \mathcal{C}$, satisfying the following property: whenever $F, F' \in \mathcal{F}$ are two adjacent facets, then $c(F) \neq c(F')$.

We are only interested in the way a colouring partitions the set of facets: in particular, two colourings $c\colon \mathcal{F} \to \mathcal{C}$ and $c'\colon \mathcal{F} \to \mathcal{C}'$ are considered to be equivalent if there is some bijection of the colours $\varphi\colon \mathcal{C} \to \mathcal{C}'$ satisfying $c' = \varphi \circ c$. From now on, all colourings will be considered up to equivalence.

Usually, we will have $[k] = \{1, \dots, k\}$ as palette of colours, although any finite set is fine.

Let us give some examples to fix ideas.

Example 3.8 (Trivial colouring)**.** Let P be any polytope. The identity $\mathrm{id}\colon \mathcal{F} \to \mathcal{F}$ is a valid colouring, where we are colouring all the facets with different colours. If one prefers using $[k]$ as palette of colours, one can equivalently choose any numbering of the facets and map each facet to the corresponding number.

Example 3.9. Let P be the n-cube $[0,1]^n$, as in Figure 3.1, left. There exists exactly an n-colouring up to equivalence, which can be defined by sending the facets $\{x_i = 0\}, \{x_i = 1\}$ to the colour i.

Example 3.10. Let P be an ideal hyperbolic n-gon, as in Figure 3.1, right. The 1-colouring sending every facet to the same colour is valid, since no two facets are adjacent (see Remark 3.2).

Now that we have got a grasp of what is a colouring, we are ready to use it to produce manifolds.

Let P be a right-angled hyperbolic n-polytope, meaning that whenever two facets are adjacent, they intersect orthogonally. In particular, the polytope P

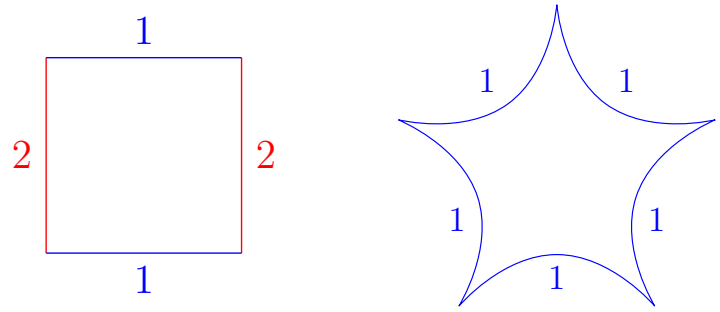

Figure 3.1: On the left, the only 2-colouring of the square; on the right, the constant colouring on a hyperbolic pentagon.

is simple, since the intersection of k pairwise orthogonal hyperplanes has always codimension k.

Let $k \in \mathbb{N}$, let $c\colon \mathcal{F} \to \mathcal{C}$ be a k-colouring, and let V denote the vector space $\mathbb{F}_2^{\mathcal{C}}$ over the field $\mathbb{F}_2$, which has a canonical basis $(e_i)_{i\in\mathcal{C}}$. For every $v \in V$ we consider a copy of P denoted by P_v, for a total of 2^k polytopes; these are all canonically isometric to P. We refer to this latter P as the *abstract* P, as it is the model of which the P_v are copies of.

We construct a manifold by taking

$$M = \bigsqcup \{P_v : v \in V\} /_{\sim},$$

where the equivalence relation is defined as follows. Let $x \in P_v$ and $y \in P_w$ be two points: then $x \sim y$ if and only if:

- x and y project to the same point in the abstract P,
- whenever the i-th component of v and w differ, then x and y must belong to a facet coloured with the colour i.

Intuitively, we are taking the disjoint copies of P and gluing together P_v with P_{v+e_i} by the identity along all the facets coloured with i. Another way to describe the same construction is that we take P and we consider its double along the facets coloured with the first colour; then we double again along the facets coloured with the second colour, and so on.

Proposition 3.11. *The space M is a complete finite-volume hyperbolic manifold.*

Proof. We use the Poincaré disk model for the hyperbolic space.

Let x be contained in the facets $F_1, \dots, F_m$ of P_v. Since the polytope is simple, then it is contained in the interior of an m-codimensional face. Since it is right-angled, we can embed P_v inside the orthant $\{x_i \geq 0 : i = 1, \dots, m\}$, sending x to the origin, and in such a way that the facet F_i is embedded inside $\{x_i = 0\}$. We may suppose that the palette of colours is $[k]$, and the colour of F_i is i.

By the definition of the equivalence relation, x is identified with the corresponding point in P_{v+w} for $w \in \mathbb{F}_2^m \subseteq \mathbb{F}_2^k$. We will therefore embed P_{v+w} in $\{(-1)^{w_i} x_i \geq 0, i = 1, \dots, m\}$ where the $\mathbb{F}_2$-component w_i is represented by either 0 or 1.

These embeddings pass to the quotient by $\sim$, and therefore map isometrically a neighbourhood of x inside M to a neighbourhood of the origin in $\mathbb{H}^n$.

Note also that, since we are gluing a finite number of finite-volume polytopes, the resulting manifold will be finite-volume (but may not be compact, if P was not compact to begin with). Completeness of M can be obtained from the completeness of P, by using the fact that all gluings are via the identity, so Cauchy sequences for M project to Cauchy sequences on P. □

We have constructed a hyperbolic manifold tessellated into copies of P. From this, one can construct its dual tessellation, with the following procedure.

Consider the barycentric subdivision of the tessellation. If σ is an m-dimensional cell of the tessellation, one can consider the subcomplex spanned by barycentres of cells $\tau \geq \sigma$; this is the cell dual to σ. The union of these dual cells forms a cell complex.

Since we are using right-angled polytopes, the dual tessellation happens to be a cube complex.

Proposition 3.12. *The dual tessellation is a cube complex C which is a* spine *of M, i.e. the manifold M deformation retracts on C.*

Proof. Consider an m-cell σ of this tessellation. Since P is right-angled, a neighbourhood of a point $x \in \sigma$ is necessarily of the form $\mathbb{R}^m \times \mathbb{R}^{n-m}$, where $\mathbb{R}^{n-m}$ is tessellated into the 2^{n-m} orthants. So F is dual to a $(n-m)$-cube; this proves the dual is a cube complex C.

By construction, the union of all dual cells is the union of all simplices of the barycentric subdivision which do not contain an ideal vertex. So the cube complex C tessellates $\bar{M}$, which is obtained from M by removing some neighbourhoods of the cusps, and it is a deformation retract of M. □

Note that C in general will not be homeomorphic to M. The cubulation C may not even be a manifold with boundary, as it may not be full-dimensional. For example, if P is the ideal n-gon in Example 3.10 with the constant colouring, then M is just the double of P, which is an n-punctured sphere, and the cubulation C is a graph with two vertices and n edges joining them.

3.1.2 States

Now that we know a straightforward way to build a manifold by attaching polytopes, we would like to define some circle-valued Morse function on it to study the topology. As we know from Chapter 2, we only need to define a cellular 1-cochain to obtain a Bestvina-Brady Morse function on the barycentric subdivision. The plan is to use the dual cubulation C for this.

To define the cocycle, we want to orient every edge of the cubulation, and put a positive weight on each. The weight will not play a very important role, as we will put unit weight on every edge (although by choosing different weights one could have some more freedom, it is not needed for our purposes). The crucial part is the choice of the orientation, as it will have a great impact on the ascending and descending links.

To define an orientation, we will observe an edge from the point of view of one of its endpoints. If e is an oriented edge, with endpoints e_+, e_- such that $\partial e = e_+ - e_-$, we say that the edge e is oriented *outwards* with respect to e_-, and *inwards* with respect to e_+.

This leads to the following definition.

Definition 3.13. Let P_v be some copy of P inside the tessellation of M, and let F be a facet of P_v. A *status* of F is the choice of a label which can be either I (for Inwards) or O (for Outwards). A *state* for P_v is the choice of a status for every facet of P_v.

The idea behind this definition is that dual to a face F of P_v there is an edge e of the cubulation, with a preferred endpoint (which is the barycentre of P_v). We orient the edge e outwards with respect to the barycentre of P_v if the status of F is O, and inwards of the status of F is I.

To define a cellular 1-cocycle on C, we need to choose a state on every polytope of the tessellation such that it satisfies the following two conditions.

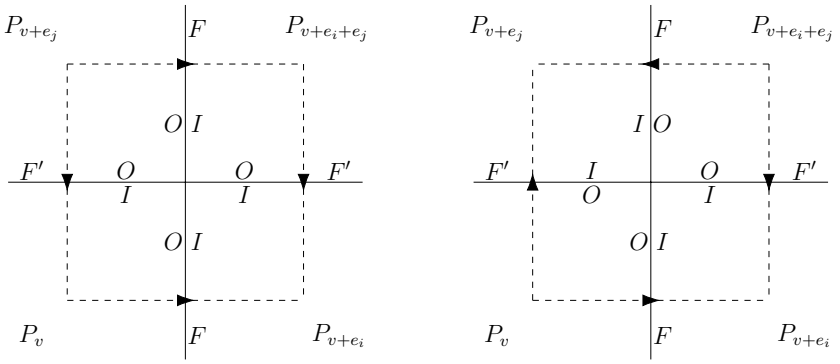

Figure 3.2: The two possible orientations on a square producing a 1-cocycle, up to rotation.

Consistency. Let F be a facet of P, coloured with the colour i. We require that the status of F in P_v is the opposite of the status of F in P_{v+e_i}.

Closedness. Let F, F' be two adjacent facets of P with colours i and j respectively (recall that $i \neq j$ by definition of colouring). For every $v \in \mathbb{F}_2^{\mathcal{C}}$ consider the status of F and F' inside P_v. We distinguish two cases:

- If F and F' have different status inside P_v, as in Figure 3.2 (left), then we require that the status of F' inside P_{v+e_i} coincides with the status of F' inside P_v, and similarly the status of F inside P_{v+e_j} must be the same as the status of F inside P_v.
- If F and F' have the same status, as in Figure 3.2 (right), then we only require that the status of F' inside P_{v+e_i} and of F inside P_{v+e_j} coincide.

Let us comment briefly on the geometric meaning behind these two combinatorial constraints. The first one simply assures that an edge inherits a well-defined orientation: since the polytopes P_v and P_{v+e_i} are attached along F, then the two glued facets of P_v and P_{v+e_i} are dual to the same edge of C, and the status of the two facets must yield the same orientation on it.

The second condition is in place to ensure that the constructed 1-cochain is a cocycle. When F and F' are adjacent, their intersection is dual to a square, and we need that the sum of the signed weights of the edges, read cyclically, yields zero. That only leaves two possibilities for the orientations, considering we are only using unit weights, which are the ones depicted in Figure 3.2 (up to rotation). The

one on the left has parallel edges oriented in the same direction, and we will refer to it as a *good square*. The one on the right will be instead referred as a *bad* square: this might cause the appearance of some non-collapsible descending links, as we will see later.

We obtain the following.

Lemma 3.14. *Let M be a manifold obtained from a colouring of a right-angled polytope, and suppose that we have a state on every polytope of the tessellation, satisfying consistency and closedness. This defines naturally an integral cellular 1-cocycle, where every edge has unit weight.*

3.1.3 Moves

To define states on every copy of P which satisfy both consistency and closedness, the plan is the following, inspired by [JNW19]. First, we choose some state on a fixed copy of P; then, we extend this state to all copies of P by using some rules which we are going to define.

Definition 3.15. A *set of moves* for P is a partition of the facets of P into subsets called *moves*, such that facets of the same colour belong to the same move.

Remark 3.16. This is a bit different from Jankiewicz, Norin and Wise's *system of moves*, which is a map $\mathcal{F} \to 2^{\mathcal{F}}$, where $\mathcal{F}$ denotes the set of facets, assigning to each facet F a subset of the facets m_F such that $F \in m_F$ and $F' \notin m_F$ for every F' adjacent to F.

A set of moves induces an assignment $F \mapsto m_F$, by defining m_F to be the element of the partition containing F; the condition about adjacent facets is however not guaranteed, so it does not necessarily produce a system of moves.

Since all facets of the same colour belong to the same move, a set of moves defines a partition of the available colours. Then it makes also sense to say that a colour belongs to a certain move.

Definition 3.17. A state is *compatible* with a set of moves if adjacent facets in the same move have the same status. A state is *balanced* if facets in the same move are adjacent if and only if they have the same status.

In particular, a balanced state is also compatible. Only compatibility is required for the construction to work; however, balancedness will make everything

more symmetric and ease computations, so in our examples most of the states will be chosen balanced.

Remark 3.18. A compatible state always exists (for example, put the same status to all the facets). The existence of a balanced state is not always guaranteed, as we need that the facets belonging to each move form one or two connected components which are cliques in the adjacency graph; the balanced status can be constructed assigning status I to the facets of a clique, and O to the facets of the other clique.

Given some set of moves $\mathcal{M}$, we choose a compatible state and we assign it to P_0 (where 0 is intended as a vector of $\mathbb{F}_2^{\mathcal{C}}$); this is called the *initial state*.

Each colour c acts on the set of all possible states on P by inverting the status of the facets in the move containing c. Since these actions commute, this defines an action of $\mathbb{F}_2^{\mathcal{C}}$ on the possible states: we assign to P_v the state obtained by acting with v on the initial state. We therefore call the set of states assigned to all the copies P_v of P the *orbit* of the initial state.

Lemma 3.19. *Let P_v be any copy of P, let $i \in \mathcal{C}$ be a colour and let F be a facet of P (of any colour). Then F in P_v has the same status of the analogue facet in P_{v+e_i} if and only if i does not belong to the same move as F.*

Proof. Since we are changing a single component of v, the state on P_{v+e_i} is obtained from the state on P_v by acting with the colour i; so the status of F changes if and only if i is the colour of some facet in the same move as F, which is exactly as required. □

More informally, this is equivalent to saying that when crossing some facet F, we invert the status of F and of all other facets belonging to the same move.

We give some examples to fix ideas.

Example 3.20. If the colouring is the trivial colouring, the set of moves can be any partition of the facets. If the set of moves is the partition of the facets into singletons, the orbit contains every possible assignment of I and O.

Example 3.21 (Chromatic set of moves)**.** The colouring itself is a valid set of moves, i.e. two facets are in the same move if and only if they are of the same colour. In this case, we have the additional property that adjacent faces are in different moves. However, not assuming this allows for more freedom and this will be crucial for our purpose. This is an important difference from [JNW19].

We call this set of moves the *chromatic set of moves*.

Recall that we started with a set of moves and a compatible state; we need to check that this property is preserved on the other copies.

Lemma 3.22. *Since the initial state is compatible, all the copies P_v inherit a compatible state. If the initial state is also balanced, then all copies inherit a balanced state, and in particular the states in the orbit are precisely all balanced states.*

Proof. If F and F' belong to the same move, then every colour acts by preserving or inverting the status of both F and F', so F and F' have the same status in P_v if and only if they had the same status in the initial state. This proves that both compatibility and balancedness are preserved by the action.

The only thing left to prove is that if we start from a balanced state, then all possible balanced states appear. This is because a balanced state, if there exists one, is uniquely determined by the status of some chosen facet for each move. In particular, by acting with $\mathbb{F}_2^{\mathcal{C}}$, we can let these chosen facets assume every possible configuration of status, and therefore obtain all the balanced states. □

Theorem 3.23. *Let P be a hyperbolic right-angled polytope, with a given colouring, set of moves and compatible initial state. The procedure described above defines a cellular 1-cocycle on the dual cubulation of M.*

Proof. We have a well-defined state on every copy of P, we only need to check that is satisfies the consistency and closedness conditions.

Consistency follows directly from Lemma 3.19, by applying it in the case where F is of colour i. Closedness also follows from the same lemma, but with slightly more work. Consider two adjacent facets F, F' of colours i, j in some P_v. We have two possibilities:

- If they belong to different moves, then the state of F in P_{v+e_j} coincides with the state of F in P_v, and the state of F' in P_{v+e_i} coincides with the state of F' in P_v; this is because j acts preserving the status of F, and i preserves the status of F'. This implies closedness, and the two edges form a *good square*.

- If they belong to the same move, by compatibility of the state they must have the same status. The colours i and j both act by inverting the status of F and F', so the status of F in P_{v+e_j} is opposite to the status of F in P_v, and similarly the status of F' in P_{v+e_i} is opposite to the state of F' in P_v. In particular, it follows that the status of F in P_{v+e_j} coincides with the status

of F' in P_{v+e_i}, as requested by the closedness condition. The two edges span a *bad square*. □

From Theorem 3.23 we get a cellular 1-cocycle, which can be promoted to Bestvina-Brady Morse function $f\colon C \to S^1$ via the low-barycentric affine extension studied in Chapter 2.

Remark 3.24. We described the algorithm only for hyperbolic polytopes, since they are the ones of interest to us. However, one may also start from an affine or spherical right-angled polytope, and the algorithm is still valid: of course, it will produce a flat or spherical manifold, instead of a hyperbolic one.

Remark 3.25. The interesting part of this structure is actually the set of moves. Suppose to have some colouring $c\colon \mathcal{F} \to \mathcal{C}$, some initial state S and some set of moves $\mathcal{M}$ that produce some manifold M, with a map $f\colon M \to S^1$. Replacing c with the trivial colouring, while keeping the same S and $\mathcal{M}$, yields a manifold N, which is a finite cover $\pi : N \to M$, with a map $g\colon N \to S^1$ such that $g = f \circ \pi$.

Therefore, one may always consider the trivial colouring, and the only price to pay is that the resulting manifold will be much larger.

3.2 Ascending and descending links

Given a hyperbolic right-angled polytope P, equipped with a colouring, an initial state and a set of moves, we want to study the ascending and descending links of the Bestvina-Brady map $f\colon \operatorname{sd} C \to S^1$ which arises from the algorithm. From now on, all ascending and descending links refer to this function, which is the low-barycentric affine extension of the cocycle obtained in Theorem 3.23.

Recall that the links at the barycentre of a cell split as a join of face and coface links, see Definitions 2.9 and 2.11 and Lemmas 2.10 and 2.12. We plan to use this to compute ascending and descending links.

3.2.1 Good and bad cubes

Let Q be an m-cube of the dual cubulation C. Let P_v be a copy of P which intersects Q: since P is simple, Q is dual to the intersection of m facets of P_v, which we denote with $F_1, \dots, F_m$.

We start by studying the face descending link $\mathrm{fLk}_\downarrow(Q)$, which we recall to be the intersection of the descending link at the barycentre of Q with Q itself, and we

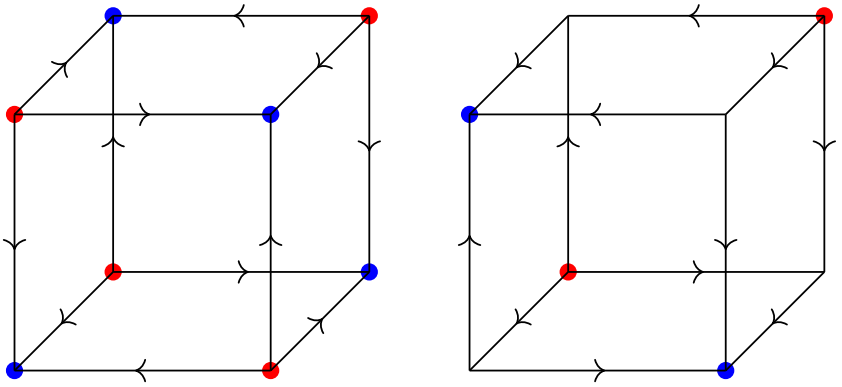

Figure 3.3: On the left, an irreducible cube, while on the right the product of an irreducible square with an interval. In both, the minima are in red while the maxima are in blue.

prove that it is collapsible under some conditions. By Lemma 2.12, collapsibility of the face descending link is enough to deduce that the whole descending link is collapsible, and this allows to skip the computation of the coface descending link.

Let us warm up considering the simple case where all the F_i belong to the same move (and $m \geq 1$). Then the edges of Q are all oriented in such a way that every square of Q is *bad*: at every vertex either every edge is oriented inwards or every edge is oriented outwards. We call this an *irreducible m-cube*; an example with $m = 3$ is depicted on the left of Figure 3.3.

Lemma 3.26. *If Q is an irreducible m-cube then $\mathrm{fLk}_{\uparrow}(Q)$ is the disjoint union of 2^{m-1} points, while $\mathrm{fLk}_{\downarrow}(Q)$ is homotopically equivalent to S^{m-1} with 2^{m-1} punctures.*

Proof. It suffices to prove the lemma for $\mathrm{fLk}_{\uparrow}(Q)$, as $\mathrm{fLk}_{\downarrow}(Q)$ is the complement (up to collapses) of the former inside the full $\mathrm{fLk}(Q)$ which is a PL $(m-1)$-sphere.

By Lemma 2.15, we know that a barycentre of a cell of the cube belongs to $\mathrm{fLk}_{\uparrow}(Q)$ if and only if the cell does not contain a minimum of Q (see Definition 2.13). Note that, by construction, the vertices are precisely split into 2^{m-1} minima and 2^{m-1} maxima, with every edge joining a minimum with a maximum, as in Figure 3.3, left. It follows that a cell does not contain a minimum if and only if it is 0-dimensional (a vertex) and it is a maximum, as desired. □

So an irreducible cube has collapsible $\mathrm{fLk}_{\uparrow}$ and $\mathrm{fLk}_{\downarrow}$ if and only if it is 1-dimensional, i.e. an interval.

We are now ready to see the general case in which $F_1, \dots, F_m$ do not necessarily belong to the same move. In this case, the moves partition the facets into some subsets, so we obtain that the cube Q is naturally a product of irreducible cubes, with the cocycle defined on it as in Section 2.1.2. We call these irreducible cubes the *factors* of Q. An example is depicted in Figure 3.3 (right).

Proposition 3.27. *The ascending and descending face links of Q are collapsible if and only if at least one of the factors is an interval.*

Proof. Since $Q = \prod Q_i$, with every Q_i being an irreducible cube, by Proposition 2.21 we know that $\mathrm{fLk}_\downarrow(Q)$ is a subdivision of the join of $\mathrm{fLk}_\downarrow(Q_i)$. Since a join is collapsible if one of the components is, we obtain that when one of the factors is the interval then ascending and descending links are collapsible.

Vice versa, we have that $1 - \chi(\mathrm{fLk}_\downarrow(Q)) = \prod_i (1 - \chi(\mathrm{fLk}_\downarrow(Q_i)))$ by the properties the join: since collapsible complexes have Euler characteristic equal to 1, if $\mathrm{fLk}_\downarrow(Q)$ is collapsible then at least one Q_i must have $\chi(\mathrm{fLk}_\downarrow(Q_i)) = 1$, and by Proposition 2.21 the cube Q_i must be an interval. □

Therefore, the only cubes in which a singularity may appear are the products of irreducible cubes of dimension ≥ 2. This leads to the following definition, which extends the notion of good and bad square to higher-dimensional cubes.

Definition 3.28. If one of the irreducible factors of Q is an interval, we say that Q is *good*, otherwise we say it is *bad*.

Whether a cube is good or bad is determined by how the set of moves partitions the facets $F_1, \dots F_m$. In particular, if two cubes are dual to cells in the tessellation that project to the same face of the abstract P, they are either both good or both bad. It makes sense to say that a face of P is *good* or *bad* if it is dual to good or bad cubes.

Proposition 3.29. *If the set of moves is the chromatic one, then all positive dimensional cubes are good, and therefore their barycentres have both ascending and descending link that are collapsible.*

Proof. Since there are no adjacent faces in the same move, all the factors are intervals, and therefore all positive-dimensional cubes have collapsible descending and ascending face link. This implies that the ascending and descending links at their barycentres are collapsible. □

Remark 3.30. Jankiewicz, Norin and Wise's original construction only produces good cubes. In their setting, all the theory developed in Chapter 2 was not needed, as in this case one can define a Morse function directly on the cubulation, without passing to the barycentric subdivision.

This discussion also makes sense for 0-dimensional cubes: in this case there are no factors, so by definition a 0-cube is always bad, and the face descending link is not collapsible (it is empty). This is why ascending and descending links of vertices of the cubulation are always to be checked with a different strategy.

3.2.2 Coface links of bad cubes

As we have just seen, whenever Q is bad, then $\mathrm{fLk}_\uparrow(Q)$ and $\mathrm{fLk}_\downarrow(Q)$ are not collapsible, and therefore we want to compute $\mathrm{cofLk}_\uparrow(Q)$ and $\mathrm{cofLk}_\downarrow(Q)$.

For the following, let v be a vertex of the cubulation, and P_v the corresponding copy of P. Note that we are using the same letter v to denote both a vector of $\mathbb{F}_2^{\mathcal{C}}$ and a vertex of the cubulation, but this is fine since there is a canonical correspondence between the two objects.

The state of P_v induces a labelling of vertices of the dual P^* with I and O. Recall from Proposition 3.5 that the boundary of P^*, with facets dual to ideal vertices removed, is a simplicial complex.

Definition 3.31. Let S be a state for P. The *descending* (resp. *ascending*) *link of* S is the full subcomplex of the boundary of P^* spanned by vertices dual to facets with status I (resp. O).

The reasoning behind this definition is immediately clear.

Proposition 3.32. *Let v be a vertex of the dual cubulation, dual to a copy P_v, which has state S. Then $\mathrm{Lk}_\uparrow(v)$ is the barycentric subdivision of the ascending link of S, while $\mathrm{Lk}_\downarrow(v)$ collapses on the barycentric subdivision of the descending link of S.*

Proof. This follows from Lemma 2.16, by noting that the ascending and descending link of S are by definition the subcomplexes denoted by $Y_\uparrow$ and $Y_\downarrow$ in Remark 2.18. The technical hypothesis of Lemma 2.16, requiring that local minima are global minima, is always satisfied for products of irreducible cubes. □

This provides a combinatorial way to compute ascending and descending links of a vertex v of the dual cubulation, up to collapse, by using only the state of P_v.

In particular, if all states of the orbit have collapsible ascending and descending links, then all vertices of the cubulation have collapsible ascending and descending link.

We would like to have a similar tool to compute coface ascending and descending links of higher dimensional cubes. To do so, we need to let faces of P inherit a state. Let us first introduce a standard definition, which generalizes the link of a vertex of a simplicial complex.

Definition 3.33. Let Y be a simplicial complex, and let $\sigma \in Y$ be a simplex. The *link* of σ is the subcomplex of Y made by all simplices τ such that $\sigma \cap \tau = \varnothing$ and $\sigma * \tau$ is a simplex in Y.

Let F be a face of P, which is the intersection of the facets $F_1, \dots, F_m$. If G is a facet of P which is adjacent to all the F_i, then $G' = F \cap G$ is a facet of F. This defines a bijection between facets of F and facets of P which are adjacent to all the F_i. This bijection preserves adjacency, so we have the following.

Lemma 3.34. *Let F be a face of P, and let σ be its dual simplex in the boundary of P^*. Then the boundary of F^* is canonically isomorphic as a simplicial complex to the link of σ in the boundary of P^*.*

Since we have associated a facet of P to each facet of F, we can define a state on F.

Definition 3.35. Let F be a face of P, which is the intersection of the facets $F_1, \dots, F_m$ of P. Let P be equipped with a state and a set of moves. If G' is a facet of F, call G the facet of P adjacent to all the F_i such that $G' = G \cap F$.

The *inherited state* on F is defined by assigning to every facet G' the status of G in P.

The *modified inherited state* is obtained from the inherited state by assigning the status O to a facet G' whenever G is in the same move as some F_i.

The inherited state is more natural; however, the modified inherited state is the one that makes the following proposition hold.

Lemma 3.36. *Let Q be a cube of the cubulation, and let v be a vertex of Q. Let P_v be its dual copy of P, equipped with a state and set of moves, and let F be the face of P which is dual to Q.*

The ascending and descending coface links of Q collapse on the barycentric subdivision of the ascending and descending links of the modified inherited state on F.

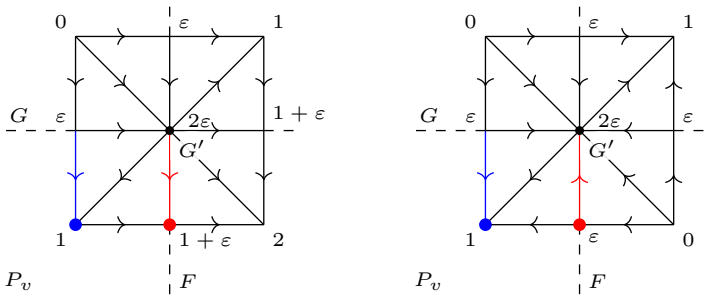

Figure 3.4: In this picture, we represented a cube of the cubulation: the blue vertex is the barycentre of P_v, and the blue edge is dual to a facet G of P_v with status I. When computing the coface link at the red vertex, which is the barycentre of a face F, we need to know the orientation of the red edge, corresponding to the status of the facet $G' = G \cap F$ of F. In the picture on the left, the square is good, so the orientation of the red edge coincides with the orientation of the blue one: the status of G' coincides with the status of G. Vice versa, on the right, we have a bad square: in this case, the red edge is always oriented outwards, so the status of G' is always O, independently of the status of G.

An intuition of why we need to change some status to O can be obtained by looking at Figure 3.4.

Before proving the proposition, we describe how to compute the modified inherited state operatively. The state on some P_v induces a labelling on the vertices of the dual P^*. A face F of P_v is dual to some simplex σ in P^*, and by Lemma 3.34 F^* embeds inside P^* as the link of σ. So F^* obtains a labelling of its vertices, by being a subcomplex of P^*: this is the *inherited state*. To obtain the *modified* inherited state, one must then override with status O all the vertices of F^* belonging to the same move as some vertex of σ.

Proof of Lemma 3.36. The coface link of Q is the barycentric subdivision of a simplicial complex whose vertices correspond to cofacets of Q, see Remark 2.18. This is isomorphic to the boundary of the dual F^*. By Proposition 2.17 it suffices to study which edges, connecting the barycentre of Q to the barycentre of a cofacet, are in the ascending link and which in the descending link.

Let Q' be the cube which is dual to a facet G' of F, so Q is a facet of Q'. Let G be the facet of P satisfying $G' = F \cap G$. If G is not in the same move as any of the F_i, then Q' factors as the product of Q and an interval, so the edge connecting the barycentre $\widehat{Q}$ to the barycentre $\widehat{Q'}$ is in the ascending link of $\widehat{Q}$ if and only if

the status of G is O, as in Figure 3.4, left.

If G is in the same move as some F_i, then Q always contains a minimum of Q' (see Figure 3.4, right); so the edge connecting $\widehat{Q}$ and $\widehat{Q'}$ is always in the ascending link of $\hat{Q}$. Therefore the modified inherited status has ascending and descending link which coincide to the subcomplexes denoted by $Y_\uparrow$ and $Y_\downarrow$ in Remark 2.18, and Proposition 2.17 allows us to conclude. □

We sum up the tools we have obtained to compute ascending and descending links with the following proposition.

Proposition 3.37. *Let F be a non-empty face of some copy P_v of P. The face F is dual to some cube Q of the cubulation, it is the intersection of some collection of facets $F_1, \dots, F_m$ of P_v, and it inherits a modified state S (see Definition 3.35).*

The ascending and descending link of the low-barycentric affine extension at the barycentre of Q is collapsible if at least one of the following holds:

- *there exists an F_i which is in a different move from F_j for every $j \neq i$, in which case Q is a good cube;*
- *the ascending and descending link of the state S are collapsible.*

Proof. If the first condition holds, collapsibility follows from Proposition 3.27. If the second condition holds, it follows from Lemma 3.36. □

3.2.3 The extended cubulation

So far, we were able to construct a Bestvina-Brady Morse function on the dual cube complex C: we would like to smoothen it to obtain a smooth Morse function.

However, as we already mentioned, the cubulation C is not a manifold with boundary, but it is just a spine of M: it might have some maximal $(n-1)$-dimensional cube separating two cusps. We want to extend C to another cubulation $\overline{C}$, which is a manifold with boundary whose interior is homeomorphic to M. To do so, we proceed as follows.

We take a right-angled hyperbolic polytope P, we choose colouring, set of moves and initial state. This produces a hyperbolic manifold M tessellated into copies of P. Its dual cubulation is denoted with C, and it has a low-barycentric affine extension $f\colon C \to S^1$.

For every cusp (that is, ideal vertex) c of P, draw a small horosphere around c. This way, the polytope P is subdivided into a truncation of P, which we denote

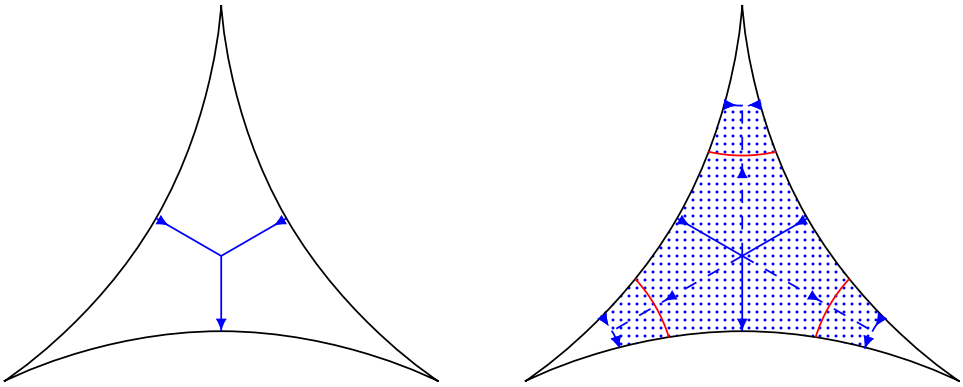

Figure 3.5: An ideal triangle, with the dual cube complex C in solid blue. If we cut with the red horospheres, the triangle is subdivided in a hexagon and three collars, and the extended cubulation, dual to this subdivided tessellation, is C with the addition of the dashed edges and the shaded squares. The dashed edges intersecting the horospheres are oriented towards the boundary, while the others have the same orientation as the edges in C to which they are parallel to.

by $\bar{P}$, and some collars of the cusps, which are a product of a Euclidean cube and $[0, \infty)$ and we denote with $\bar{P}^c$. These are not polytopes, since the horosphere is not totally geodesic, but they are still right-angled. If F is a face of P, we denote with $\bar{F}$ and $\bar{F}^c$ the pieces in which it is subdivided, where c denotes a cusp the face F is incident to.

Recall that M is tessellated by copies of P: if we make the above subdivision, the manifold is now tessellated into copies of $\bar{P}$ and collars. This new tessellation is dual to another cube complex $\overline{C}$, in which C is naturally embedded, as we can see from Figure 3.5. We call $\overline{C}$ the *extended cubulation*.

We want to orient edges of $\overline{C}$, and to do so we define states for the copies of $\bar{P}$ and for the collars. Every copy $\bar{P}_v$ has two kinds of facets: the ones of the form $\bar{F}$, where F is a facet of P_v, and the horospheres. We assign to $\bar{F}$ the same status of F in P_v, and to horospheres we assign status O.

We also need to assign a state for the collars $\bar{P}_v^c$ of P_v: similar to what we did for $\bar{P}$, we assign to facets of the form $\bar{F}^c$ the status of F in P_v, and to the horospheres status I.

This defines an integral cellular cocycle on $\overline{C}$, which in turn defines a low-barycentric affine extension $\bar{f}$ on $\overline{C}$; note that $\bar{f}\big|_C = f$.

We would like to compare ascending and descending links of $\bar{f}$ with ascending

and descending links of f: the key here is that the restriction on every boundary component of $\overline{C}$ should also be a fibration. This can be checked with the following combinatorial condition.

Definition 3.38. We say that a hyperbolic polytope P, equipped with a set of moves and a state, has *fibering cusps* if for every cusp c there is a pair of disjoint facets F, F' of P incident to c, which are in the same move and have opposite status. Moreover, we also ask that the other facets incident to c belong to moves different from the one containing F and F'.

Remark 3.39. Since P is right-angled, the intersection of P with a small horosphere around a cusp c combinatorially yields an $(n-1)$-cube. So the facets incident to c are partitioned into $n-1$ pairs of opposite facets, where two facets are adjacent if and only if they belong to different pairs.

We only need to check this fibering cusps condition on one copy P_v of P of the polytope (as it is naturally preserved when moving to other copies).

When P has fibering cusps, passing to the extended cubulation $\overline{C}$ does not produce significant changes: the homotopy type of the ascending and descending links is preserved, and the newly introduced vertices have collapsible ascending and descending links.

Proposition 3.40. *Suppose that P, equipped with an initial state, has fibering cusps. Let $f\colon C \to S^1$ be the Morse function produced by the algorithm, and let $\bar{f}\colon \overline{C} \to S^1$ be the extension to $\overline{C}$ obtained by truncating P, as above.*

Let v be the barycentre of some cube Q in $\overline{C}$.

- *If $Q \in C$, then $\mathrm{Lk}_\downarrow(v;\bar{f})$ and $\mathrm{Lk}_\uparrow(v;\bar{f})$ collapse on $\mathrm{Lk}_\downarrow(v;f)$ and $\mathrm{Lk}_\uparrow(v;f)$ respectively.*
- *If $Q \notin C$, then $\mathrm{Lk}_\downarrow(v;\bar{f})$ and $\mathrm{Lk}_\uparrow(v;\bar{f})$ are collapsible.*

Additionally, if $Q \in \partial\overline{C}$, then the restrictions to the boundary $\mathrm{Lk}_\downarrow(v,\partial\overline{C};\bar{f})$ and $\mathrm{Lk}_\uparrow(v,\partial\overline{C};\bar{f})$ are also collapsible.

Proof. First, if one copy of P satisfies the fibering cusps condition, then all of them do, since the moves either invert or preserve the status of both F and F'.

We now analyse the cubes of $\overline{C}$, depending on whether they are in the boundary, in a collar of the boundary, or in the original cube complex. Recall that $\overline{C}$ is

embedded inside M, so if two cells are dual then they are transverse and intersect in a point.

Boundary case. Let $Q \in \partial\overline{C}$, with barycentre $\hat{Q}$. Let P_v be a copy of P which intersects Q, so that one of the vertices of Q is dual to a collar $\bar{P}_v^c$, where c is a cusp of P_v.

By the fibering cusp condition, there are two facets F, F' of P_v which are incident to c, are in the same move and have opposite status, and such that all other facets incident to c are in different moves. There are two possibilities: either Q intersects F or F', or it intersects neither of them. It cannot intersect both as they are not adjacent.

In the first case, the cube Q is good, as it decomposes as $Q' \times I$, where the interval component corresponds to edges dual to either $\bar{F}^c$ or $\bar{F}'^c$, and Q' is some cube. This is because all other facets incident to c are in a move which is different from the one containing F and F'. By Proposition 3.27 ascending and descending links at the barycentre of Q are collapsible.

In the second case, let us restrict to the boundary component D of $\overline{C}$ containing Q. The subcomplex D is dual to a neighbourhood of the cusp, tessellated into copies of $\bar{P}^c$. The cube Q is dual to some face G of $\bar{P}_v^c$ which has some opposite facets of the form $G \cap F$ and $G \cap F'$. The face G has a modified inherited state from Definition 3.35, but since all other facets of P incident to c are in different moves from F and F' by hypothesis, this state assigns opposite states to $G \cap F$ and $G \cap F'$, and therefore the ascending and descending links collapse on the vertices dual to F and F'. By Lemma 3.36 we conclude that $\mathrm{cofLk}_\uparrow(Q)$ and $\mathrm{cofLk}_\downarrow(Q)$ are collapsible inside $\partial\overline{C}$.

We now compute the ascending and descending inside the whole $\overline{C}$. Since the facet of $\bar{P}_v^c$ contained in the horosphere has status I, we obtain that $\mathrm{Lk}_\uparrow(\hat{Q}, \partial\overline{C}) = \mathrm{Lk}_\uparrow(\hat{Q}, \overline{C})$, while $\mathrm{Lk}_\downarrow(\hat{Q}, \overline{C})$ is the cone of $\mathrm{Lk}_\downarrow(\hat{Q}, \partial\overline{C})$, so the ascending and descending links inside $\overline{C}$ are collapsible as well.

Collar case. The case where Q intersects the horosphere is straightforward: since all edges intersecting the horosphere are oriented towards the boundary, then Q is isomorphic to a good cube and by Proposition 3.27 we conclude.

Interior case. Finally, we need to study the links of the vertices contained in C. Good cubes remain good cubes, so if $\mathrm{fLk}_\downarrow(Q)$ was collapsible in C, then it is also collapsible in $\overline{C}$. Otherwise, suppose that Q is bad.

In the original cubulation C, the cube Q is dual to B, which is a bad face of some P_v, and inherits a modified state from P_v by Definition 3.35, which we denote

by S. We know from Lemma 3.36 that the ascending and descending coface links inside C collapse on the ascending and descending links of S.

However, now we are considering the extended cubulation $\overline{C}$: here Q is dual to the truncated face $\bar{B}$, which inherits a modified state $\bar{S}$. The state $\bar{S}$ is obtained from S by simply putting status O on the new facets, i.e. the facets contained in the horospheres, that appear after the truncation. We claim that the ascending and descending link of $\bar{S}$ collapse on ascending and descending link of S respectively.

Since we only added facets with status O, the descending link of $\bar{S}$ is the same as the descending link of S. The ascending link of $\bar{S}$ is obtained from the ascending link of S by adding, for every cusp c of B, a cone over the subcomplex of B^* spanned by vertices dual to facets of $\bar{B}$ which are adjacent to the cusp c and have status O.

Let G be the facet of $\bar{B}$ corresponding to the truncation near some cusp c. Denote with F, F' the facets incident to c which are provided from the fibering cusp condition. Since Q is bad, none of its edges can be dual to F or F', or otherwise by what we discussed for the case $Q \in \partial\overline{C}$ we would have that Q decomposes as $Q' \times I$. So G, which is combinatorially a cube, has two opposite facets which are contained in the facets F, F' of P_v.

Since exactly one of the facets $F \cap B$ and $F' \cap B$ of B has status O, by adding G we are adding to the ascending link of S the cone over a collapsible subcomplex. So the ascending link of $\bar{S}$ collapses on the ascending link of S; this implies that $\mathrm{Lk}_\uparrow(v; \bar{f})$ collapses on $\mathrm{Lk}_\uparrow(v; f)$. This is because coface ascending/descending links are appropriate neighbourhoods of the ascending/descending links of the state, see Proposition 2.17 and Lemma 3.36. □

Note that the fibering cusp condition is necessary: indeed, the following holds.

Proposition 3.41. *Suppose that some P_v has a cusp c such that all opposite facets adjacent to it are either in different moves or have the same status. Then the restriction $\bar{f}\big|_c$ is homotopic to a constant. In particular, f cannot be homotoped to a fibration.*

Proof. Consider the boundary component D of $\overline{C}$ corresponding to that cusp, which is a torus, dual to a neighbourhood of c tessellated into copies of $\bar{P}^c$.

Let ℓ be any geodesic curve which is also contained in the 1-skeleton of D (in particular, we require that ℓ is orthogonal to the standard coordinate system of the torus). Assuming that every cube has unit length, the curve ℓ has length two

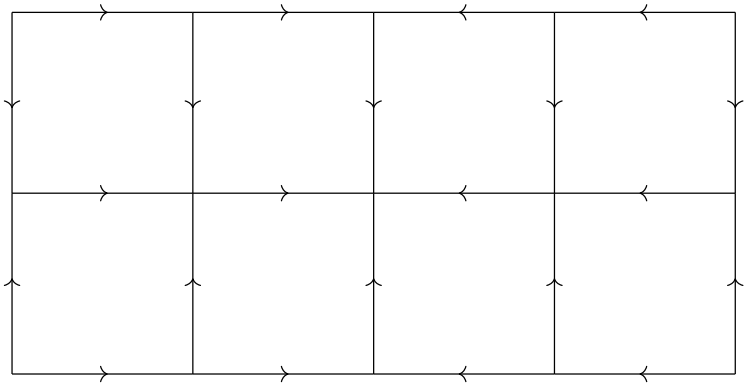

Figure 3.6: The two possible orientations on a square producing a 1-cocycle.

or four, depending on whether it is transverse to facets of $\bar{P}^c$ with the same or different colour.

If it has length two, the two facets have the same colour and are therefore in the same move. The curve will be as the vertical curves in Figure 3.6, since the facets have the same state by hypothesis, and in particular $\bar{f} \circ \ell$ will be null-homotopic. The case where they have different colours but are in the same move is similar.

If they are in different moves, then ℓ has length 4 and will be as the horizontal curves in Figure 3.6, which are null-homotopic as well.

We proved that the map $\bar{f}_* \colon H_1(D) \to \mathbb{Z}$ is trivial, so $\bar{f}\big|_c$ is null-homotopic.

Note that D is parallel to a subcomplex $D' \subset C$, which is another horosphere around c; so $D \cong D'$, and by construction $f|_{D'} = \bar{f}\big|_D$. Since a fibration must restrict by definition to a fibration on every cusp, this in particular means that the restriction to a horosphere cannot be homotopically trivial, and therefore f is not homotopic to a fibration. □

Putting everything together, we obtain the following.

Theorem 3.42. *Let P be a hyperbolic polytope, equipped with a colouring, a set of moves and a compatible initial state. The algorithm produces a manifold M tessellated into copies of P, whose dual is a cube complex C.*

Suppose that every vertex and bad cube of C has descending link which is either collapsible or collapses to a PL sphere; suppose also that P has fibering cusps.

Then M admits a smooth $f \colon M \to S^1$ which is Morse, which has critical points of index k in correspondence with the descending links which collapse to $(k-1)$-spheres.

In particular, if all links are collapsible, then f is a fibration.

Proof. Consider the extended cubulation $\overline{C}$, and construct the low-barycentric affine extension. By Proposition 3.40, we are not creating new critical vertices in doing so. Moreover, the restriction of f to $\partial\overline{C}$ is a fibration: by Theorem 1.40 we can smoothen this to a Morse function with the same critical vertices. □

4

Applications to hyperbolic manifolds

The aim of this chapter is to construct some circle-valued Morse functions on hyperbolic manifolds in various dimensions. The way we proceed is by considering a family of hyperbolic right-angled polytopes and applying the machinery we have developed in Chapter 3.

4.1 The polytopes P^n

Let us start by introducing the family of polytopes we are going to work with. The polytopes P^n are a family of right-angled hyperbolic polytopes, one in each dimension $2 \leq n \leq 8$. Their first appearance was in [ALR01], and later they were described by Potyagailo and Vinberg in [PV05].

We briefly report the idea behind the constructions of these polytopes. For every dimension $3 \leq n \leq 8$, there exists some Coxeter n-simplex with the property that some facet F has dihedral angle either $\frac{\pi}{2}$ or $\frac{\pi}{4}$ with all the others. The polytope P^n is then obtained by reflecting the simplex along all its facets except F. This way, after the reflections, these angles are doubled so they either become π and disappear, with the two adjacent facets merging into one, or become right.

As we can see by this construction, the resulting polytopes possess a huge quantity of symmetries. The first thing to note is that, for $n \geq 3$, every facet of P^n is isometric to P^{n-1} and the group of isometries acts transitively on the facets.

We will be interested in particular in the adjacency graph of P^n, as it will be useful to choose colourings, states and moves. Adjacency graphs can be viewed as the 1-skeleton of the dual affine polytopes, which form a family which was discovered by Gosset [Gos00]. We denote this polytopes with G^n.

The Gosset polytopes G^n have some facets which are hyperoctahedra, and they are dual to ideal vertices of P^n. If we remove these facets from the boundary of G^n, we obtain a simplicial complex (since P^n is simple), which has the additional property of being *flag*, i.e. whenever $k+1$ vertices are pairwise adjacent, they span a k-simplex.

So the structure of the Gosset polytopes is entirely encoded in their 1-skeleton, and there is a canonical bijection between $(n-k)$-faces of P^n and k-cliques in the adjacency graph.

Another important property of the Gosset polytopes is that the link of a $(k-1)$-simplex in the boundary of G^n is isomorphic to G^{n-k} for $n-k \leq 2$: this is a consequence of the fact that every k-codimensional face of P^n is isometric to P^{n-k}.

4.2 Some low-dimensional examples

Given this family of polytopes, we want to use it to construct some hyperbolic manifolds, together with a Bestvina-Brady Morse function, controlling the resulting ascending and descending links. One can find most of these examples on [IMM20] or [JNW19].

We briefly summarize the procedure described in the previous chapter. We start from a right-angled hyperbolic polytope P, and choose a colouring, a set of moves and a compatible initial state. This produces a hyperbolic manifold M tessellated into copies of P, with a state assigned to each. It also defines a piecewise-linear map $f\colon C \to S^1$, which is Morse on the barycentric subdivision of the dual cubulation C of M. We need to compute ascending and descending links of this map.

For every copy of P, we compute the ascending and descending link of its state, i.e. we consider the dual polytope P^*, which gets a labelling of its vertices from the state, and we take the full subcomplexes spanned by vertices with label I and O respectively. This is, up to collapses, the ascending and descending link of f at the barycentre of that copy of P.

If the set of moves coincides with the colouring, all the other barycentres have collapsible ascending and descending links by Proposition 3.29; this was called the chromatic set of moves. Otherwise, we need to check higher-dimensional cubes as well, by using Proposition 3.37. We proceed as follows.

We consider a face F of some copy of P; this is dual to some simplex σ of P^* (recall that since P is simple, P^* is simplicial). Vertices of P^* are dual to facets of P, so they have a move and status assigned.

If the simplex σ has a vertex whose move is different from the moves of all its other vertices, the face F is dual to a good cube, so we call the simplex *good*: the barycentre of F has collapsible ascending and descending links. Otherwise, we look at the link of σ, which is a subcomplex Y of P^* (see Definition 3.33). This is isomorphic to F^* by Lemma 3.34, and therefore we can use it to compute the modified inherited state on F, as in Definition 3.35. This just means that Y inherits a labelling of its vertices by being a subcomplex of P^*, and we modify it by putting an O to vertices which belong to the same move of some vertex of σ. Then we take the full subcomplexes of Y spanned by vertices with status O or I, and check whether they are collapsible.

Finally, if we want to produce a smooth Morse $f : M \to S^1$, we need to check the fibering cusp condition of Definition 3.38.

Remark 4.1. To describe colourings, states, and set of moves, we will usually depict the dual polytope P^*. Its vertices are dual to faces of the polytope P, and so we will assign colours, status, and moves to vertices of P^*.

We use dimension 3 to warm up, by giving also examples using polytopes different from P^3.

4.2.1 Ideal octahedron

We can consider the ideal hyperbolic octahedron, which is right-angled, and put on it the checkerboard colouration, as done in [JNW19]. As set of moves, we consider the chromatic set of moves.

The dual is the cube, with all squares dual to ideal vertices. We can take the initial state in Figure 4.1, upper left diagram. We obtain a hyperbolic manifold tessellated into four copies of the octahedron, which is the complement of the minimally twisted chain link with 6 components (see [KM13]) and the possible states are all depicted in Figure 4.1. Every label on a vertex in the picture determines the state of the corresponding dual facet.

Since we are using the chromatic set of moves, by Proposition 3.29, the only bad cubes are the vertices of the cube complex, so we only need to check that all the ascending and descending links of the states in the orbit are collapsible (see Definition 3.31).

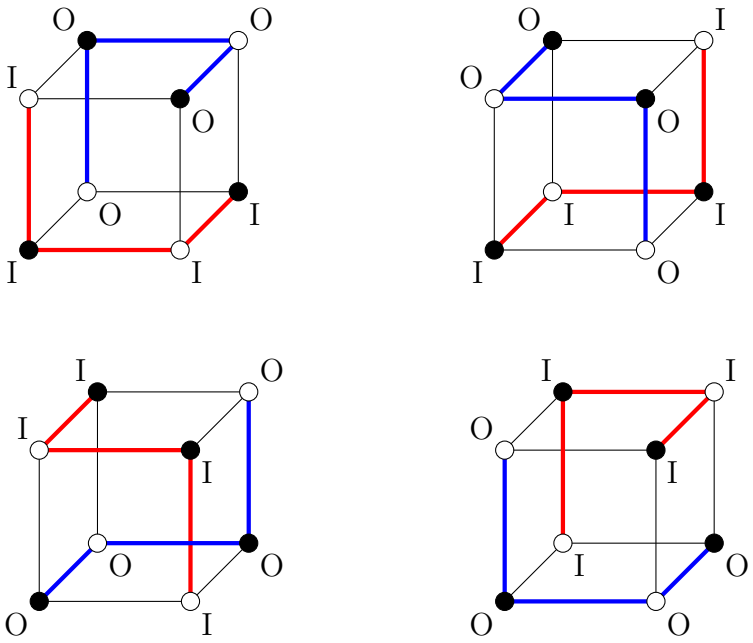

Figure 4.1: The states on the cube, which is the dual of the octahedron. Moving horizontally changes the state of the white vertices, while moving vertically changes the states of the black vertices. In blue and red the ascending and descending link of the states.

Recall that, to compute ascending and descending link of a state, one must consider the boundary of the dual polytope, with facets dual to ideal vertices removed. Then one should take the full subcomplex spanned by vertices dual facets with status O or I respectively. By looking at Figure 4.1, one can see that all these are intervals, with a cell structure with four vertices and three edges; in particular, they are collapsible.

It remains to check that the octahedron has fibering cusps. A square of the cube is dual to an ideal vertex of the octahedron, and the vertices of the square are dual to facets of the octahedron incident to that cusp. Note that every square has a pair of opposite vertices with the same colour and opposite status, and this guarantees the fibering cusp condition.

Having checked all the conditions, by Theorem 3.42, the resulting map to S^1 can be smoothened to a fibration.

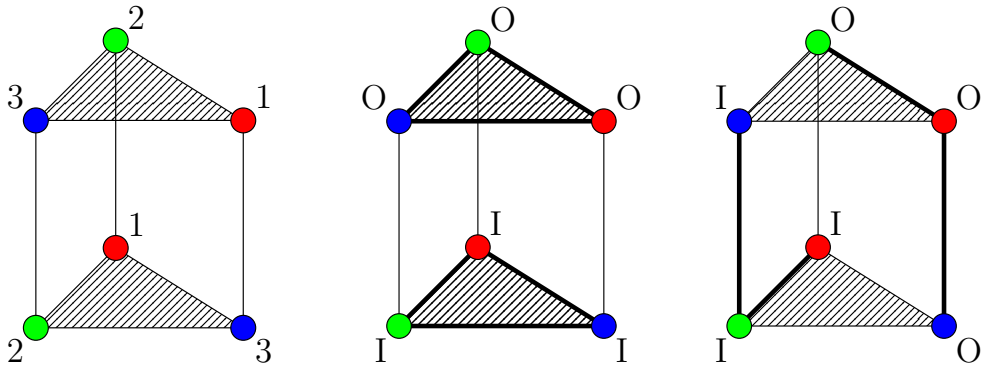

Figure 4.2: On the left, the colouring of the vertices of the triangular prism, dual to P^3. On the right, the two possible states, up to combinatorial isomorphism.

4.2.2 The polytope P^3

The polytope P^3 is the triangular bipyramid, with the three base vertices ideal and the two summits finite. The dual is the triangular prism G^3, which is shown in Figure 4.2 (left). The 3 cusps are dual to the three squares in the lateral surface of the prism. The bases are shaded to remind that the squares are removed from the boundary of the prism.

As before, we use the chromatic set of moves, and we put on P^3 the colouring and initial state given in Figure 4.2 (centre). Actually many choices of initial state were possible: we only need that they are balanced (see Definition 3.17).

By choosing any balanced state, we know by Lemma 3.22 that the orbit is precisely made of all balanced states, which are, up to symmetries of the polytope, the two depicted in the figure. Again one can check that the ascending and descending links are collapsible, and again the map can be smoothened to a fibration (after checking the fibering cusps condition). It is also possible to deduce that this manifold is the complement of the Borromean rings.

4.2.3 The hyperbolic dodecahedron

We now consider the right-angled hyperbolic dodecahedron, which is a compact polytope. The dual is the icosahedron.

The natural choice for the colouring would be the 6-colouring that assigns the same colour to opposite facets of the dodecahedron. Here we do something different, and we choose the 6-colouring in Figure 4.3. This time we are not taking

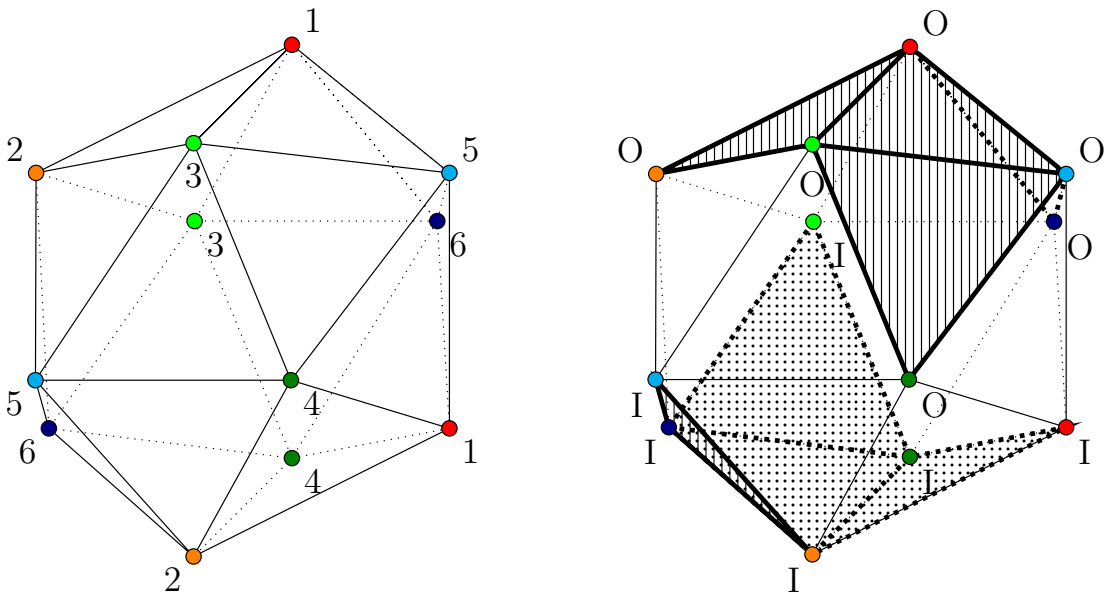

Figure 4.3: On the left, the colouring on the dodecahedron, represented by colouring the vertices of the dual icosahedron; on the right the choice for the initial state, with highlighted the ascending and descending links.

the chromatic set of moves: we partition the colours into three pairs, $(1, 2), (3, 4)$ and $(5, 6)$, which are conveniently associated to similar actual colours in the picture (red and orange, light green and dark green, blue and cyan), and each move is made of all the facets with a colour belonging to a pair, so we have partitioned the facets into three moves.

An example of a possible choice of initial state can be seen in Figure 4.3 (right). As before, any balanced state does the job, as the orbit will consist of all balanced states.

The perhaps surprising thing that happens is that all the ascending and descending links of the states of the cubulation are combinatorially isomorphic to the simplicial complex in Figure 4.4, which is collapsible. To see that they are all isomorphic, note that for each move $m \in \mathcal{M}$ there exists a reflection of the icosahedron which:

- fixes each move (as a set);
- sends vertices in m with status O to vertices with status I (and vice versa);
- preserves the statuses of the vertices of the other moves.

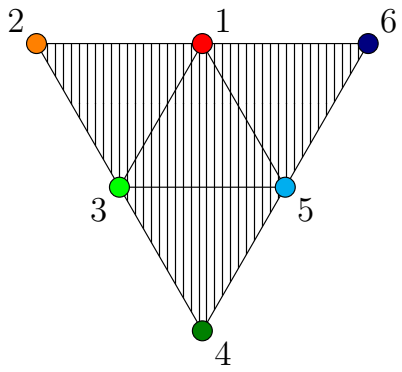

Figure 4.4: The ascending and descending link of all vertices of the cubulation, up to isomorphism.

For example, the reflection on the plane containing vertices with colours 3 and 4 fixes pointwise these vertices, sends the colour 1 to the colour 2 preserving the status and fixes the colours 5 and 6 inverting the status.

When we are crossing a facet of the dodecahedron, this corresponds to inverting the labels of the corresponding move; however, the new ascending and descending link will be the image of the former by the above-mentioned reflection, so they will be in particular combinatorially isomorphic.

Since we did not choose the chromatic set of moves, we need to check the bad cubes. Since all the simplices of the icosahedron have dimension at most 2, a bad simplex must be an edge, connecting two vertices in the same move. By checking them all by hand or by using the symmetries of the polytope to reduce computations, it turns out that the link of these edges of the icosahedron is two disconnected points of the same colour.

Since every state is balanced, those two points have opposite status, and hence both the ascending and descending coface links of the corresponding bad squares are collapsible. By Theorem 3.42 the resulting manifold fibers over the circle.

This construction, which seems to be coming a bit out of nowhere, is none other that the translation into the combinatorial setting of colours and moves of a construction by Thurston. We will see this better in Chapter 5, as it is similar to what happens in dimension 5.

4.2.4 The polytope P^4

The polytope P^4 is a 4-dimensional polytope with 10 facets, 5 cusps and 5 finite vertices. Its dual is the rectified 5-cell G^4.

The 1-skeleton of G^4 may be described as follows: the vertices V correspond to the set of the 10 unordered pairs in $\{1, 2, 3, 4, 5\}$, with an edge connecting two vertices if the corresponding pairs intersect in an element. There are five tetrahedra, dual to the finite vertices of P^4, and corresponding to the 4-cliques formed by the four pairs containing a certain element in $\{1, 2, 3, 4, 5\}$. We also have five octahedral facets of G^4, dual to the cusps of P^4 and whose vertices correspond to the six pairs *disjoint* from a fixed element. Note that every cusp is opposed to a real vertex, and every facet is incident to either the vertex or the cusp (but not to both).

Considering that we are in even dimension, our best hope is to find some hyperbolic manifold with a perfect-valued Morse function. This construction was due to [BM22].

With the identification of the facets with pairs of numbers in mind, we assign the same colour to the pairs $\{k, k+1\}$ and $\{k+2, k+4\}$ (where all numbers are intended modulo 5). We consider the chromatic set of moves, and as initial state, we take the one that assigns O to all facets corresponding to cyclically adjacent numbers, and I to the others (as usual, we could have chosen any other balanced state).

With some effort, one may show that most ascending and descending links are collapsible, save for the states isomorphic to the initial one. In this latter case, both ascending and descending links are circles, and this produces the Morse singularities of index 2. We leave the reader to [BM22] for details.

4.3 Constructions in higher dimension

Now that we have seen some examples we are ready to tackle the higher dimensional constructions. Since the polytopes are now harder to visualize, it will be convenient to have a deep understanding of the combinatorics of these polytopes, and to do so it turns out that we will also need to employ some algebraic tools, such as quaternions and octonions.

4.3.1 Dimension 5

With the techniques described in the previous chapter, we now build a hyperbolic 5-manifold M^5 fibering over S^1, starting from the right-angled hyperbolic polytope P^5, which we now describe following [RT03].

The polytope P^5 has 16 facets, 10 cusps and 16 finite vertices.

Although the high dimension does not help, P^5 has still a surprisingly intuitive geometric description. For the following, we see $\mathbb{H}^5$ with the Poincaré disk model.

Consider an ideal regular hyperbolic 5-hyperoctahedron, centred in the origin of the Poincaré disk, which has dihedral angles $\frac{2}{3}\pi$. By cutting along the coordinate planes, we can decompose it in 32 copies of a simplex Σ, which has all facets orthogonal to the axes except for one "diagonal" facet, which is also a facet of the hyperoctahedron.

Put the checkerboard colouring on the hyperoctahedron, and glue to every white facet another copy of Σ along the diagonal facets. Every ridge of the hyperoctahedron was incident to two copies of Σ; after the gluing operation, it is incident to three copies, so the dihedral angle becomes $\frac{2}{3}\pi + \frac{\pi}{3} = \pi$. Every black facet therefore merges with a facet of each of the five neighbouring Σ's we added, so in the end we obtain a polytope with 16 facets. Moreover, the ridges of this polytope are made by attaching two ridges of two copies of Σ, and the dihedral angle is right. This polytope, which is subdivided into 48 copies of Σ, is the right-angled hyperbolic polytope P^5.

We now describe the dual polytope G^5, which is the 5-demicube; in particular we write explicitly its 1-skeleton, as we know that it contains all the information about the polytope.

Since the facets of an ideal 5-hyperoctahedron are in natural correspondence with $\{1, -1\}^5$, and facets of P^5 are in bijection with black facets of the hyperoctahedron, it is natural to label the vertices of G^5 with the 5-uples $(\pm 1, \pm 1, \pm 1, \pm 1, \pm 1)$ with an even number of -1. Two vertices are adjacent if and only if their labels differ for exactly two components.

Remark 4.2. We can check that the link at any vertex of G^5 is indeed G^4: given some vertex v of G^5, the adjacent vertices are the ones that differ for exactly two components: therefore there is a correspondence between the vertices in $\mathrm{Lk}(v)$ and the unordered pairs in $\{1, 2, 3, 4, 5\}$, which are the labels assigned to the vertices of G^4.

The 4-simplices in G^5, dual to finite vertices of P^5, are in bijection with the

5-tuples $(\pm 1, \pm 1, \pm 1, \pm 1, \pm 1)$ with an odd number of minus signs, by sending every such tuple (x_i) to the simplex whose vertices are labelled with the tuples which differ from (x_i) for exactly one component. Again we have this opposition phenomenon we witnessed in P^4, but this time it is between facets and finite vertices of P^5: changing all the signs of the label of a facet F yields the label of a vertex v, and every other facet of P^5 is either adjacent to F or incident to v (but not both).

The 10 cusps are dual to some 4-hyperoctahedra in G^5: each 4-hyperoctahedron has 8 vertices, which are labelled with 5-tuples that all coincide on a component (note there is a choice from 5 components on which they may agree, and two possible values for each, for a total of 10 cusps). For example, the vertices of one of these 4-hyperoctahedra are all the ones with label of the form $(\pm 1, -1, \pm 1, \pm 1, \pm 1)$.

The isometries of P^5 are also very simple. They coincide with the symmetry group of the 5-demicube, which is an index 2 subgroup of the symmetries of the 5-cube. Precisely, it is the subgroup that preserves the checkerboard colouring on the vertices of the cube, so it is generated by compositions of an even number of reflections upon the coordinate hyperplanes, and by the isometries of $\mathbb{H}^5$ that permute the coordinates. It is indeed isomorphic to a semidirect product $(\mathbb{Z}/2\mathbb{Z})^4 \rtimes S_5$, which has order 1920.

Inside this group there is a particularly symmetric embedding of the quaternion group $Q_8 = \langle i, j, k : i^2 = j^2 = k^2 = -1,\ ij = -ji = k \rangle$. This is seen as follows: we may identify the ambient $\mathbb{R}^5$ in which the Poincaré disk is embedded as $\mathbf{H} \times \mathbb{R}$, where $\mathbf{H}$ here denotes the quaternions. This way, we can define a natural action of Q_8 by left multiplication on the first component.

To emphasize this action of Q_8, we also change the labels of the facets: we put on the facet labelled with $(\pm 1, \pm 1, \pm 1, \pm 1, \varepsilon)$ the label $\pm 1 \pm i \pm j \pm k$; doing this we are ignoring the last component, as it is determined by the other four thanks to the parity condition. With this new labelling, two facets are adjacent if their labels differ for one or two signs.

It is now natural to consider only a subgroup of the isometries of P^5, made by all the isometries that factor into the product of an isometry of $\mathbf{H}$ and an isometry of $\mathbb{R}$.

The group Q_8 acts on $\mathbf{H}$, and so acts on P^5 by isometries. In particular, it acts permuting the facets: this action coincides with the action by left-multiplication on the new labels, which preserves the parity of minus signs. Actually, the elements $Q_8 \cup \{\frac{1}{2}(\pm 1 \pm i \pm j \pm k)\}$ together form a group, called the *binary tetrahedral group*

and denoted with T_{24}, which is made of all the unitary elements inside the Hurwitz quaternions (see for example [CS03] for more details).

For the construction, we will use this quaternionic labelling of the facets, as it is the one that carries the most information on the symmetries which are of interest to us. The elements $\pm 1 \pm i \pm j \pm k$ can be placed on the vertices of a 4-dimensional hypercube, since they are naturally in bijection with $\{\pm 1\}^4$. However, the 1-skeleton of G^5 is bigger than the 1-skeleton of the hypercube: to obtain it, we should add all the diagonals of all the 2-dimensional squares contained in the hypercube (since two vertices are adjacent if they differ for at most two signs). This embedding of the 1-skeleton of the hypercube into the 1-skeleton of G^5 is not intrinsic, as it depends on the choice of the component we are "forgetting" (in our case, the fifth).

The first colouring. The most natural colouring appears to be the 8-colouring obtained by assigning the same colour to opposite vertices in the hypercube: that is, we are assigning the same colour to the facets with label t and $-t$ (where $t = \pm 1 \pm i \pm j \pm k$). Note that this notion of opposition is not intrinsic, as it depends on the embedding of the hypercube: in particular, every pair of non-adjacent facets is equivalent, meaning that there is an isometry sending one pair to the other. This is of course not a problem; it is just good to be aware that there is an actual choice involved.

The colouring is depicted in Figure 4.5. We consider the chromatic set of moves; as for the initial state, we choose any balanced state.

These were the colouring and moves considered in [IMM20]. There are $2^8 = 256$ states in the orbit, and for each state one has to compute the ascending and descending link, so the numbers start becoming big. Both checking by hand and with the help of a Sage program (which can be found at [Mar]), the possible states could be narrowed down to seven classes of combinatorial isomorphism, of which four have collapsible ascending and descending link, and the other states are subdivided in the following:

- 32 states that have ascending and descending link collapsing to S^2;
- 8 states that have ascending and descending link collapsing to S^3;
- 8 states that have ascending and descending link collapsing to a wedge of three circles.

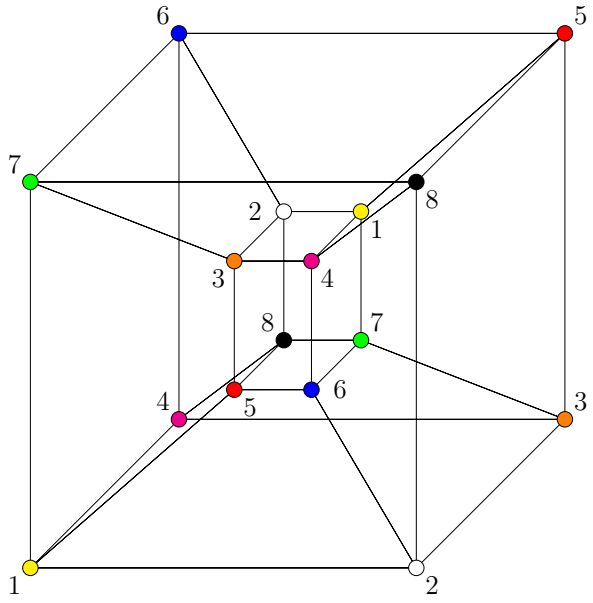

Figure 4.5: A colouring for P^5. The dual is represented here as a hypercube, but it is actually a 5-demicube. To obtain the 1-skeleton one should add all the diagonals of every square, which are not depicted for readability.

One can also double-check with the Euler characteristic: each S^3 contributes with a -1, each S^2 with a $+1$ and each $\bigvee_3 S^1$ with a -3, so we get

$$32 \cdot 1 + 8 \cdot (-1) + 8 \cdot (-3) = 0$$

as expected.

While the ascending and descending links are not all collapsible, they are at least all connected, so by Theorem 1.37 the induced map $f_*\colon \pi_1(M) \twoheadrightarrow \mathbb{Z}$ is surjective with finitely generated kernel, i.e. the map f is an algebraic fibration.

The second colouring It turns out that this result can be improved by considering the colouring shown in Table 1. As a palette of colours, instead of the usual integers, we consider the set Q_8 (the reasoning behind this will be apparent later). The colouring is also shown in Figure 4.6.

Here we consider the set of moves that partitions the facets of P^5 in four moves, each containing facets whose colour belongs to one of the following pairs: $\{1, -1\}$, $\{i, -i\}$, $\{j, -j\}$, $\{k, -k\}$. As the initial state we take any balanced state, as they are all equivalent by Lemma 3.22. A possible choice is pictured on the right of Figure 4.6, and it corresponds to assigning O to all the facets of the first column of Table 1, and I to all the facets of the second.

Facets		Colour
$1+i+j+k,$	$1-i-j-k$	1
$-1+i+j+k,$	$-1-i-j-k$	-1
$1+i+j-k,$	$-1+i-j+k$	i
$1-i+j-k,$	$-1-i-j+k$	$-i$
$1-i+j+k,$	$-1+i+j-k$	j
$1-i-j+k,$	$-1+i-j-k$	$-j$
$1+i-j+k,$	$-1-i+j+k$	k
$1+i-j-k,$	$-1-i+j-k$	$-k$

Table 1: A different colouring for P^5.

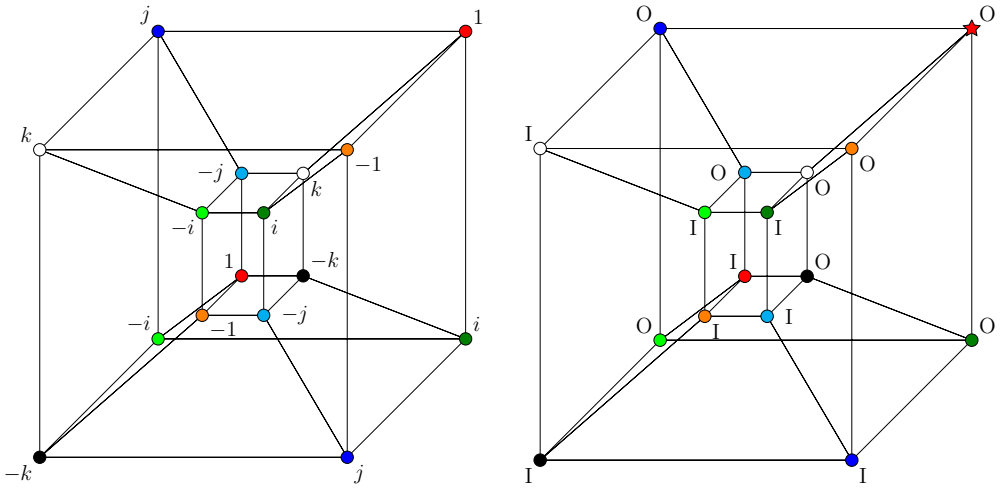

Figure 4.6: On the left, another colouring of P^5. On the right, a choice of an initial state. The vertex marked with a star is the only one which has the property that every vertex with status O is adjacent to it.

Lemma 4.3. *Consider the action of Q_8 on P^5 by isometries. This induces an action which is by left multiplication on the labels of the facets of P^5; moreover, it also acts by left multiplication on the colours. The colouring is Q_8-equivariant as a map from the set of facets $\mathcal{F}$ to the palette of colours Q_8, that is, if we denote with $c(F)$ the colour of a facet, we have that $c(q \cdot F) = q \cdot c(F)$.*

Proof. One can prove by hand that the statement holds for facets with colour 1, i.e. that for every $q \in Q_8$ then both $q \cdot (1 + i + j + k)$ and $q \cdot (1 - i - j - k)$ have the colour q. Then given any facet F, one can write $F = q' \cdot F'$ with $c(F') = 1$. We conclude noting that

$$c(q \cdot F) = c(q \cdot q' \cdot F') = q \cdot q' \cdot c(F') = q \cdot c(q' \cdot F') = q \cdot c(F). \qquad \square$$

It would be nice if the action were also transitive on the facets of P: this is of course not possible, since Q_8 has only eight elements, and we have 16 facets. To obtain a transitive action, we consider the involution τ of Q_8 defined as follows:

$$\tau(\pm 1) = \pm 1, \qquad \tau(\pm i) = \mp j, \qquad \tau(\pm j) = \mp i, \qquad \tau(\pm k) = \mp k.$$

The involution $\tau \colon Q_8 \to Q_8$ is actually a group automorphism. Both τ and Q_8 act on Q_8 (the latter by left multiplication) so they can be interpreted as elements of the permutation group $\mathrm{Sym}(Q_8)$. In this sense, τ normalizes Q_8, so the subgroup generated by Q_8 and τ has order 16; we denote this subgroup by R_{16}.

We extend τ to an automorphism of $\mathbf{H}$. We want τ to act on $\mathbf{H} \times \mathbb{R}$; this way, the map τ can also be seen as an isometry of P^5. Since τ does not preserve the parity of minus signs, to obtain an actual isometry of P^5 it must act on $\mathbb{H} \times \mathbb{R}$ by $(\tau, -\mathrm{Id})$. The induced action on the facets corresponds to the action of τ on the labels as elements of $\mathbf{H}$.

Lemma 4.4. *The colouring is R_{16}-equivariant; in particular, it preserves moves and colours (as partitions).*

Proof. As we already know that the colouring is Q_8-equivariant, it suffices to check that it is equivariant with respect to τ. Denote with $c(F)$ the colour of the facet F: we have that

$$c(\tau(1 + i + j + k)) = c(1 - i - j - k) = 1 = \tau(1) = \tau(c(1 + i + j + k)),$$
$$c(\tau(1 - i - j - k)) = c(1 + i + j + k) = 1 = \tau(1) = \tau(c(1 - i - j - k)),$$

so equivariance holds for facets with colour 1.

If $F = q \cdot F'$, with $c(F') = 1$, we have

$$c(\tau(F)) = c(\tau(q \cdot F')) = c(\tau(q) \cdot \tau(F')) = \tau(q) \cdot c(\tau(F')) = \\ = \tau(q) \cdot \tau(c(F')) = \tau(q \cdot c(F')) = \tau(c(F)),$$

where we used that $\tau(a \cdot b) = \tau(a) \cdot \tau(b)$ for $a, b \in \mathbf{H}$, and that c is Q_8-equivariant by Lemma 4.3. □

Now we have a group that acts freely and transitively on the facets, and preserves all the structure of colouring and moves. We want to use this to study the states: in fact, by acting on the facets, it also acts on the states. This is the analogue of the reflections we considered in the dodecahedron in Section 4.2.3.

Lemma 4.5. *For every facet F there exists exactly one balanced state that assigns status O to F, and status I to all facets not adjacent to F. This induces a bijection between facets and balanced states.*

In Figure 4.6, the starred vertex corresponds to the facet F in the statement.

Proof. Since R_{16} acts transitively preserving the colouring and moves, it sends balanced states to balanced states. Therefore, we may assume that the facet F is $1 + i + j + k$ without loss of generality.

Suppose S is a balanced state assigning status O to $1 + i + j + k$ and status I to all facets not adjacent to it. Since among these latter facets there is at least one facet for every move, all the status of all the other facets are forced by balancedness.

It suffices then to check that in the state obtained in this way the only facet which is adjacent to all the others with status O is $1 + i + j + k$; this can be done directly on Figure 4.6. This shows the map that assigns to each facet the state constructed above is injective, and since there are 16 facets and 16 balanced states (two choices for each move) it is a bijection. □

By combining Lemmas 4.4 and 4.5 we obtain the following.

Lemma 4.6. *The group R_{16} acts on the balanced states of P, and this action is free and transitive.*

Proof. By using the bijection in Lemma 4.5, every balanced state is identified with a facet, and this identification is naturally equivariant with respect to the isometries of P. In particular, since the action of R_{16} on the facets is free and transitive, so is the action on the balanced states. □

Theorem 4.7. *The colouring and initial state in Figure 4.6, along with the set of moves mentioned above, produce a hyperbolic* 5*-manifold* M^5 *along with a fibration* $f\colon M \to S^1$.

Proof. Unlike the previous construction, the number of moves was reduced from 8 to 4, so there are only 16 possible states. Moreover, by Lemma 4.6, we obtain that the balanced states, which are the ones appearing in the orbit, are all combinatorially isomorphic.

We just need to check collapsibility for a particular state: since we proved that there exists a facet with status O that is incident to all the facets with status O (since all the facets not adjacent to it have status I), it follows that the ascending link is a cone over the vertex dual to that facet. The same holds for the descending link (one way to see this is that the multiplication by $-1 \in Q_8$ yields an isometry of P^5 which inverts the whole state, so it sends the ascending link into the descending link isomorphically).

Next, we need to check the bad cubes. There are no tetrahedra in G^5 whose vertices are split into two pairs, with each pair belonging to one move (we can check this on a particular state since they are all isomorphic), so the only bad simplices are edges connecting vertices in the same move. These are the link of some bad square inside the dual cubulation.

Pick two adjacent vertices of G^5 which are in the same move; they are dual to a pair of facets F, F' and they are connected by an edge e. The link of this edge is isomorphic to G^3, which is dual to the ridge $F \cap F'$, and it inherits the same colouring and set of moves we described for P^3. The modified inherited state on $F \cap F'$ coincides with the inherited state, as every facet adjacent to F and F' is in a move different from F and F'. The inherited state is balanced, and we have already seen in Section 4.2.2 that balanced states for P^3 yield collapsible ascending and descending links.

The only thing left is to check the fibering cusps condition. The cusps of P^5 are dual to the hyperoctahedra in G^5. Eight of these have as vertices the vertices of a facet of the hypercube: by adding all the diagonals of squares in a 3-cube one obtains precisely the 1-skeleton of 4-hyperoctahedron. The other two hyperoctahedra have as vertices the vertices with an odd (even) number of signs in their labels in $\mathbf{H}$.

For the facets of the hypercube, one can note that for every one of them there is exactly a pair of vertices which are opposite in that cube (and therefore not

adjacent in G^5) and belong to the same colour; in particular, by the balancedness property, they must always have opposite status. Regarding the other two cusps, it turns out that every pair of opposite facets belongs to the same move, so we can conclude similarly.

Having checked all the conditions, we can apply Theorem 3.42 to conclude. □

We have thus obtained a hyperbolic 5-manifold M^5 that fibers over the circle, which is tessellated into 2^8 copies of P^5. This manifold has still a lot of symmetries; we will see later that these may be used to quotient down M^5 to a smaller manifold.

Remark 4.8. The set of moves we have just used was the same that was considered in [IMM22]. However, the colouring considered there was the one we saw in the first example (see Figure 4.5). This does not change much, as the resulting manifold M' will be commensurable to M, by what we observed in Remark 3.25. In particular, in Chapter 5 we will construct a manifold N which is a quotient of M, and it is the same obtained in the paper.

4.3.2 Dimension 6

The polytope P^6 has 27 facets, 27 cusps and 72 finite vertices [ERT12]. The symmetries of P^6 that stabilize a facet F coincide with the symmetries of that facet, which is isometric to P^5, and any isometry of F can be extended univocally to an isometry of the whole P^6.

Similarly to the previous section, we want to use P^6 to construct a hyperbolic manifold M^6 with a perfect circle-valued Morse function (since we are in even dimension, we cannot obtain a fibration).

The labelling of the facets. The general plan is to consider only the symmetries that fix some preferred facet, to recycle all the symmetries of P^5 we have just studied. The labelling we choose to refer to the facets will reflect that.

We fix a facet of P^6, and label it with the letter A. Recall that we labelled the facets of P^5 with elements of the form $\pm 1 \pm i \pm j \pm k$. The facet A is isometric to P^5; every isometry between A and P^5 induces a labelling of the facets of A, which are in natural bijection with the facets of P^6 adjacent to A. We choose such an isometry, and obtain a labelling of the 16 facets adjacent to A with the elements $\pm 1 \pm i \pm j \pm k$.

The facet A has 10 cusps. For every cusp c of A, there is a unique facet of P^6 that is incident to c but is not adjacent to A. This induces a bijection between the 10 cusps of A and the 10 facets not adjacent to A.

For every element $q \in Q_8$ there is a cusp of P^5 which is incident to precisely all the facets whose label has positive Euclidean scalar product with q. So for example, if $q = -i$, the corresponding cusp is incident to facets with label $\pm 1 - i \pm j \pm k$. We assign to the facets of P^6 which are disjoint from A and are incident to a cusp of A of this form the corresponding label $q \in Q_8$.

The remaining two cusps are adjacent to facets whose label has an even (resp. odd) number of minus signs. We assign label B (resp. C) to the corresponding facet of P^6.

This completes the assignment of the labels. To sum up, we have assigned to the 27 facets of P^6 the 24 elements of the binary tetrahedral group T_{24}, and some special labels A, B, C. This of course translates to a labelling of the vertices of the dual polytope, which is the Gosset polytope 2_{21}, denoted by G^6 to be consistent with the notation we used for lower dimensions.

Remark 4.9. To be precise, the elements of $T_{24} \backslash Q_8$ are of the form $\frac{1}{2}(\pm 1 \pm i \pm j \pm k)$, but we never write the $\frac{1}{2}$ factor since it is not relevant for our purpose.

Definition 4.10. We call the three facets with label A, B, C *special facets*, and their dual *special vertices*.

The adjacencies between facets can be read directly from the labels.

Lemma 4.11. *With the labelling above, the following hold:*

- *two facets with labels in T_{24} are adjacent if and only if their labels have non-negative Euclidean scalar product;*
- *special facets are pairwise not adjacent;*
- *the facet A is adjacent to another facet if and only if its label is in $T_{24} \setminus Q_8$;*
- *the facet B (resp. C) is adjacent to a facet if and only if its label is in Q_8, or if it is in $T_{24} \setminus Q_8$ and has an even (resp. odd) number of minus signs.*

Proof. Most of the adjacencies follow directly from the construction. However, we also give in Table 2 an explicit isomorphism with the description in [ERT12]. Vertices of G^6 are embedded in the 7-dimensional space, and two vertices are adjacent if and only if their Lorenzian scalar product with signature $(++++++-)$ is zero. □

Vertex	Label	Vertex	Label
$(0,0,0,0,0,-1,0)$	A		
$(0,0,0,0,-1,0,0)$	$1+i+j+k$	$(1,1,1,1,1,0,2)$	$-1-i-j-k$
$(1,1,0,0,0,0,1)$	$1+i-j-k$	$(1,0,1,0,0,0,1)$	$1-i+j-k$
$(1,0,0,1,0,0,1)$	$1-i-j+k$	$(1,0,0,0,1,0,1)$	$1-i-j-k$
$(0,1,1,0,0,0,1)$	$-1+i+j-k$	$(0,1,0,1,0,0,1)$	$-1+i-j+k$
$(0,1,0,0,1,0,1)$	$-1+i-j-k$	$(0,0,1,1,0,0,1)$	$-1-i+j+k$
$(0,0,1,0,1,0,1)$	$-1-i+j-k$	$(0,0,0,1,1,0,1)$	$-1-i-j+k$
$(-1,0,0,0,0,0,0)$	$-1+i+j+k$	$(0,-1,0,0,0,0,0)$	$1-i+j+k$
$(0,0,-1,0,0,0,0)$	$1+i-j+k$	$(0,0,0,-1,0,0,0)$	$1+i+j-k$
$(1,0,0,0,0,1,1)$	1	$(0,1,1,1,1,1,2)$	-1
$(0,1,0,0,0,1,1)$	i	$(1,0,1,1,1,1,2)$	$-i$
$(0,0,1,0,0,1,1)$	j	$(1,1,0,1,1,1,2)$	$-j$
$(0,0,0,1,0,1,1)$	k	$(1,1,1,0,1,1,2)$	$-k$
$(0,0,0,0,1,1,1)$	C	$(1,1,1,1,0,1,2)$	B

Table 2: The explicit labelling of the vertices of G^6, with respect to the description in [ERT12]. Two vertices are adjacent if their Lorenzian scalar product in $\mathbb{R}^7$ with signature $(++++++-)$ is zero.

Algebraically speaking, the group Q_8 is a normal subgroup of T_{24}, and each of the special vertices is adjacent to two of the three cosets.

The chosen labels allow us to use the symmetries of the group R_{16}, studied for P^5. This group acts on the facet A by isometries, which can be univocally extended to isometries of P^6 that fix A. This defines an action on the labels, which is as follows:

- the action on the labels in T_{24} is the restriction of its action on $\mathbf{H}$;
- the subgroup $Q_8 < R_{16}$ acts by fixing A, B, C, while τ fixes A and swaps B and C.

As one can possibly suspect from the equality between the numbers of cusps and facets, every facet F of P^6 is opposed to a cusp, in the sense that every other facet is either adjacent to F or incident to the cusp (and not to both).

Colouring and moves. To define the colouring and set of moves for P^6, the general idea is to try to extend the ones that worked for P^5.

We start with the set of moves. We put the special facets in three different moves. It would actually be more efficient to put them in the same move, but we choose to sacrifice efficiency to build a more symmetric example, which is easier to describe.

To define the moves on the facets with label in T_{24}, we consider the action of Q_8 by left multiplication: this partitions T_{24} into three orbits. We choose a base point in each: in particular, we pick 1, $1 + i - j - k$, and $1 + i - j + k$. Every $t \in T_{24}$ is of the form $q \cdot t'$, with t' one of the base points and $q \in Q_8$. We define $r \colon T_{24} \to Q_8$ by setting $r(t) = q$. Note that r is *not* a group homomorphism.

To motivate this strange choice of base points, we note that these are pairwise adjacent; furthermore, they have the property to be invariant, as a set, under the involution τ.

The facets with label in T_{24} are then subdivided into four sets of six facets each, that are the preimages of $\{\pm 1\}, \{\pm i\}, \{\pm j\}, \{\pm k\}$ via r; these four sets coincide with four moves. The explicit values of $r(t)$ are computed in Table 3.

Summing up, the moves consist into 3 singletons $\{A\}, \{B\}, \{C\}$ and 4 sets of 6 facets each.

Finally, we should choose the colouring. We could divide the 24 facets with label in T_{24} in 12 pairs; however this only changes the resulting hyperbolic manifold

t			$r(t)$
$1,$	$1+i-j-k,$	$1+i-j+k$	1
$-1,$	$-1-i+j+k,$	$-1-i+j-k$	-1
$i,$	$-1+i+j-k,$	$-1+i-j-k$	i
$-i,$	$1-i-j+k,$	$1-i+j+k$	$-i$
$j,$	$1-i+j-k,$	$1+i+j-k$	j
$-j,$	$-1+i-j+k,$	$-1-i-j+k$	$-j$
$k,$	$1+i+j+k,$	$-1+i+j+k$	k
$-k,$	$-1-i-j-k,$	$1-i-j-k$	$-k$

Table 3: The values of r on each facet. The facets in each row are pairwise adjacent; the horizontal lines divide the facets into four moves. The three columns form the three orbits of the action of Q_8 by left multiplication.

by commensurability, so to simplify the description we will just take the trivial colouring.

Lemma 4.12. *The map $r\colon T_{24} \to Q_8$ is R_{16}-equivariant with respect to the natural action of R_{16} on T_{24} and Q_8.*

Proof. Suppose that some facet has label t with $r(t) = q'$; be definition $t = q' \cdot t'$, with $t' \in \{1, 1+i-j-k, 1+i-j+k\}$.

If $q \in Q_8$, then r clearly satisfies $r(q \cdot t) = q \cdot r(t) = q \cdot q'$. On the other hand, since τ is a group automorphism of T_{24}, we have that $\tau(t) = \tau(q' \cdot t') = \tau(q') \cdot \tau(t')$, and since the base points are invariant under τ we obtain $r(\tau(t)) = \tau(q') = \tau(r(t))$, as desired. □

Note that τ swaps two of the three base points, and therefore swaps the corresponding orbits of the action of Q_8 on T_{24} by left-multiplication.

Corollary 4.13. *The restriction of the moves to facets adjacent to A produces the same set of moves used for P^5.*

Proof. Note that $1+i+j+k$ and $1-i-j-k$ are in the same move, and conclude by using that both r and the colouring $c\colon \mathcal{F} \to Q_8$ of P^5 are Q_8-equivariant. □

We choose as initial state the balanced state which assigns the status O to A, B, C, and all the facets with $r(t) \in \{1, i, j, k\}$, and the status I to all the other facets.

Theorem 4.14. *The above choice of colouring, set of moves and initial state produces a hyperbolic manifold M^6, tessellated into 2^{27} copies of P^6, with a piecewise-linear map $f\colon M^6 \to S^1$ which can be smoothened to a perfect circle-valued Morse function.*

Proof. We need to check the conditions required to apply Theorem 3.42. The first thing to check is the ascending/descending link of the states of the orbit, which consists of all the balanced states. These correspond to ascending and descending links of vertices of the dual cubulation.

Note that R_{16} acts transitively on the balanced states, if we ignore the status of A, B, and C: more precisely, given two balanced states S and S' there is some $\varphi \in R_{16}$ such that $\varphi(S)$ and S' coincide on all facets except possibly on A, B, and C. This can be seen by restricting the status to the facets adjacent to A and using that R_{16} acts transitively on the balanced states of P^5; then, if two states coincide on the facets adjacent to A, they must also coincide on the other non-special facets by balancedness, since they belong to the same move as some facet adjacent to A.

In particular, it is enough to prove collapsibility for the ascending link of all the states obtained from the initial one by changing the state of some special facets. Pick one such state; the vertices of G^6 with status O are therefore the following:

$$\begin{array}{lll} 1, & 1+i-j-k, & 1+i-j+k, \\ i, & -1+i+j-k, & -1+i-j-k, \\ j, & 1-i+j-k, & 1+i+j-k, \\ k, & 1+i+j+k, & -1+i+j+k, \end{array}$$

plus eventually some special vertices. Denote by L the ascending link of the state, which is the full subcomplex of G^6 spanned by these vertices.

Start with the vertex with label A. If it has status I, skip to the following step; otherwise, we would like to remove it from L with a collapse. Consider the link of A inside L: this is precisely the ascending link of a balanced state of P^5. Since the link of A is collapsible inside L, we can collapse A on its link, and remove it from L.

The same can be done with B and C: one could show that the facets adjacent to each of them are in correspondence with the facets of P^5, with the same moves. However, since defining the isomorphism is not straightforward, we prove directly that $\mathrm{Lk}(B, L)$ and $\mathrm{Lk}(C, L)$ are collapsible. The first is spanned by the first two columns in the list above, and they are all adjacent to $1 + i + j + k$, while the

second is spanned by the first and third column, and they are all adjacent to i. So they are both cones and therefore collapsible.

After collapsing B and C, the next vertex we want to collapse is $-1+i-j-k$. Its link inside L is spanned by the following vertices:

$$\begin{array}{rrr} & 1+i-j-k, & 1+i-j+k, \\ i, & -1+i+j-k, & \\ & & 1+i+j-k, \\ & & -1+i+j+k. \end{array}$$

It is the cone over i, and therefore collapsible.

After removing $-1+i-j-k$ from L every other vertex collapses on $1+i+j+k$; L is therefore collapsible.

The situation regarding bad cubes is complicated, as there are a lot of them. To check them, we need to study all the simplices σ of G^6 such that no move contains exactly a vertex of σ, and compute the modified inherited state on their link in G^6.

Fix a k-simplex σ. The moves partition the vertices of σ, so they determine a partition λ of the integer $k+1$. We subdivide the study of the simplices based on this partition.

Case $\lambda = (2)$. We start from edges of G^6 with vertices on the same move. By acting with R_{16}, we may suppose that the endpoints are either $1+i+j+k$ and $-1+i+j+k$, or $1+i+j+k$ and k. We analyse separately the two cases.

In the first case the link of the edge in G^6 has the vertices indicated in Figure 4.7. Note that they are 10, as the spanned simplicial complex is isomorphic to G^4.

This inherits a modified state, which is balanced. There is another constraint on the state, i.e. that k has always status O, since it is in the same move as $\pm 1+i+j+k$ (see Definition 3.35); this however will not important when computing the ascending and descending links.

We start by computing the ascending link of this state (the descending link is analogous), that is the subcomplex of G^4 spanned by vertices with status O and we denote by L. We want to collapse A onto its link if it has status O, otherwise we just skip to the following step.

The link of A in G^4 is spanned by the six vertices with label $\pm 1 \pm i \pm j \pm k$, and it is represented in Figure 4.8 (left). It is isomorphic to G^3, with the set of moves being the same we considered in Section 4.2.2. We already saw that

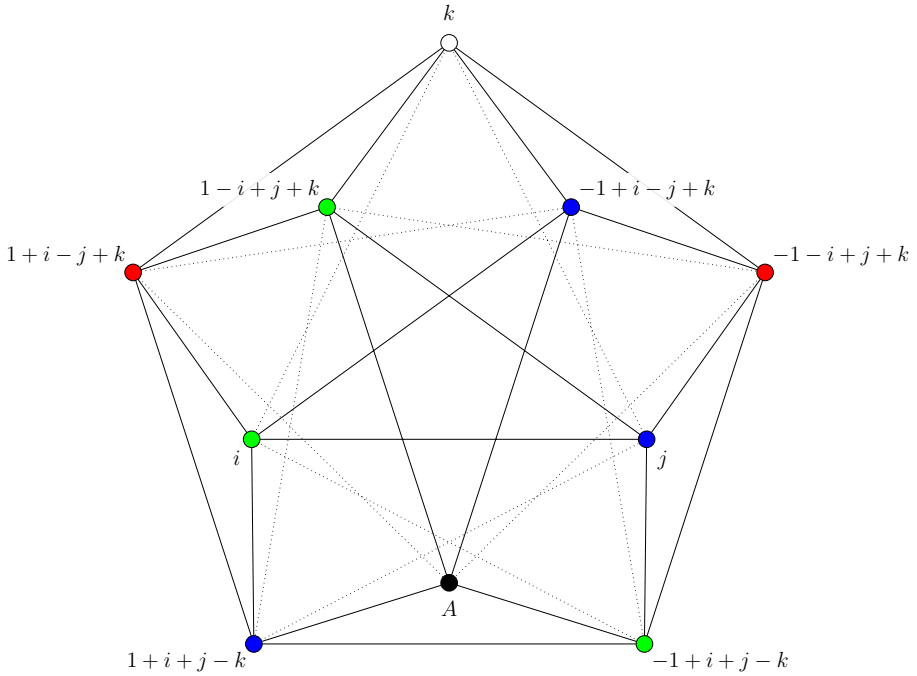

Figure 4.7: The link of the edge in G^6 connecting $\pm 1+i+j+k$. It is the dual polytope of the ridge obtained by intersecting the facets with those labels.

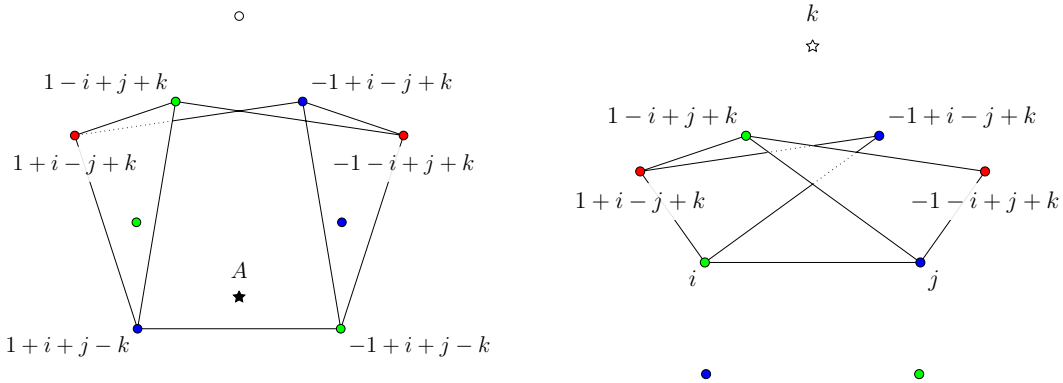

Figure 4.8: The links of A and k inside the coface link: they both form a triangular prism.

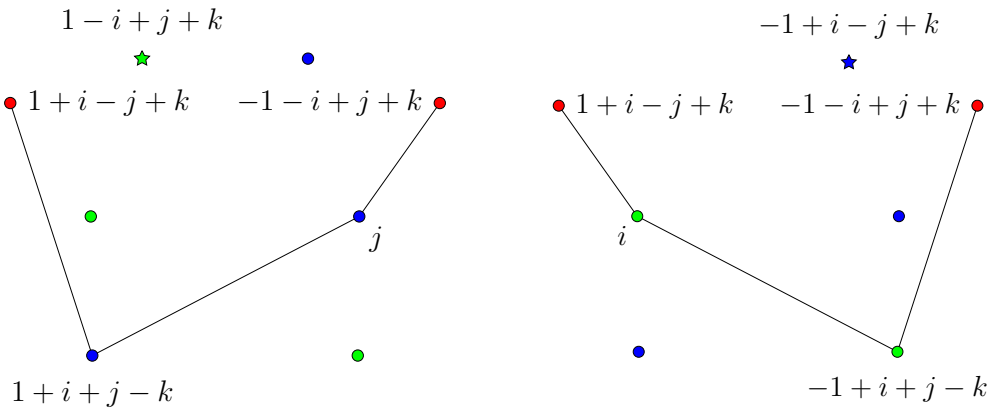

Figure 4.9: The links of $1-i+j+k$ and $-1+i-j+k$ inside the coface link.

balanced states of P^3 yield collapsible ascending and descending link, so $\mathrm{Lk}(A, L)$ is collapsible and we can safely collapse A onto its link. We also remove A from G^4.

The same can be done with the vertex k: the adjacent vertices are shown in Figure 4.8 (right), and again they span a G^3 with the same set of moves.

Next up is $1-i+j+k$: its link is spanned by the vertices in Figure 4.9 (left). Since j and $1+i+j-k$ are adjacent and in the same move, they have the same status by balancedness; similarly, $1+i-j+k$ is not adjacent to $-1-i+j+k$, so they have opposite status and exactly one of them will belong to the ascending link. In every case, if we restrict to vertices with status O we obtain a collapsible link, so we can collapse $1-i+j+k$. Similarly, we can also collapse away $-1+i-j+k$ (see Figure 4.9).

After these collapses, the vertices remaining in G^4 are shown in Figure 4.10. Note that exactly one of $1+i-j+k$ and $-1-i+j+k$ has status O; depending on the status of the other vertices, by using again the balancedness of the state, the possible ascending links are either a single point, two segments joined on a vertex, or a triangle and a tetrahedron joined on an edge. All of them are collapsible, so we are done.

We should also analyse the second case, i.e. the case where the bad edge connects k and $1+i+j+k$. The vertices of its link are shown in Figure 4.11; it is isomorphic to the first case, so we conclude in the same way.

Case $\lambda = (3)$. We now study triangles in G^6 whose vertices are in the same move. We may suppose by using R_{16} that the triangle is spanned by $1+i+j+$

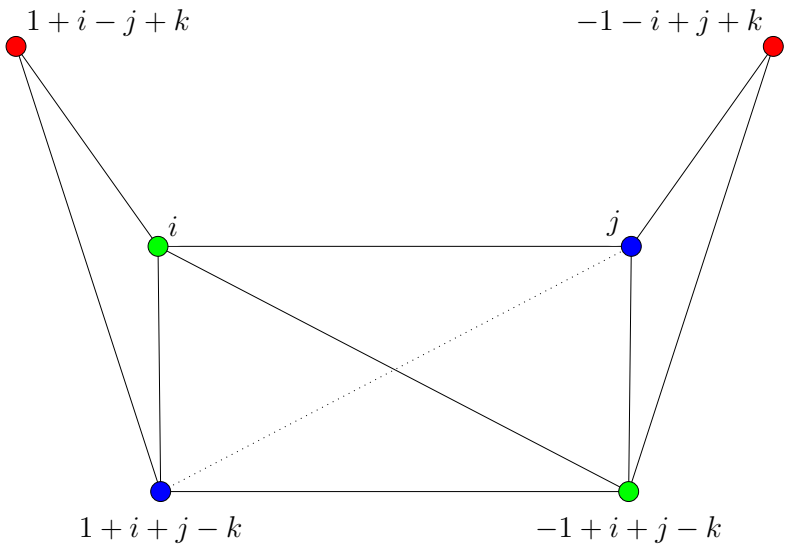

Figure 4.10: The coface link after all the collapses.

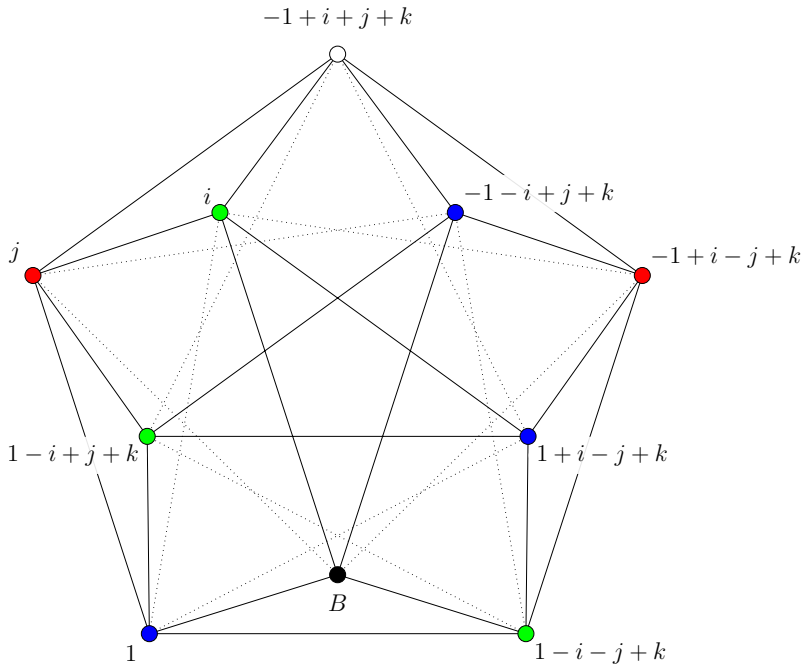

Figure 4.11: The coface link of the bad square spanned by k and $1+i+j+k$; the result is isomorphic to the case obtained before.

$k, -1+i+j+k, k$. We already computed the link of this triangle, and it is the one drawn in Figure 4.8 (right); since it is isomorphic to G^3 with the usual set of moves, the ascending and descending links of the modified inherited state are collapsible.

Case $\lambda = (2,2)$. We consider tetrahedra σ in G^6 whose vertices are split into two pairs, each pair belonging to a move. This is the link of a product of two irreducible bad squares inside the dual cubulation.

We know that by acting by R_{16} we may send any edge connecting two vertices in the same move to the edge connecting $1+i+j+k$ and $-1+i+j+k$, or k and $1+i+j+k$. Without loss of generality, we may suppose two of the vertices of σ are $\pm 1+i+j+k$ (the other case produces isomorphic results). We can see in Figure 4.7 the possibilities for the other two vertices of σ: since they are in the same move, they are either i and $-1+i+j-k$, or j and $1+i+j-k$. By symmetry of the picture we may consider only the first case.

So the vertices of σ are $1+i+j+k$, $-1+i+j+k$, i and $-1+i+j-k$, and its link in G^6 is spanned by $1+i+j-k, j, -1+i-j+k$: they form a disjoint segment and point, and they are all in the same move. In particular, the ascending link of the modified inherited state is made of one of these two collapsible components.

Case $\lambda = (3,2)$. There is no 4-simplex whose vertices are split in a pair and a triple, each made by vertices in the same move.

Case $\lambda = (3,3)$. There is also no 5-simplex whose vertices are split into two triples, each of vertices in the same move.

Case $\lambda = (2,2,2)$. There are, however, 5-simplices whose vertices are split into three pairs, each pair made of vertices in the same move. These are links of products of three bad squares inside the dual cubulation. Let σ be such a simplex.

The simplex σ is maximal inside G^6, and therefore its link is empty. This implies that a cube Q which is the product of three bad squares is maximal inside the cubulation, and so the descending link of f at the barycentre of Q coincides with the descending face link of Q. By applying Proposition 2.21 and Lemma 3.26, we obtain that the descending face link of Q collapses on the join of three S^0, which is a PL 2-sphere. The barycentre of Q is therefore a critical point of index 3.

A quick Euler characteristic check: the number of 5-simplices inside G^6 whose vertices are partitioned in three pairs by the moves is 8. Indeed, every such simplex has exactly one pair of vertices in the same move adjacent to A, and this determines all the vertices, as one can deduce by looking at Figure 4.7; this pair can be chosen in 8 ways. We can conclude that, since every bad 6-cube has 64 vertices,

every vertex of the cubulation contributes to the total Euler characteristic with $-1 \cdot \frac{8}{64} = -\frac{1}{8}$, which is exactly the Euler characteristic of P^6.

The cusps. After computing all the descending links of f, we need to check the fibering cusp condition to obtain a perfect-valued Morse function. Recall that every cusp c of P^6 is opposed to a facet F, and the facets incident to c are the 10 facets not adjacent to F (and different from F itself).

- The cusp opposed to A has every pair of opposed facets of the same colour, and except for the pair (B, C) they have opposite status by balancedness.
- The two facets $-1 + i - j - k$ and $-i$ are incident to the cusp opposed to $1 + i + j + k$, they are in the same move, and since they are disjoint they have opposite status. By using R_{16}, this proves that every cusp opposed to a facet adjacent to A satisfies the fibering cusps condition.
- Take a cusp c opposed to the facet with label $q \in Q_8$: the facets incident to c are A, $-q$ and all the facets adjacent to A and to $-q$, which correspond to the facets incident to some cusp of the facet A, isometric to P^5 with the same colouring and set of moves described in the previous section. Since P^5 has fibering cusps, we conclude that c satisfies the condition. The same argument applies to the cusps opposed to B and C.

We conclude that P^6 has fibering cusps.

Having checked all the hypotheses of Theorem 3.42, we can conclude that M^6 admits a perfect circle-valued Morse function. □

4.3.3 Dimension 7

Starting from dimension 7, the combinatorics become complicated very quickly. To understand the symmetries of P^7, we need to introduce the octonions. We refer to [CS03].

Recall that the octonions $\mathbb{O}$ are a vector space with basis $1, e_1, \dots, e_7$. The rules for multiplication can be summarized by the Fano plane.

The Fano plane is a diagram on the projective plane, containing seven points $e_1, \dots, e_7$. There are seven oriented circles, each connecting e_n, e_{n+1} and e_{n+3}, where all numbers are to be intended modulo 7. It is represented in Figure 4.12: all the lines depicted are circles, containing precisely three points and oriented in such a way that e_n, e_{n+1}, e_{n+3} is a positively oriented triple.

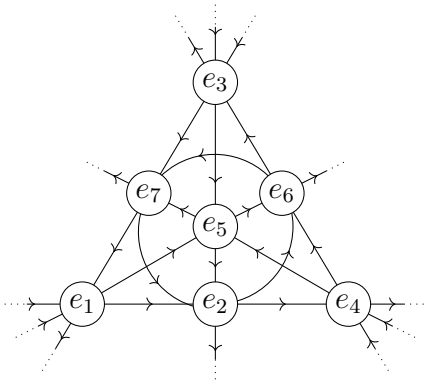

Figure 4.12: The Fano plane.

With that in mind, we can define the multiplication as follows:

- $e_i \cdot e_i = -1$;
- if $i \neq j$, then $e_i \cdot e_j = \pm e_k$, where k is the only subscript such that e_i, e_j, e_k are three distinct points in a circle on the Fano plane, and the sign is positive if e_i, e_j, e_k is a positively oriented triple, and negative otherwise.

By definition, if we restrict to the vector space generated by 1 and by the three elements on a Fano circle, we obtain an embedding of the quaternions.

Remark 4.15. Note that the product is not associative! In fact, one can check that $(e_i \cdot e_j) \cdot e_k = \pm e_i \cdot (e_j \cdot e_k)$, where the sign is positive if and only if e_i, e_j, e_k belong to the same line (in which case equality follows from the associativity of the quaternions).

Now that we have refreshed the definitions, we are ready to describe P^7. It has 56 facets, 126 ideal vertices and 576 finite vertices. Its facets are in correspondence with the elements of the form $\frac{1}{2}(1 \pm e_n \pm e_{n+1} \pm e_{n+3})$, and two facets are adjacent if and only if their scalar product is $\frac{1}{2}$. Therefore, one may use the symmetries of the octonions to find symmetries of P^7, which form the exceptional group E_7. The dual is the Gosset polytope 3_{21}, which we denote by G^7.

Vertices and cusps. We also give a combinatorial description of finite vertices and cusps. To do so, we think of an element of the form $\frac{1}{2}(1 \pm e_n \pm e_{n+1} \pm e_{n+3})$ as a line in the Fano plane, together with a choice of a sign for each of the three points of that line. In this interpretation, two facets are adjacent either if the two lines are different and they intersect in a point with the same sign, or if the

two lines coincide and they differ for exactly a sign. Note that this description already contains some symmetry breaking: in fact, we are distinguishing two types of adjacencies even if they are intrinsically the same.

We work on the dual G^7, whose vertices have the same labelling as the facets of P^7.

Let us start with the description of the finite vertices of P^7. They are dual to the 6-simplices of G^7, which are of the following two types:

- Choose a sign for each of the seven points of the plane, and consider all the vertices of G^7 whose label has the prescribed sign on every point of its line. There are seven such labels (one per line) and they are all pairwise adjacent by construction, so the vertices from a 6-simplex. There are $2^7 = 128$ simplices of this form.

- Choose three points on a line ℓ in the Fano plane and one other point e_k not contained in ℓ. For each of these four points choose a sign, and consider all the vertices of G^7 whose label intersects at least two chosen points with the prescribed signs. There are 7 such labels (three lines intersecting e_k with two choices of sign each, plus ℓ with all the prescribed signs), and they are all pairwise adjacent, so they span a 6-simplex.

  There are 7 available choices for ℓ, 4 for e_k, and $2^4 = 16$ choices for the signs, for a total of $7 \cdot 4 \cdot 16 = 448$ simplices of this form.

This concludes the characterization of the $128 + 448 = 576$ finite vertices. The cusps, dual to hyperoctahedra of G^7, are similarly subdivided in two types:

- Choose a point e_k of the Fano plane and a sign; then consider all the labels whose line intersects that element with the given sign. There are 3 lines intersecting e_k and 4 choices of sign, for a total of 12 labels, corresponding to vertices of G^7. They are all pairwise adjacent except for pairs of labels with the same line and the signs of the two points different from e_k inverted. These are the vertices of a hyperoctahedron in G^7, dual to a cusp of P^7; there are $7 \cdot 2 = 14$ cusps of this type.

- Choose a line ℓ and a sign for each of the four points *not* in ℓ, and consider all vertices of G^7 labelled with a line different from ℓ, and with the prescribed sign on the points outside ℓ. There are 6 lines different from ℓ, and two choices of sign for the intersection with ℓ. All facets with such a label are

pairwise adjacent except for the pairs of distinct lines intersecting in ℓ with different sign.

There are $7 \cdot 2^4 = 112$ cusps of this type; together with the 14 cusps of the first form, we obtain a total of 126, which is precisely the number of cusps of P^7.

We note that even for P^7 there is some sort of opposition: this time, every facet F is opposed to another facet F', which is the one with all signs inverted. Every other facet is adjacent to exactly one of F and F'.

Colouring and states. The colouring we choose is a 14-colouring, where we assign the same colour to all the facets labelled with $\frac{1}{2}(1 \pm e_n \pm e_{n+1} \pm e_{n+3})$ with the same n and with the same parity of number of minus signs. By definition, there are four facets for each colour. Here we use the chromatic set of moves.

This time there is an actual choice to make regarding the initial state. It is easier to describe the initial state by inheriting this from the one we will give for P^8. Since P^7 is a facet of P^8, a colouring and state for P^8 induces some colouring and state for P^7 by looking at a facet. We refer to the next section for the description of the initial state we use here.

By Proposition 3.29, all the cubes are good, so we only need to check are the ascending and descending links of the states in the orbit. However, the numbers are way too big to even attempt doing the computations by hand: we have a manifold tessellated into 2^{14} copies of P^7, for a total of 16384 ascending links and 16384 descending links. By using a Sage program which can be found in [Mar], one can find out that, after quotienting by isomorphism, these links reduce to 106 classes, which are all simply connected.

By applying Theorem 1.37 we obtain some map $f\colon M^7 \to S^1$ whose induced map in homotopy $f_*\colon M^7 \to S^1$ has finitely presented kernel.

A fibration? Following what we have obtained in dimension 5 and 6, it is natural to ask the following.

Question 4.16. *Does there exist a complete, finite volume hyperbolic 7-manifold which fibers over the circle?*

One might hope to promote the map above to a fibration. However, the following obstruction stands.

Proposition 4.17. *Let $f\colon M^7 \to S^1$ be the map constructed above. There is some cusp c of M^7 on which the restriction $f|_c$ is homotopic to a constant. In particular, f cannot be homotoped to a fibration.*

Proof. Consider one of the 112 cusps of the second form. The 12 facets incident to it have all distinct colours and are in distinct moves, therefore by Proposition 3.41 the restriction to such a cusp is homotopic to a constant. □

There might be a way to use some non-chromatic set of moves to improve the result. However, we could not find any suitable colouring and set of moves that does not have some problems on the cusps.

For example, one could try to partition the 56 facets into 7 moves, such that each move contains two disjoint 4-cliques. In this way, one could choose a balanced initial state, and hope that the construction produces a fibration.

For the fibering cusps condition, one needs every cusp to contain at least a pair of opposite facets in the same move: however, there are at most $16 \cdot 7 = 102$ pairs of non-adjacent facets in the same move, and $14 \cdot 9 = 126$ cusps: since each pair of non-adjacent facets belongs to at most one cusp, there are always at least 14 cusps which are not fibering.

4.3.4 Dimension 8

In dimension 8 we need the full power of the octonions to describe P^8. It has 240 facets, 2160 cusps and 17280 real vertices. The facets can be identified with the following unitary elements in $\mathbb{O}$:

- the 16 elements ± 1 and $\pm e_n$;
- the half integral elements $\frac{1}{2}(\pm 1 \pm e_n \pm e_{n+1} \pm e_{n+3})$, which amount to a total of $7 \cdot 2^4 = 112$;
- the 112 elements of the form $\frac{1}{2}(\pm e_{n+2} \pm e_{n+4} \pm e_{n+5} \pm e_{n+6})$.

Remark 4.18. While it is tempting to assume that these 240 elements are closed under multiplication, as it is for the binary tetrahedral group, this is not the case here! While this property may be obtained by considering a slightly different lattice, we will never need it, so we keep this description.

Similarly to P^7, two facets are adjacent if and only if their labels have Euclidean scalar product equal to $\frac{1}{2}$. In particular, the facets adjacent to 1 have the same

label as the facets of P^7, which is coherent with the fact that every facet of P^8 is isometric to P^7. The dual of P^8, denoted by G^8, is the Gosset polytope 4_{21}.

Next, we want to choose a colouring that induces the colouring described for P^7 when restricting to the facet labelled with 1. We partition the facets into 15 *hextets*, each comprised of 16 mutually disjoint facets.

- The first hextet contains all the elements $\pm 1, \pm e_1, \dots, \pm e_7$;
- Other seven hextets can be constructed by fixing n and considering all elements $\frac{1}{2}(\pm 1 \pm e_n \pm e_{n+1} \pm e_{n+3})$ and $\frac{1}{2}(\pm e_{n+2} \pm e_{n+4} \pm e_{n+5} \pm e_{n+6})$ with an even number of minus signs;
- The last seven can be built as above by considering odd number of minus signs.

This partition is a 15-colouring of P^8; we would like to pick an initial state (the set of moves is the chromatic one). Since every colour contains 16 facets, it is natural to pick a state where each colour has 8 facets with status I and 8 with status O. We explain how we perform this choice.

Let $S = \{\pm 1, \pm e_1, \dots, \pm e_7\}$. We would like to let it act by left multiplication on the facets, except for the fact that this is not a group action since the octonions are not associative. However, with some caution, we can still obtain the following.

Lemma 4.19. *For any x, y belonging to the same hextet, there is a unique $s \in S$ such that $s \cdot x = y$. We say, by an abuse of notation, that S acts freely and transitively on each hextet.*

Proof. For the first hextet the proof is straightforward. Regarding the others, by using the symmetries of the Fano plane we can reduce ourselves to prove it only for the hextet corresponding to $n = 1$. After that, the proof reduces to a tedious but easy check, by using the orientation of the Fano plane, that the parity of minus signs is preserved. □

Inside S there are some copies of Q_8, for example the one obtained by sending $i \to e_1$, $j \to e_2$, and $k \to e_4$. We want to use the action of $Q_8 \subset S$ to separate each hextet into two orbits, and give status I to one orbit and O to the other. Again, even if Q_8 is now a group, the action is still not a group action, as it is multiplying octonions and therefore associativity is not satisfied.

We can however fix some base point in each hextet, namely 1, $1 + e_n + e_{n+1} + e_{n+3}$, and $-1 + e_n + e_{n+1} + e_{n+3}$. If we take an hextet with base point x_0, the set $Q_8 \cdot x_0$ is well-defined and consists of 8 elements in that hextet; we give status I to the corresponding facets. All the other facets receive status O.

Again we need the help of Sage to analyse the ascending and descending links. There are 2^{15} descending links to analyse, which reduce to 185 classes of isomorphism. The links are quite complicated: indeed, since $\chi(P^8) = 17/2$, every link should contribute to an average of $17/2$ to the Euler characteristic, so on average one should expect the wedge of at least 8 spheres of various dimensions.

However, it turns out that all these links are connected and simply connected. We obtain the following.

Theorem 4.20. *For $n = 7, 8$ there exists a finite volume hyperbolic manifold M^n along with a map $f\colon M^n \to S^1$ such that the induced map in homotopy $f_*\colon \pi_1(M^n) \to \mathbb{Z}$ has finitely presented kernel.*

The cover $\widetilde{M^n}$ associated with this kernel has finitely presented fundamental group, and infinitely many cusps of maximal rank. In particular, it has infinite Betti number b_{n-1}.

Proof. The manifolds M^n are the ones obtained above; since all the descending links are simply connected, then we may apply Theorem 1.37.

Let $\widetilde{M}$ be the cyclic cover corresponding to $\ker f_*$. We want to show that the restriction of f to some cusp is null-homotopic; then we would conclude that the cusp lifts to infinitely many cusps in $\widetilde{M^n}$.

We already saw that there are some cusps in M^7 on which f is null-homotopic, so it remains to check M^8.

By using Sage, it turns out that the cusps are subdivided into 1920 whose adjacent facets form a 14-coloured cube, and 240 that form a 7-coloured cube. By Proposition 3.41, the restriction on the cusps of the first type is null-homotopic. □

5

The fibering 5-dimensional hyperbolic manifold

In the previous chapter, we constructed hyperbolic manifolds M^n in various dimensions with some associated map $f\colon M^n \to S^1$. In particular, the manifold M^5 constructed in dimension 5 stands out, as it is the first example of a hyperbolic 5-manifold fibering over the circle.

In this chapter we study this manifold. Since it is quite large, as it is tessellated into 256 polytopes, we are interested in finding commensurable fibering manifolds with smaller volume. To do so, we quotient M^5 by a group of isometries so that the quotient is tessellated by a small amount of copies of P^5.

After giving some explicit data about this manifold, we discuss some consequences of the existence of a fibering hyperbolic 5-manifold.

5.1 Quotienting M^5

Recall that M^5 is built by attaching copies of P^5, each indexed by a vector in an $\mathbb{F}_2$-vector space. This vector space has as basis the palette of colours; since our palette of colours was chosen to be $\mathcal{C} = Q_8$, the vector space we are using is $V := \mathbb{F}_2^{Q_8}$, generated by the elements $\{e_q : q \in Q_8\}$. The copy of P^5 associated to some $v \in V$ is denoted with P_v.

To obtain a small quotient of M^5 we would like to have a large subgroup $\Gamma < \operatorname{Isom} M^5$ acting freely and properly discontinuously. Moreover, we also need it to preserve the fibration, so that the quotient still fibers over the circle.

Definition 5.1. An isometry Φ of M^5 is *cellular* if it preserves the tessellation into polytopes. It is *fibered* if it preserves the circle-valued fibration: that is, we ask that $f \circ \Phi = f$.

Every P_v is canonically identified with the abstract P^5, so given two copies P_v and $P_{v'}$ and an isometry $\varphi\colon P_v \to P_{v'}$ between them, then φ is naturally an isometry of an abstract P^5, and vice versa. The group R_{16} acts on P^5 by isometries, so it can be considered as a subgroup of $\mathrm{Isom}\, P^5$.

Lemma 5.2. *For every pair of polytopes P_v and $P_{v'}$, there exists a unique cellular fibered isometry Φ of M^5 that sends P_v to $P_{v'}$ via some isometry $\varphi \in R_{16}$.*

Proof. Note that a fibered cellular map should map P_v to $P_{v'}$ preserving the state, so there is exactly one $\varphi \in R_{16}$ that satisfies this by Lemma 4.6. Uniqueness is guaranteed from the general fact that two isometries of a connected Riemannian manifold which coincide on an open subset must coincide everywhere.

The existence follows from the fact that the map that sends P_v to $P_{v'}$ via φ extends to a cellular isometry Φ of M^5, as it preserves the colouring (as a partition). Since it also preserves the set of moves and the state, it is fibered. □

If Φ sends P_v to $P_{v'}$ via some $\varphi \in R_{16}$, then it acts with the same φ on every other copy P_w; this follows from the fact that the copies are glued altogether along the facets via the identity map of P^5. So the isometries which are cellular, fibered, and whose restriction on some P_v belongs to R_{16} form a group G.

One must be careful that the action of G on M^5 is not free. For example, the map Φ that sends P_0 to $P_{e_1+e_{-1}}$ acts as the identity on the abstract P^5. The two polytopes P_0 and $P_{e_1+e_{-1}}$ intersect on the two ridges which are the intersection of a facet with colour 1 and a facet with colour -1: these ridges are fixed by Φ.

One could ignore this and quotient anyway: the result would be an orbifold, obtained from P^5 by gluing together pairs of facets, with some conical singularities with angle π corresponding to the bad ridges. We will see more about this in the next section.

Instead we take some subgroup $\Gamma < G$ of index 2 such that the action of Γ is free. To do so, we construct a bipartition $X_1 \sqcup X_2$ of the set of copies P_v of P^5 such that:

- every isometry $\Phi \in G$ preserves the bipartition of the copies of P^5 into X_1 and X_2 (possibly sending X_1 to X_2 and vice versa);
- if P_v and $P_{v'}$ intersect in a bad ridge, i.e. the intersection of two facets in the same move, then they belong to different sets of the bipartition.

This way we obtain the subgroup of index 2 we desire, which is made of all the fibered cellular isometries that stabilize both X_1 and X_2.

To define the bipartition, we describe the set of facets which separate X_1 from X_2. Consider the subset of facets in M^5 obtained in the following way. First, define the *parity* of a facet F of P^5 as the parity of minus signs in its label $\pm 1 \pm i \pm j \pm k$; similarly, define the *parity* of $v \in V$ as the parity of the number of components which are non-zero.

For every copy P_v, consider all its facets F that have:

- either status I and the parity of F equals the parity of v;
- or status O and the parity of F differs from the parity of v.

Since when crossing a facet one inverts both the status and the parity of v, the definition is independent on which of the two polytopes which are incident in the same F we consider. Call $\mathcal{T}$ the set consisting of all these facets.

Lemma 5.3. *For any colour $q \in Q_8$ and any P_v, the set $\mathcal{T}$ contains exactly either all the facets of P_v with colour q or all the facets with colour $-q$.*

Proof. This follows from the fact that facets of the same colour differ for three signs, and they have opposite status. Facets of opposite colour have same status and differ for one sign (if adjacent), or have opposite status and differ for all the signs. □

Lemma 5.4. *Let F, F' be two facets of some P_v, with colour q, q'. Denote with $\overline{F}, \overline{F'}$ the corresponding facets in $P_{v+e_q+e_{q'}}$. Then the intersection $\{F, F', \overline{F}, \overline{F'}\} \cap \mathcal{T}$ has even cardinality.*

Proof. Denote with $s(F)$ the status of a facet.

If q, q' belong to different moves, $s(F) \neq s(\overline{F})$ and $s(F') \neq s(\overline{F'})$. In particular, exactly one between F and $\overline{F}$ belongs to $\mathcal{T}$, and exactly one between F' and $\overline{F'}$ belongs to $\mathcal{T}$.

Similarly, if they belong to the same move, then $s(F) = s(\overline{F})$ and $s(F') = s(\overline{F'})$, so it holds that $F \in \mathcal{T} \Leftrightarrow \overline{F} \in \mathcal{T}$ and $F' \in \mathcal{T} \Leftrightarrow \overline{F'} \in \mathcal{T}$.

In both cases the number of facets belonging to $\mathcal{T}$ is even. □

Start from the polytope P_0, and put it into X_1. Given $v \in V$, take any path that starts from the interior P_0, ends in the interior of P_v, and is transverse to all the facets; if the number of facets in $\mathcal{T}$ crossed by the path is even, put P_v in X_1, otherwise put it in X_2.

Lemma 5.5. *The definition of X_1 and X_2 is well-posed.*

Proof. We need to show that it does not depend on the chosen path. First, we may suppose that the path is contained in the 1-skeleton $C^{(1)}$ of the dual cube complex.

Note that $C^{(1)}$ can be obtained by the 1-skeleton of a 8-cube by replacing every edge with two. By attaching a bigon on every pair of edges joining the same vertices, one obtains (up to homotopy equivalence) the 1-skeleton of the cube; by attaching in addition all the squares of the 8-cube one obtains the 2-skeleton, which is simply connected.

Therefore every loop in the 1-skeleton of $C^{(1)}$ can be turned into the trivial loop via a sequence of discrete homotopies, using some bigons and/or some squares. A bigon corresponds to crossing two facets of the same colour in succession, while a square corresponds to crossing F, F', and then again F and F', for some pair of facets F and F' (not necessarily adjacent).

By Lemma 5.3 and Lemma 5.4 these discrete homotopies do not change the parity of the number of faces of $\mathcal{T}$ crossed. □

Lemma 5.6. *The group G fixes $\mathcal{T}$.*

Proof. Define the *parity* of a state as the parity of the facet associated to it by Lemma 4.5.

Let S, S' be the states associated to two adjacent polytopes P_v, P_{v+e_i}: one may check that the parity of S and S' differ, so it follows that v and v' have the same parity if and only if their state have the same parity.

Since G acts by preserving states, given $\Phi \in G$, there are two cases:

- either Φ preserves the parity of vectors in V, so the associated $\varphi \in R_{16}$ preserves parity of states, and therefore Φ also preserves parity of facets (because it preserves the parity of a particular facet, which is the one associated to the status);
- or Φ inverts parity of the vectors, so similarly it also inverts parity of facets.

The isometry Φ preserves or inverts the parity of both the vectors in V and the facets, so it sends facets in $\mathcal{T}$ to facets in $\mathcal{T}$, as required. □

Since G fixes $\mathcal{T}$, it follows that it preserves the bipartition into $X_1 \sqcup X_2$. We may henceforth quotient M^5 by the group of isometries $\Gamma < G$ that stabilize X_1 and X_2, which is a subgroup of index 2.

Proposition 5.7. *The group Γ acts freely on M^5.*

Proof. The group Γ acts on the dual cube complex by preserving the orientations, and without fixing any vertex.

Suppose by contradiction that $\Phi \in \Gamma$ fixes some bad square Q. Then the only possibility in order to preserve orientations would be that Φ acts as a rotation of angle π around the centre. However, this is excluded, since a bad square alternates edges in $\mathcal{T}$ with edges not in $\mathcal{T}$; this is because edges in a bad squares are dual to facets with colours q and $-q$, and so we can apply Lemma 5.3. Thus, opposite vertices are dual to polytopes in different sides of the bipartition, so Φ does not stabilize X_1, a contradiction.

Suppose now that Φ fixes a cube. If the cube does not contain bad squares, then its minimum should be fixed by Φ, a contradiction. Otherwise, the only other possibility is that it is the product of a bad square with a good cube; therefore it has two minima, which are the vertices of a bad square which should be fixed, again a contradiction. □

The quotient M^5/Γ is a manifold tessellated with two copies of P^5; we denote it with N.

Remark 5.8. This construction of N is quite different from the one in [IMM22]: this is due to the fact that we are using a different colouring, and so the manifold M that we are quotienting is different; however, it turns out the quotient manifold N obtained is the same. The advantage of the construction presented here is that we do not need to pass to a cyclic covering, but we can directly define N as a quotient of M^5; however, the subgroup of index 2 was easier to describe in the original construction of [IMM22].

One can use Regina [BBP+23] to study N, with the code available at [Mig].

The facet identification is described in Table 4: for every facet F of the two polytopes tessellating N it is listed the state, the polytope and facet to which F is attached to, and the gluing isometry. The latter is described via a permutation of the vertices: every finite vertex of every facet is labelled with a number from 1 to 5, each number corresponding naturally to a coordinate in the ambient space $\mathbf{H} \times \mathbb{R} \cong \mathbb{R}^5$, and an isometry between two facets is determined by the image of the finite vertices. Note that the fifth coordinate is always fixed, since R_{16} acts separately on $\mathbf{H}$ and $\mathbb{R}$, and the permutation is always odd, so that the pasting maps are all orientation reversing.

	Facet	Status	To Polytope	To Facet	Permutation
Polytope A	$-1-i-j-k$	In	A	$1+i-j+k$	24135
	$-1-i-j+k$	Out	A	$1+i-j-k$	42315
	$-1-i+j-k$	In	B	$-1+i-j+k$	24135
	$-1-i+j+k$	Out	B	$1+i-j+k$	13245
	$-1+i-j-k$	In	B	$1+i+j+k$	42315
	$-1+i-j+k$	In	A	$1-i+j+k$	13245
	$-1+i+j-k$	In	A	$-1+i+j+k$	31425
	$-1+i+j+k$	Out	A	$-1+i+j-k$	24135
	$1-i-j-k$	In	B	$-1-i+j+k$	31425
	$1-i-j+k$	Out	B	$1-i+j+k$	24135
	$1-i+j-k$	Out	B	$1-i-j-k$	42315
	$1-i+j+k$	Out	A	$-1+i-j+k$	13245
	$1+i-j-k$	In	A	$-1-i-j+k$	42315
	$1+i-j+k$	Out	A	$-1-i-j-k$	31425
	$1+i+j-k$	In	B	$-1+i+j-k$	13245
	$1+i+j+k$	Out	B	$1+i+j-k$	31425
Polytope B	$-1-i-j-k$	In	B	$-1+i+j+k$	13245
	$-1-i-j+k$	Out	B	$1-i+j-k$	31425
	$-1-i+j-k$	Out	B	$1-i-j+k$	42315
	$-1-i+j+k$	Out	A	$1-i-j-k$	24135
	$-1+i-j-k$	Out	B	$1+i-j-k$	24135
	$-1+i-j+k$	Out	A	$-1-i+j-k$	31425
	$-1+i+j-k$	Out	A	$1+i+j-k$	13245
	$-1+i+j+k$	Out	B	$-1-i-j-k$	13245
	$1-i-j-k$	In	A	$1-i+j-k$	42315
	$1-i-j+k$	In	B	$-1-i+j-k$	42315
	$1-i+j-k$	In	B	$-1-i-j+k$	24135
	$1-i+j+k$	In	A	$1-i-j+k$	31425
	$1+i-j-k$	In	B	$-1+i-j-k$	31425
	$1+i-j+k$	In	A	$-1-i+j+k$	13245
	$1+i+j-k$	In	A	$1+i+j+k$	24135
	$1+i+j+k$	Out	A	$-1+i-j-k$	42315

Table 4: The facet pairing of the two polytopes of N.

Regina also tells us that N is combinatorially isomorphic to the manifold constructed by Ratcliffe and Tscahntz in [RT03], which is the hyperbolic 5-manifold with the smallest volume known.

The computer also gives a description of the fiber F of the fibration $N \to S^1$. It has a triangulation with 144 simplices, which Regina simplifies to a triangulation with 40 simplices. Its signature is given below:

```
OvLLAALzzwLvAAMvPQwLPMQQQQQwLQQQQQcfcgdgfjgkoqpuvmxwAurBvxGHHIFI
GwFEwzDEzCDJACEMLNLNMGKLKKNMKNML2a2aDaJaaaJaaaVbqbaa3akbaaVb2a7aVba
aqbOaUb9aKaHa3aHaVbpaaapaJa3aSbPb2aJaKbRagavaaa2aJa8adbVbDaaaDaaava
UbUbcbUbUb2aJa2aHbHb
```

This is a different triangulation than the one given in [IMM22]; this is probably because the simplification algorithm of Regina is not invariant under isomorphism, so different representations of the same object may lead to different results.

By using Regina we can compute the Euler characteristic of F, which is equal to 1; this implies that N is the smallest quotient of M we can obtain.

5.2 Orbifolds

As we mentioned before, if we are happy to work with orbifolds, we can quotient by all the isometries of M^5 without restricting to a subgroup of index 2. What happens in this case is that every bad square is quotiented by an isometry that rotates of an angle π around its centre, so the centre becomes a singular point of order 2.

In particular, the singular locus S is precisely the union of the bad ridges, which are transverse to the bad squares. By looking at the double cover N, it turns out that f restricts to a fibration on the preimage of the bad ridges, with fiber a torus with three punctures.

Quotienting a bad square by a rotation of angle π can be translated in terms of colouring. Define a *pseudocolouring* as a colouring in which adjacent faces are allowed to be in the same colour, i.e. it is a partition of the facets without any restriction.

Given a right-angled hyperbolic polytopes and a pseudocolouring, one can repeat the same construction we did in Section 3.1.1. In this case, however, the resulting space is not necessarily a hyperbolic manifold, since one may have two right angles around a ridge instead of four. We obtain instead an orbifold $\mathcal{O}$, where

the intersection of two facets with the same colour becomes singular with angle π. The orbifold $\mathcal{O}$ is still tessellated into copies of P.

This is precisely the point behind the notion of moves. Consider a polytope P, equipped with a colouring, set of moves and initial state, which produce a manifold M. The set of moves can be interpreted as a pseudocolouring, which produces a hyperbolic orbifold $\mathcal{O}$ as above.

Since the pseudocolouring is coarser than the colouring as a partition (meaning that facets of the same colour are of the same pseudocolour), the manifold M covers the orbifold $\mathcal{O}$, with the covering map sending polytopes to polytopes preserving the state. This means that the map $f\colon M \to S^1$ passes to the quotient, and defines a map $g : \mathcal{O} \to S^1$.

It turns out that this map g can sometimes be described geometrically. We now give a motivating example, which is due to Thurston.

Example 5.9. Consider the cube in Figure 5.1, where every facet is subdivided into two by a segment. Combinatorially, this has become a polytope with 12 facets and 20 vertices, which is a dodecahedron. In particular, if we put the Euclidean metric of the cube on it, we have that almost every dihedral angle is $\frac{\pi}{2}$ save for the new edges, which have angle π.

Now we can consider the unique 3-colouring of the cube, and via the procedure explained in Section 3.1.1 we get a 3-torus T^3 tessellated into eight copies of the cube. However, we can also put the hyperbolic metric on the cube, induced by the metric on the hyperbolic right-angled dodecahedron we considered in Section 4.2.3. This gives T^3 the structure of a hyperbolic orbifold, but since in this metric the new edges have angle $\frac{\pi}{2}$, they produce a conical singularity in T of angle π along a link. This hyperbolic orbifold is naturally a quotient of the manifold constructed in Section 4.2.3, corresponding to the 3-pseudocolouring of the dodecahedron obtained by giving the same colour to facets in the same move.

On $T^3 \cong {}^{[0,1]^3}\!/\!_{\sim}$ one can define a diagonal map onto S^1, given by $f(x, y, z) = x+y+z \pmod{\mathbb{Z}}$. The connected components of the singular locus are all parallel to some coordinate axis, so f restricts to a fibration on the singular locus, and therefore lifts to a fibration of some covering manifold.

If we were to interpret this in terms of states, we should be assigning the status O on a facet if the gradient of f pointed outside the cube, and I otherwise. Note that the two facets in the same square have the same status (the gradient of f points in the same direction, since the facets are parallel), and opposite facets have

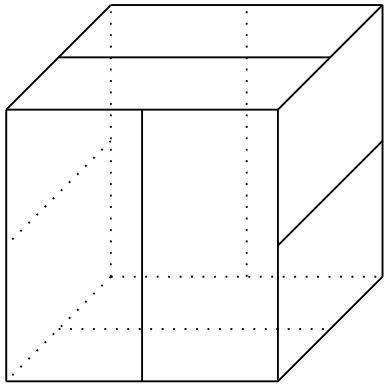

Figure 5.1: An unusual representation of a dodecahedron.

opposite status. This is coincides with the notion of balanced state we have used all along Chapter 4.

One could translate the construction of P^5 into this setting. However, this time the situation is more complicated, not only because of the higher dimension and the richer combinatorics, but also because now our polytope has cusps: therefore, one does not get a compact 5-cube, but a (subdivided) cube with some faces of different dimensions removed, one for every cusp. We will not go into the details of this.

5.3 Finiteness properties of groups

We conclude with some group-theoretical considerations. As we mentioned in the introduction, the fiber bundle structure does not behave very well with the hyperbolic metric, in the sense that the fiber is necessarily far from being a totally geodesic submanifold. This fact can be used as a source for constructing complicated subgroups of hyperbolic groups.

Hyperbolic groups were introduced by Gromov in [Gro87].

Definition 5.10. Let X be a proper geodesic metric space. We say that X is *δ-hyperbolic* if geodesic triangles are δ-thin, meaning that every edge is contained in a δ-neighbourhood of the union of other two.

Definition 5.11. A group G is *hyperbolic* if it acts properly discontinuously and cocompactly on a δ-hyperbolic space by isometries.

Hyperbolic groups are always finitely generated and finitely presented; they also satisfy a more general notion of finiteness.

Definition 5.12. A group G is *of type* $\mathcal{F}_n$ for $n \geq 1$ if it admits a classifying space X (i.e. an aspherical space X with $\pi_1(X) \cong G$) with finite n-skeleton.

If G is of type $\mathcal{F}_n$ for every n, then G is said to be *of type* $\mathcal{F}_\infty$; if moreover the classifying space is finite, G is said to be *of type* $\mathcal{F}$.

Being of type $\mathcal{F}_1$ is equivalent to being finitely generated, while type $\mathcal{F}_2$ translates to finitely presented.

A hyperbolic group G is always of type $\mathcal{F}_\infty$: this can be shown by using the Vietoris-Rips complex, which is contractible and on which G acts cocompactly with finite stabilizers (see [Gro87]). If G is torsion-free, one can deduce that G is of type $\mathcal{F}$.

A natural question to ask is whether hyperbolicity and finiteness properties are hereditary in some sense. For example, a subgroup H of a hyperbolic group G might not be hyperbolic, as it may not be finitely generated (for example, take the commutators subgroup of the free group of rank 2). What if we ask whether H is hyperbolic under the assumption that it is finitely generated? Or that it is of type $\mathcal{F}_n$ for some n?

Theorem 5.13 ([Rip82, Gro87, LIMP21, LIP22, IMM22])**.** *For every n, there exists a hyperbolic group G with a subgroup $H < G$ which is of type $\mathcal{F}_n$ but not $\mathcal{F}_{n+1}$ (and therefore not hyperbolic).*

Moreover, there exists a hyperbolic group G with a subgroup H of type $\mathcal{F}$ which is not hyperbolic.

The case $n = 1$ is due to Rips [Rip82]: he finds a subgroup of a hyperbolic group which is finitely generated but not finitely presented.

A sketch of a counterexample for $n = 2$ was given by Gromov in his fundamental paper [Gro87], but later Bestvina showed during a talk in 1993 that Gromov's example was not working, as the ambient group could not be hyperbolic. Later Brady provided a proper counterexample in [Bra99].

More recently Llosa Isenrich, Martelli and Py [LIMP21] were able to prove that the kernel constructed for $n = 8$ in Theorem 4.20, which we already know that is of type $\mathcal{F}_2$ but not $\mathcal{F}_7$ (this can be deduced from the fact that the covering has infinite Betti number b_7), is actually of type $\mathcal{F}_3$ and not $\mathcal{F}_4$. Note that $G = \pi_1(M^8)$ is not hyperbolic since M^8 is cusped, but this problem can be circumvented by an appropriate Dehn filling.

Finally, Llosa Isenrich and Py were able to prove in [LIP22] the theorem for all $n \in \mathbb{N}$ by using complex hyperbolic geometry.

The last statement of the theorem, i.e. that there exists a hyperbolic group containing a subgroup of type $\mathcal{F}$ which is not hyperbolic, can be proved by using the fibering hyperbolic manifold M^5. We give an idea on how to do so, without going into details as it would become quite technical.

Sketch of proof. The rough idea is to take $G = \pi_1(M^5)$ and $H = \pi_1(F)$, where F is the fiber. Note that F is aspherical: the cyclic covering $\widetilde{M}^5$ is hyperbolic and aspherical, and is homeomorphic to $F \times \mathbb{R}$, and therefore homotopically equivalent to F. So F is a classifying space for H, and thus H is of type $\mathcal{F}$.

However, since M^5 is cusped, the ambient group $\pi_1(M^5)$ is not hyperbolic. Indeed, $\pi_1(M^5)$ acts by isometries on $\mathbb{H}^5$, but not cocompactly. To fix this, we need to compactify our fibering manifold.

Recall that M^5 is the interior of a compact manifold with toric boundaries, on which f restricts to a fibration. We fill these boundary tori by coning every fiber to a point; this way, the map f extends to the filling. If the fibers are large enough, i.e. each closed geodesic has length at least 2π, this is called a 2π-filling, and by a theorem of Fujiwara and Manning [FM10, Theorem 2.7] the resulting space $\hat{M}$ is locally negatively curved, which is enough to guarantee hyperbolicity of $\pi_1(\hat{M})$. To ensure that the filling is actually a 2π-filling, one may need to pass to a suitable finite cover.

So one can take $G = \pi_1(\hat{M})$ and $H = \pi_1(\hat{F})$. It remains to prove that H is not hyperbolic.

The fiber F cannot admit any hyperbolic metric. This is a consequence of Mostow rigidity: if the fiber were hyperbolic, it would follow that the monodromy could be homotoped to a unique isometry, which must have finite order since $\mathrm{Isom}(F)$ is finite: but the monodromy has infinite order in $\mathrm{MCG}(F)$, or else M would contain an essential torus, which is forbidden by the hyperbolicity.

The proof that H is not hyperbolic uses a similar idea, namely that the monodromy has infinite order in $\mathrm{Out}(H)$. For more details on this, refer to [IMM22]. □

Bibliography

[AGM13] Ian Agol, Daniel Groves, and Jason Manning. The virtual Haken conjecture. *Documenta Mathematica*, 18:1045–1087, 2013.

[ALR01] Ian Agol, Darren D. Long, and Alan W. Reid. The Bianchi groups are separable on geometrically finite subgroups. *Annals of Mathematics*, 153:599–621, 2001.

[Bar02] Alexander I. Barvinok. A course in convexity. In *Graduate Studies in Mathematics*, 2002.

[BB97] Mladen Bestvina and Noel Brady. Morse theory and finiteness properties of groups. *Inventiones mathematicae*, 129:445–470, 1997.

[BBP+23] Benjamin A. Burton, Ryan Budney, William Pettersson, et al. Regina: Software for low-dimensional topology. `http://regina-normal.github.io/`, 1999–2023.

[Ben16] Bruno Benedetti. Smoothing discrete Morse theory. *Annali Scuola Normale Superiore – Classe di Scienze*, 16:335–368, 2016.

[BM22] Ludovico Battista and Bruno Martelli. Hyperbolic 4-manifolds with perfect circle-valued Morse functions. *Transactions of the American Mathematical Society*, 375:2597–2625, 2022.

[Bra99] Noel Brady. Branched Coverings of Cubical Complexes and Subgroups of Hyperbolic Groups. *Journal of the London Mathematical Society*, 60:461–480, 1999.

[BS18] Matthias Beck and Raman Sanyal. *Combinatorial reciprocity theorems*, volume 195. American Mathematical Soc., 2018.

[CS03] John H. Conway and Derek A. Smith. *On Quaternions and Octonions: Their Geometry, Arithmetic, and Symmetry.* 2003.

[ERT12] Brent Everitt, John G. Ratcliffe, and Steven T. Tschantz. Right-angled Coxeter polytopes, hyperbolic six-manifolds, and a problem of Siegel. *Mathematische Annalen*, 354:871–905, 2012.

[FM10] Koji Fujiwara and Jason Fox Manning. CAT(0) and CAT(-1) fillings of hyperbolic manifolds. *Journal of Differential Geometry*, 85:229 – 270, 2010.

[Gos00] Thorold Gosset. On the regular and semi-regular figures in space of n dimensions. *Messenger of Mathematics*, 29:43–48, 1900.

[Gro87] Michail Gromov. *Hyperbolic Groups*. Springer New York, New York, NY, 1987.

[HM74] Morris W. Hirsch and Barry Mazur. *Smoothings of Piecewise Linear Manifolds*. Princeton University Press, 1974.

[IMM20] Giovanni Italiano, Bruno Martelli, and Matteo Migliorini. Hyperbolic manifolds that fibre algebraically up to dimension 8. *Journal of the Institute of Mathematics of Jussieu*, 2020.

[IMM22] Giovanni Italiano, Bruno Martelli, and Matteo Migliorini. Hyperbolic 5-manifolds that fiber over S^1. *Inventiones mathematicae*, 231:1–38, 2022.

[JNW19] Kasia Jankiewicz, Sergey Norin, and Daniel T. Wise. Virtually fibering right-angled Coxeter groups. *Journal of the Institute of Mathematics of Jussieu*, 20:957–987, 2019.

[KM13] Alexander Kolpakov and Bruno Martelli. Hyperbolic four-manifolds with one cusp. *Geometric and Functional Analysis*, 23, 2013.

[LIMP21] Claudio Llosa Isenrich, Bruno Martelli, and Pierre Py. Hyperbolic groups containing subgroups of type $\mathcal{F}_3$ but not $\mathcal{F}_4$. *arXiv:2112.06531*, 2021.

[LIP22] Claudio Llosa Isenrich and Pierre Py. Subgroups of hyperbolic groups, finiteness properties and complex hyperbolic lattices. *arXiv:2204.05788*, 2022.

[Mar] Bruno Martelli. Personal webpage. `http://people.dm.unipi.it/martelli/research.html`. Accessed: 2023-06-03.

[Mig] Matteo Migliorini. Code for tessellated manifolds. `https://github.com/topologia-pisa/tessellated-manifold-triangulation`.

[Min89] Hermann Minkowski. *Allgemeine Lehrsätze über die konvexen Polyeder*. Springer Vienna, Vienna, 1989.

[MSW69] John Milnor, Micheal Spivak, and Robert Wells. *Morse Theory. (AM-51), Volume 51*. Princeton University Press, 1969.

[Mun60] James Munkres. Obstructions to the smoothing of piecewise-differentiable homeomorphisms. *Annals of Mathematics*, 72:521–554, 1960.

[PV05] Leonid Potyagailo and Ernest Vinberg. On right-angled reflection groups in hyperbolic spaces. *Commentarii Mathematici Helvetici*, 80:63–73, 2005.

[Rip82] Eliyahu Rips. Subgroups of small cancellation groups. *Bulletin of the London Mathematical Society*, 14:45–47, 1982.

[RS82] Colin P. Rourke and Brian J. Sanderson. *Introduction to Piecewise-linear Topology*. Ergebnisse der Mathematik und ihrer Grenzgebiete. Springer-Verlag, 1982.

[RT03] John Ratcliffe and Steven Tschantz. Integral congruence two hyperbolic 5-manifolds. *Geometriae Dedicata*, 107, 2003.

[Wey34] Hermann Von Weyl. Elementare theorie der konvexen polyeder. *Commentarii Mathematici Helvetici*, 7:290–306, 1934.

[Wis21] Daniel T. Wise. *The Structure of Groups with a Quasiconvex Hierarchy*. Princeton University Press, Princeton, 2021.